

# UIC CLASS VI GEOLOGIC STORAGE OF CO<sub>2</sub> PERMIT APPLICATION

## Loving CCS Hub

Loving County, Texas

## Section 1: Site Characterization & Narrative

[40 CFR §146.82, §146.83]

*Prepared for:*

**EPA Region 6**

**Underground Injection Control Section**

1201 Elm Street, Suite 500 | Dallas, Texas 75270



*Prepared and submitted by:*

**Milestone Carbon Delaware CCS Hub, LLC**

840 Gessner Rd, Suite 600  
Houston, Texas 77024

*Prepared by*

# Table of Contents

<b>1.0 SITE CHARACTERIZATION [40 CFR 146.82 (a);] [40 CFR 144.31(e)(1-6)]</b>	7
1.1 Facility Information [40 CFR 146.82 (a)(1)]	7
1.2 Project Introduction [40 CFR 146.82 (a)(1)]	8
1.3 Overview Maps of AoR [40 CFR 146.82(a)(2)]	11
1.3.1 Major Roads Near Injection Site	11
1.3.2 Mines, Superfund Sites, Quarries, Other Hazardous Sites	13
1.3.3 Map of Rivers, Springs, Wells, Other Water Features	14
1.3.4 Map of Oil and Gas and Injection Wells in the Area of Review (AoR)	15
1.3.5 Map of Buildings in the Area of the Wells	16
1.3.6 Omnibus Map [40 CFR 146.82(a)(2)]	17
1.4 [REDACTED]	30
1.5 Regional Geology Background [40 CFR 146.82(a)(3)(vi)]	31
1.5.1 [REDACTED]	[REDACTED]
1.5.2 [REDACTED]	[REDACTED]
1.5.3 [REDACTED]	[REDACTED]
1.5.4 [REDACTED]	[REDACTED]
1.5.5 [REDACTED]	[REDACTED]
1.5.6 [REDACTED]	[REDACTED]
1.5.7 [REDACTED]	[REDACTED]
1.5.8 Major Geologic Features and Description on Tectonic History	47
1.6 Local Geology Introduction	50
1.7 Structural Geology [40 CFR 146.82 (a)(3)(iii)]	51
1.7.1 Structure	51
1.7.2 Thickness	61
1.7.3 Cross-sections	64
1.7.4 Lithology	68
1.8 Faults and Fractures [40 CFR 146.82 (a)(3)(ii)]	69
1.8.1 Fractures	69
1.8.2 Faults	75
1.8.3 Seismic History [40 CFR 146.82 (a)(3)(v)]	77
1.8.4 Regional Stress	82
1.8.5 Fault Slippage Potential (FSP) Analysis	82
1.8.6 Summary	89
1.9 Petrophysical Characterization [40 CFR 146.82(a)(3)(iii)] [40 CFR 146.82(a)(3)(iv)]	90
1.9.1 Type Log	90
1.9.2 Porosity	92
1.9.3 Permeability	96

1.9.4	Salinity.....	100
1.9.5	Naturally Occurring CO <sub>2</sub> .....	102
1.9.6	Capillary Pressure .....	103
1.10	Geomechanics [40 CFR 146.82(a)(3)(iv)].....	104
1.10.1	Methods.....	104
1.10.2	Pore Pressure.....	106
1.10.2.1	Top Seal .....	106
1.10.3	Stress Magnitude.....	108
1.10.4	Stress Orientation.....	111
1.10.5	Rock Strength.....	112
1.10.6	Ductility.....	113
1.10.7	Additional Testing .....	114
1.11	Geochemistry [40 CFR 146.82(a)(6)].....	115
1.11.1	Geochemistry for Central Loving Project.....	115
1.11.1.1	Brine Geochemistry .....	116
1.11.1.2	[REDACTED] Group and [REDACTED] Mineralogy.....	117
1.11.1.3	Injectate Chemistry .....	117
1.11.2	Equilibrium Geochemical Modeling .....	117
1.11.2.1	Geochemical Database .....	118
1.11.2.2	Saturation Indices .....	118
1.11.3	Geochemical Model Pressure and Temperatures .....	119
1.11.4	Geochemical Modeling Results and Discussion.....	119
1.11.4.1	Modeling Steps .....	119
1.11.4.2	Equilibrium Modeling Results.....	120
1.11.4.3	Conclusion .....	122
1.12	Mineral Resources .....	123
1.13	Site Suitability [40 CFR 146.83] .....	125
1.13.1	Subsurface Distribution of Fractures – Implications for CO <sub>2</sub> plume migration .....	125
1.13.2	Injectability .....	125
1.13.3	Carbon Dioxide Containment.....	126
1.13.4	Secondary Confinement Zones .....	126
1.13.5	Carbon Dioxide Interaction with Well Materials and Formation .....	127
1.13.6	Total Storage Capacity .....	127
1.14	Well Index Tables.....	128
1.14.1	Water Well Index Table .....	128
1.14.2	Oil and Gas Well Index Table .....	129

## List of Tables

Table 1-1: Proposed Operational Parameters.....	9
Table 1-2: Contact Information for Key Local, State and Other Authorities [40 CFR 146.82(a)(20)].....	9
Table 1-3: Additional Federal, State and Local Permits Required for Project Completion [40 CFR 146.82(a)(1)] .....	10
Table 1-4: Coordinates and Total Depth of All Injection, Monitoring Wells and Other Class Wells .....	10

Table 1-9: Ground Water Advisory Unit Determinations, All Depths in TVD Below Ground Level .....	30
Table 1-10: Subsea and TVD Depth of Tops at [REDACTED] .....	51
Table 1-11: Earthquake Catalog 10 mi Radius of the Central Loving Facility .....	81
Table 1-12: Geomechanical Input parameters for [REDACTED] FSP Models .....	83

Table 1-15: Probability of Fault Slip – [REDACTED] .....	86
--	----

Table 1-16: Probability of Fault Slip - [REDACTED]	89
Table 1-17: Log Porosity Values in Study Area [REDACTED]	92
Table 1-18: Injection Zones / Seal Stress Magnitudes [REDACTED]	109
Table 1-19: Injection Zones / Seal Stress Gradients [REDACTED]	111
Table 1-20: Avg. Unconfined Compressive Rock Strength of the Injection Unit & Top Seal Formations [REDACTED]	112
Table 1-21 Est. Minimum Net Confining Stress in Fusselman Dolostone [REDACTED]	113
Table 1-22: Composite Brine Chemistry from USGS [REDACTED]	116
Table 1-23: Mineralogy Input for PHREEQC Selected for [REDACTED]	117
Table 1-24: Injectate Chemistry Used in Geochemical and Static/Dynamic Models [REDACTED]	117
Table 1-25: Mineralogy Changes Based on Equilibrium Geochemical Modeling for [REDACTED]	121
Table 1-26: Mineralogy Changes Based on Equilibrium Geochemical Modeling for [REDACTED] and [REDACTED]	121
Table 1-27: Modeled Equilibrium Aqueous Concentrations [REDACTED]	122
Table 1-28: AoR Maximum Plume Extent [REDACTED]	127
Table 1-29: Water Well Index Table [REDACTED]	128
Table 1-30: Oil and Gas Well Index Table [REDACTED]	129

## List of Figures

Figure 1-1: Map of AoR and Wells with Respect to [REDACTED]	11
Figure 1-2: Major TxDOT Roads Near Facility [REDACTED]	12
Figure 1-3: Regional Map of Superfund Sites, Hazards and Active Mines in AoR [REDACTED]	13
Figure 1-4: Water Sources in AoR [REDACTED]	14
Figure 1-5: All Artificial Penetrations in AoR - Except Water Wells (As of 6/19/2024) [REDACTED]	15
Figure 1-6: Map of Local Buildings, Temporary and Permanent [REDACTED]	16
Figure 1-7: Omnibus map - Artificial Penetrations, Cleanup Sites, Quarries, Mines, Water Wells, Springs etc. [REDACTED]	17
Figure 1-8: Schematic Cross-section of the Aquifers in [REDACTED] A-A' West to East (Ashworth, 1990) [REDACTED]	18
Figure 1-9: AoR in relation to Major and Minor Aquifers of West Texas [REDACTED]	19
Figure 1-10: Regional Map of [REDACTED]	20

Figure 1-22: Proposed Facility Location in the Greater Permian Basin (Modified from Fairhurst et al., 2021) [REDACTED]	31
Figure 1-23: Stratigraphic Column Permian Basin, modified from Merrill et al., 2012 [REDACTED]	33
Figure 1-24: Stratigraphic Column Deep Permian Basin [REDACTED]	34
Figure 1-25: Regional Map of the [REDACTED]	

Figure 1-34: Map of West Texas Precambrian Basement (Ewing et al., 2019, Adams and Keller, 1996) [REDACTED]	46
Figure 1-35: Interpreted crustal blocks (T. Hoak et al. 1998) [REDACTED]	47
Figure 1-36: Horne Delaware Basin Faults and Recent Earthquakes (Horne et al., 2022) Red Star = Facility [REDACTED]	48
Figure 1-37: Horne Delaware Basin Orogenic History with Type-log and Strat. (Horne et al., 2022) [REDACTED]	49
Figure 1-38: Stylized West-East Cross-section through Permian (Saller and Steuber, 2018) [REDACTED]	50

Figure 1-52: A-A' Dip Cross-Section, NW to SE.....	65
Figure 1-53: B-B' Strike Cross-Section, SW to NE.....	65
Figure 1-54: A-A' / B-B' Index Map.....	66

Figure 1-65: Faults in 3-D from a bird's-eye view.....	76
Figure 1-66: Lateral 3-D view of AoR and faults (looking north).....	76
Figure 1-67: Frequency of U.S. Damaging Earthquakes.....	77
Figure 1-68: Tectonic Map of Texas, Major Structural Features of the Lone Star State.....	78
Figure 1-69: USGS Earthquakes Jan 1980 - July 2024 .....	79
Figure 1-70: West Texas Earthquake Catalog .....	80
Figure 1-71: West Texas Stress Map.....	82

Figure 1-95: Regional Maximum Horizontal Stress Map (Source: World Stress Map, 2024).....	111
Figure 1-96: Dolomite Triaxial Test from Analogous Low Porosity Dolomite.....	114
Figure 1-97: Example of Brittle and Ductile behavior .....	114
Figure 1-98: Offset Deep Oil and Gas Production.....	124

## List of Equations

(1-1 ) .....	104
(1-2 ) .....	104
(1-3 ) .....	105
(1-4 ) .....	105
(1-5 ) .....	105
(1-6 ) .....	105
(1-7 ) .....	113
(1-8 ) .....	118
(1-9 ) .....	118
(1-10) .....	119
(1-11) .....	127

## Professional Geologist Stamp

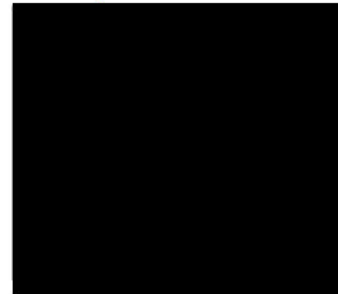
Based on my professional evaluation and analysis, I certify that the geological maps, cross-sections and figures associated with this permit are accurate and correct to the best of my knowledge based on publicly available data. The interpretations, recommendations and conclusions presented in these documents accurately represent the geological conditions as observed and analyzed in the field and in the laboratory.

Not contained here is any proprietary information that might be held by local oil and gas operators such as drilling information or proprietary wireline logs. The field measurements previously reported to RRC, TCEQ or TWDB are not guaranteed under this seal as I did not witness the testing. Uncertainty surrounding the validity of these measurements is discussed in the permit.

All interpretations, representations, and conclusions drawn from the data are based on sound geological principles and current best practices. These maps and figures have been reviewed for accuracy and completeness in accordance with established geological standards and methodologies.

Any non-geoscience work such as engineering diagrams, well designs or plugging diagrams in this permit are not covered under this stamp. Those are stamped separately by a professional engineer (P.E.) licensed in the State of Texas. This P.E. stamp may be found in Permit - **Section 3**.

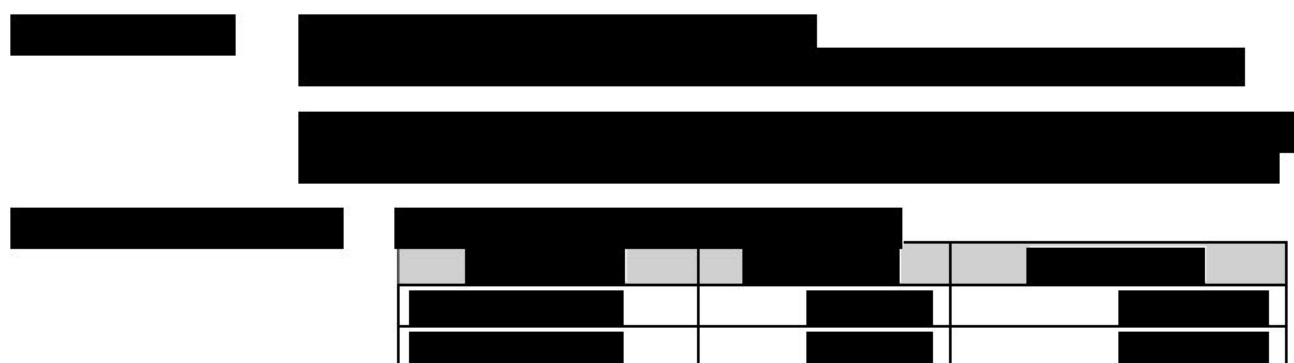
The seal appearing on this document was authorized on 7/31/2024 by



## 1.0 SITE CHARACTERIZATION [40 CFR 146.82 (a);] [40 CFR 144.31(e)(1-6)]

### 1.1 Facility Information [40 CFR 146.82 (a)(1)]

Facility Name: Central Loving Facility



Field Name: Phantom, TRCC District 8

Facility Address: Milestone Carbon –

(Injection Wells)

Owner and Operator Information: Milestone Carbon Delaware CCS Hub, LLC  
840 Gessner Rd. Suite 600 Houston, TX 77024  
Front Desk Phone: 832-739-6700  
Privately Held Delaware Limited Liability Corporation

SIC Codes: 4953 – Refuse Systems  
8999 – Environmental Consulting

**Key Terms.** For the purposes of this permit application, the following terms and their relationship to the proposed Class VI well application are as follows:

- Milestone Carbon Delaware CCS Hub, LLC (Milestone) – The Operator and “Operational Area” (including the Facility and the Wells), referred hereafter simply as “Milestone”



## 1.2 Project Introduction [40 CFR 146.82 (a)(1)]

Milestone Carbon Delaware CCS Hub, LLC (Milestone) is submitting this application to request authorization of the construction and operation of [REDACTED] Class VI Underground Injection Control (UIC) wells in Loving County, Texas. The proposed Delaware CCS #1 and Delaware CCS #2 carbon capture and sequestration (CCS) Class VI wells (the Wells) will be sited within the Milestone Central Loving Facility and will be designed to inject carbon dioxide (CO<sub>2</sub>) from nearby oil and gas processing sources, power plants and cement plants, into deep underground brine aquifer formations to sequester it safely and permanently.

Milestone has extensive experience with slurry injection and landfill operations associated with energy waste in [REDACTED]. Accordingly, Milestone understands both the technical and regulatory obligations associated with responsibly managing project operations in this area. This application demonstrates how Milestone will meet all applicable regulatory and monitoring requirements associated with the proposed Class VI Wells in order to protect underground sources of drinking water (USDW) during pre-construction, pre-injection, operation, and post-injection periods.

Objectives and benefits of the proposed wells include:

1. **Climate Change Mitigation:** Natural gas combustion accounts for 22% of the world's greenhouse gas (GHG) emissions. Sequestering the carbon dioxide (CO<sub>2</sub>) related to these emissions will help mitigate GHG effects on climate change. The Permian Basin, as one of the largest oil and gas producing provinces in the United States, emits approximately 60 million metric tonnes (MMta) of CO<sub>2</sub> annually (IEA, 2020 Report).
2. **Energy Security:** The Facility will help to ensure energy security by enabling the continued use of fossil fuels while reducing GHG. The Texas electricity market has one of the narrowest supply vs demand ranges in the USA. Therefore, disruptions in energy can have catastrophic effects on property and life in the state (Electric Reliability Council of Texas (ERCOT) Website, 2023).
3. **Economic Development:** The Facility will support economic development by creating new jobs in the area related to construction, including injection well, monitoring well, pipeline, and capture facility construction. Additional oil and gas service industry jobs related to remote monitoring and well logging will be created/retained.
4. **Technological Advancement:** The Facility will help to advance the carbon sequestration industry by demonstrating the effectiveness of long-term brine aquifer CO<sub>2</sub> sequestration while minimizing risk to USDWs in the area. Novel techniques and process efficiencies are likely to be discovered during injection and monitoring operations.

Milestone proposes to inject [REDACTED]

[REDACTED] There is a total of 16.6 MMta of emissions within a radius of 30 miles (Emissions Source: Enverus, 2024). Table 1-1 shows a summary of operational parameters. Additional information on operational parameters may be found in permit Section 4.

Milestone will be the owner and operator of the Wells and Facility. [REDACTED]

The Railroad Commission of Texas (RRC) Groundwater Advisory Unit (GAU) provides Groundwater Protection Determinations for surface casing, underground injection and other underground activities.

The GAU has determined the base of USDW is estimated to occur at a depth of [REDACTED] within the area of the Facility (GAU Determination letter, **Section 13 Appendix I**). The top of the Injection Interval, [REDACTED] of the lowest known USDW. Additional information on local aquifers, salinity, and water chemistry is detailed subsequently in **Sections 1.4, 1.9 and 1.11**. An Aquifer exemption will not be required.

The project is not located on, or near, Indian lands or Indian reservations. The nearest Indian reservation is the Mescalero Apache reservation. The reservation is located over 150 mi away, within New Mexico, northwest (NW) from the calculated Area of Review (AoR).

Milestone holds no known prior Resource Conservation and Recovery Act (RCRA), Federal UIC, National Pollution Discharge Elimination System (NPDES) or Prevention of Significant Deterioration (PSD) permits.

A list of applicable federal, state and local contacts within the AoR can be found in **Table 1-2** [40 CFR 146.82(a)(20)]. A list of non-UIC federal, state and local permits can be found in **Table 1-3** [40 Code of Federal Regulation (CFR) 146.82 (a) (1)] and a list of all Injection and Monitoring Well Coordinates is found in **Tables 1-1 through 1-4**.

[REDACTED]	[REDACTED]	[REDACTED]	[REDACTED]
[REDACTED]	[REDACTED]	[REDACTED]	[REDACTED]
[REDACTED]	[REDACTED]	[REDACTED]	[REDACTED]
[REDACTED]	[REDACTED]	[REDACTED]	[REDACTED]
[REDACTED]	[REDACTED]	[REDACTED]	[REDACTED]

[REDACTED]	[REDACTED]	[REDACTED]	[REDACTED]
[REDACTED]	[REDACTED]	[REDACTED]	[REDACTED]
[REDACTED]	[REDACTED]	[REDACTED]	[REDACTED]
[REDACTED]	[REDACTED]	[REDACTED]	[REDACTED]
[REDACTED]	[REDACTED]	[REDACTED]	[REDACTED]
[REDACTED]	[REDACTED]	[REDACTED]	[REDACTED]
[REDACTED]	[REDACTED]	[REDACTED]	[REDACTED]
[REDACTED]	[REDACTED]	[REDACTED]	[REDACTED]
[REDACTED]	[REDACTED]	[REDACTED]	[REDACTED]
[REDACTED]	[REDACTED]	[REDACTED]	[REDACTED]
[REDACTED]	[REDACTED]	[REDACTED]	[REDACTED]
[REDACTED]	[REDACTED]	[REDACTED]	[REDACTED]
[REDACTED]	[REDACTED]	[REDACTED]	[REDACTED]

Term	Organic (%)	Natural (%)	Artificial (%)
GMOs	75	75	15
Organic	85	85	10
Natural	85	85	10
Artificial	75	75	50
GMOs	75	75	15
Organic	85	85	10
Natural	85	85	10
Artificial	75	75	50
GMOs	75	75	15
Organic	85	85	10
Natural	85	85	10
Artificial	75	75	50
GMOs	75	75	15
Organic	85	85	10
Natural	85	85	10
Artificial	75	75	50
GMOs	75	75	15
Organic	85	85	10
Natural	85	85	10
Artificial	75	75	50

## 1.3 Overview Maps of AoR [40 CFR 146.82(a)(2)]

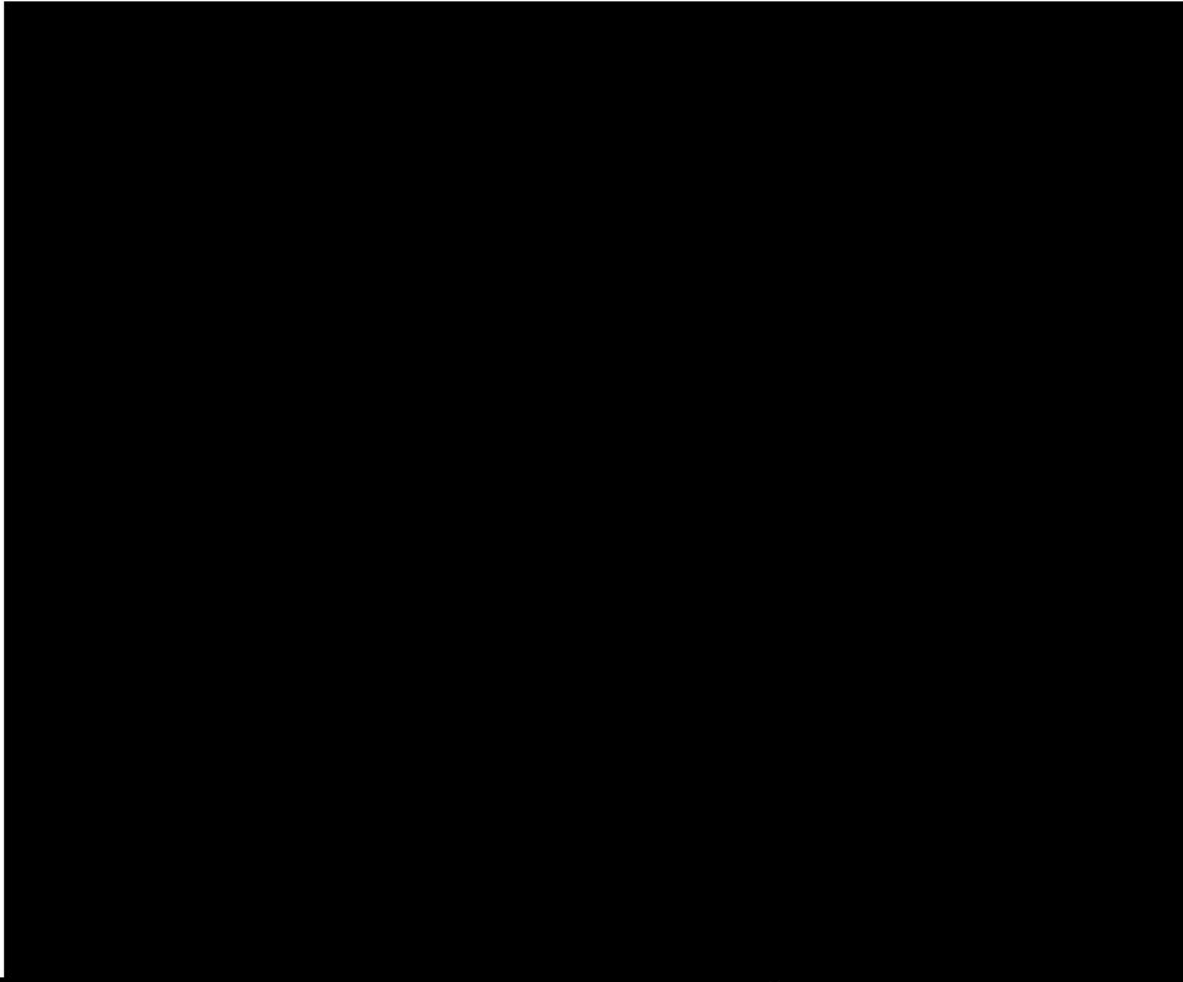
**Figures 1-1 through 1-7** show the proposed Well location, along with all pertinent items listed in 40 CFR 146.82(a)(2). This information is separated into various maps for ease of reference and discussion. An omnibus map encompassing every element in this section is found in **Section 1.3.6**. Due to the difficulty of reading well names for the large amount of water wells, and oil and gas wells above the injection zone, these wells have been indexed into tables in **Section 1.14, Tables 1-29 and 1-30**. Each existing non-project well is denoted by its index number for the remainder of **Section 1.3**. The Area of Review (AoR) is defined in permit **Section 2** based on the geologic model.

### 1.3.1 Major Roads Near Injection Site

The Facility will be situated in the central part of Loving County, Texas. The property on which the Well is located, leased by Milestone, is located at [REDACTED] and is approximately [REDACTED] of the City of Mentone, Texas. It is slightly less than [REDACTED]

[REDACTED] A list of all injection wells and monitoring wells coordinates are found in **Table 1-4** and a map of all injection and monitoring wells is found in **Figure 1-1**.

Due to the lack of population in Loving County, most of the roads are private and, in many cases, unnamed. The roads are utilized by oil and gas operators to maintain infrastructure in the area. The nearest roads to the injection wells are private roads and have not been designated by the county. [REDACTED] (**Fig. 1-2**).  
[REDACTED]



A more regional view of the project area is shown in **Figure 1-2**. A project overview is as follows:

- Mertzon, TX
  - [REDACTED]
  - An unincorporated community and the county seat of Loving County
  - Population of 22 people (source: 2020 census)
- Pecos, TX
  - [REDACTED]
  - Population of 15,193 (source: 2020 census)
  - County seat of Reeves County
  - [REDACTED]
- Orla, TX is [REDACTED]
  - An unincorporated community in northern Reeves County
  - Census data is not available for Orla
  - Population between 2-56 people (reported from various sources)

### 1.3.2 Mines, Superfund Sites, Quarries, Other Hazardous Sites

Within the AoR of the proposed Facility, [REDACTED]

[REDACTED]

Within Loving County, [REDACTED]

[REDACTED]

There are no [REDACTED] within Loving County.

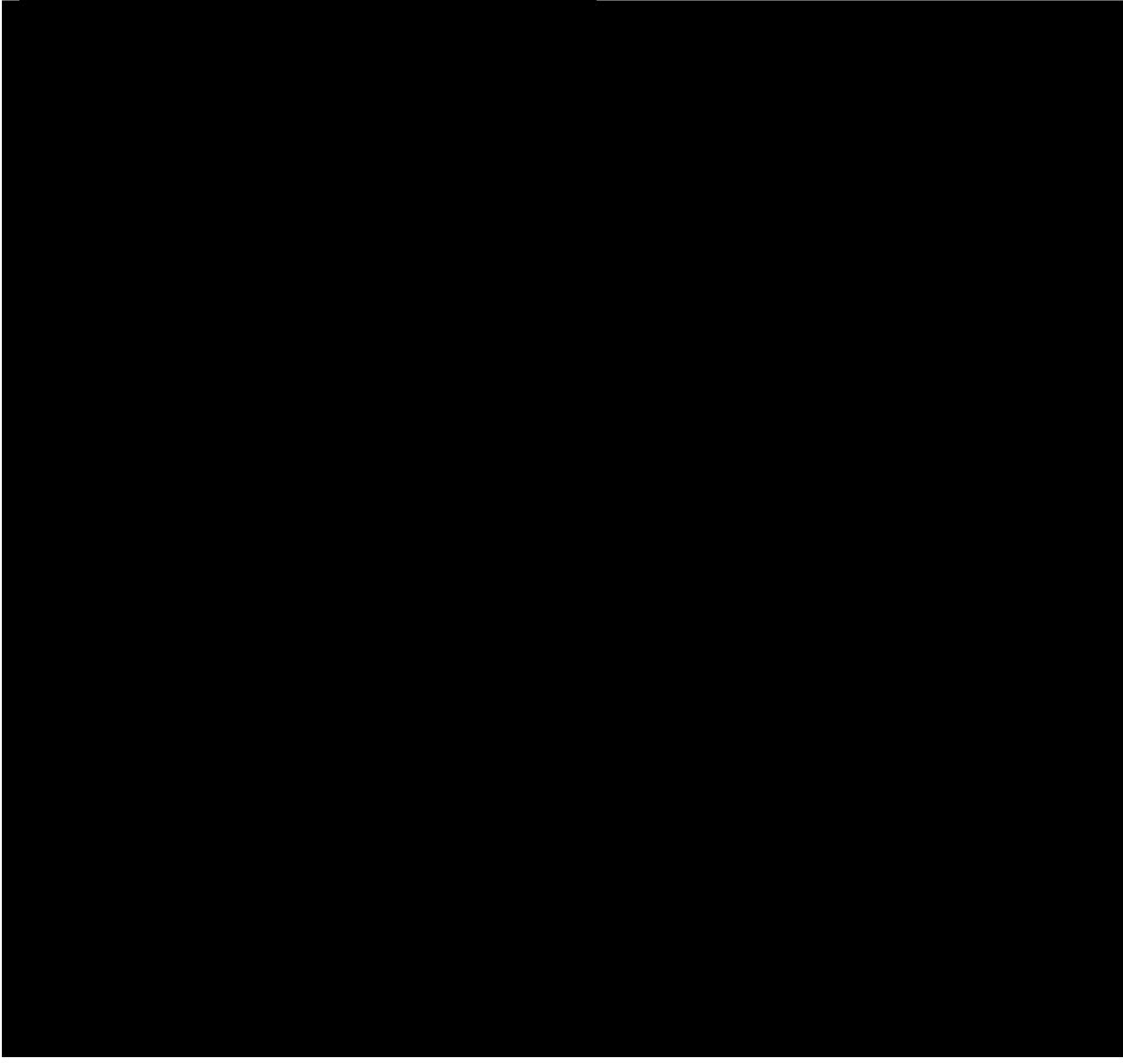
[REDACTED]

### 1.3.3 Map of Rivers, Springs, Wells, Other Water Features

Loving County has a *hot semi-arid* climate based on the Koppen climate classification (Beck, et al. 2018). There are limited natural water sources in the vicinity of the AoR.



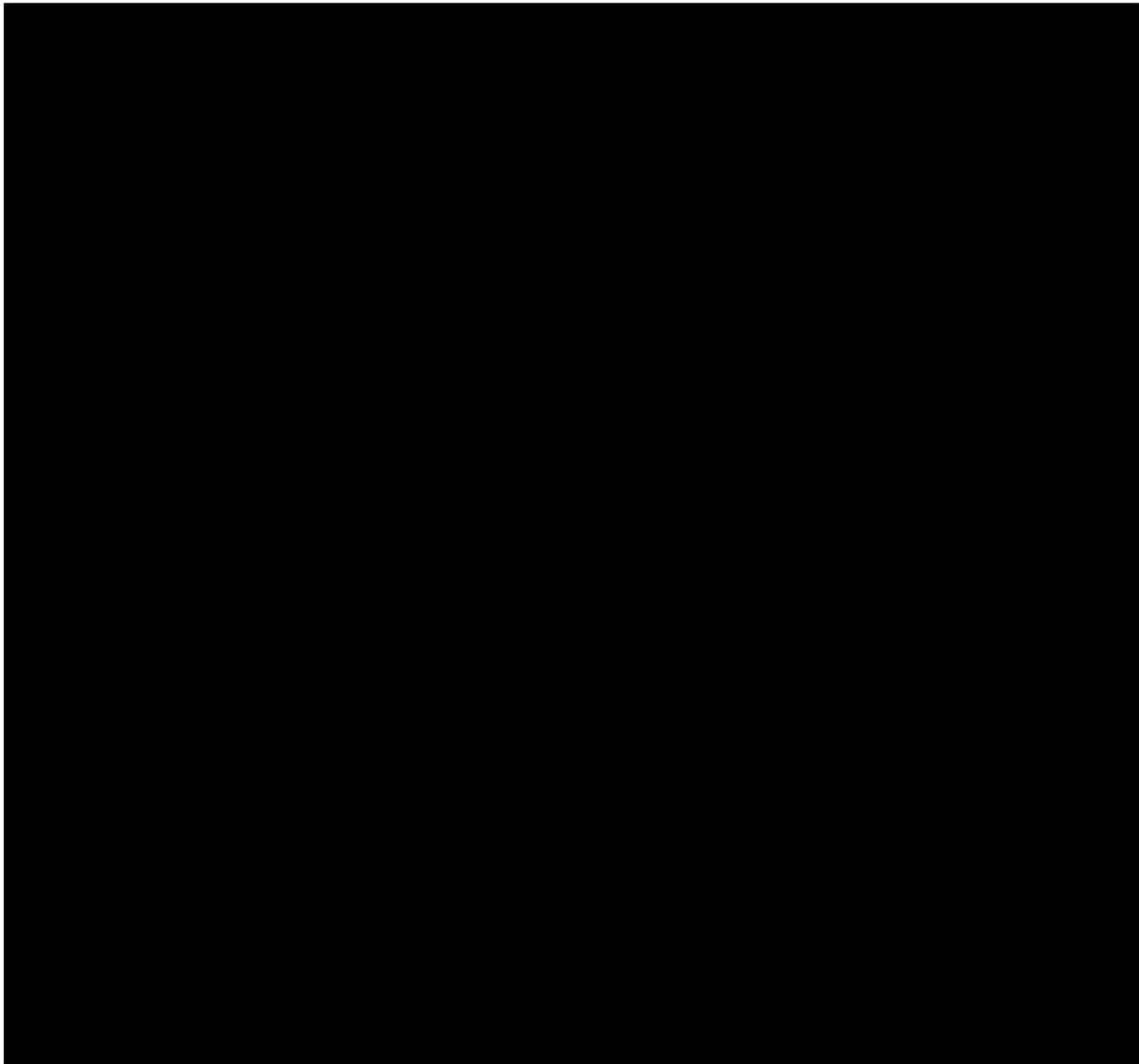
There are a total of [REDACTED] within the AoR and an [REDACTED] of the AoR (Fig. 1-4).



#### 1.3.4 Map of Oil and Gas and Injection Wells in the Area of Review (AoR)



Wells are labeled by an index number used for the remainder of **Section 1**. A table of indexed RRC records for all wells on this map is presented in **Section 1.14.2, Table 1-30**. Wells are indexed based on [REDACTED] being lowest index number and [REDACTED] being highest index number. Complete RRC files can be found as an appendix attachment [REDACTED]



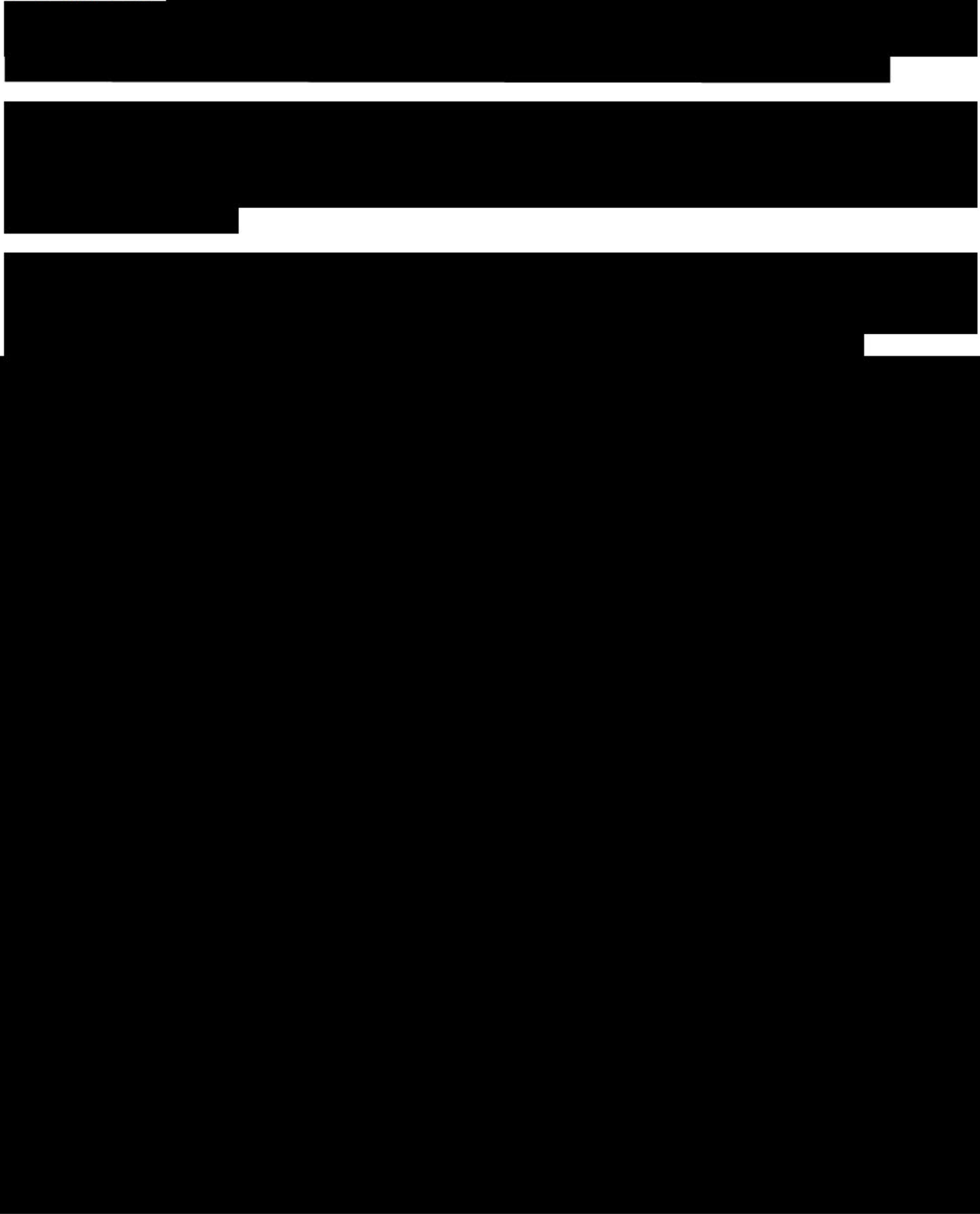
### 1.3.5 Map of Buildings in the Area of the Wells

There are [REDACTED] permanent inhabited structures in the AoR. There are [REDACTED]



### 1.3.6 *Omnibus Map [40 CFR 146.82(a)(2)]*

The information contained in **Sections 1.3.1 through 1.3.5** is referenced on the map, **Figure 1-7**. Water Wells and Oil and Gas Wells are labeled using the index numbers found **Section 1.14, Tables 1-29 and 1-30**.



#### 1.4 Regional USDW Characterization and Hydrogeology [40 CFR 146.82(a)(3)(vi), 146.82(a)(5)]

This section describes the general vertical and lateral limits of all Underground Sources of Drinking Water (USDW), water wells and springs within the AoR, their positions relative to the injection zone, and the direction of water movement, where known.

The Texas Railroad Commission Ground Water Advisory Unit (RRC GAU)

See Section 3 for a full description of casing sizes, depths and cement.

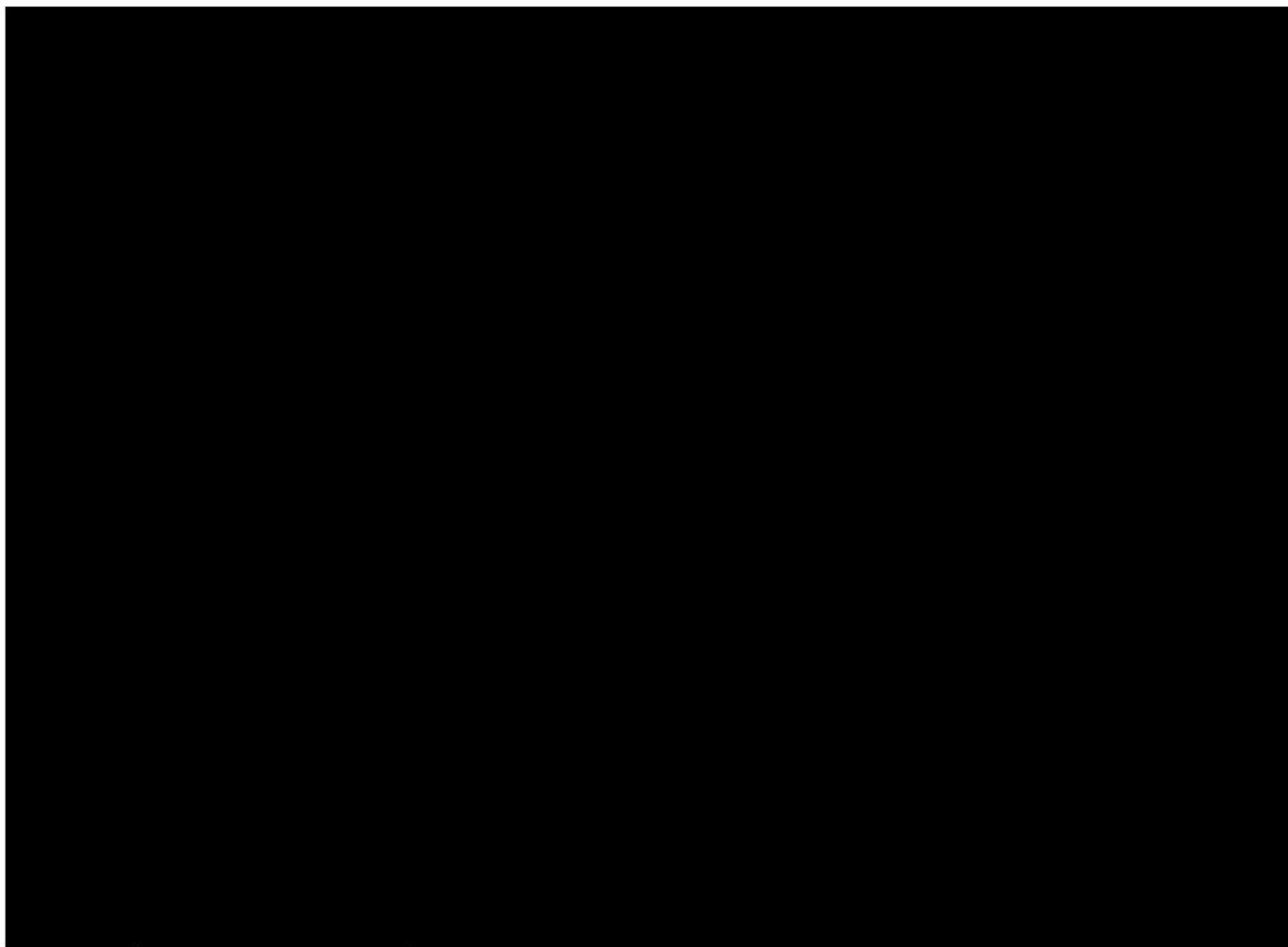
The 2011 and 2016 Aquifers of Texas Report by the Texas Water Development Board (TWDB) identified two aquifers in the vicinity of the AoR:

(Fig. 1-9) The AoR is not within a ground water conservation district.

In central Loving County, the principal source of drinking water is the [REDACTED] [REDACTED] which is a shallow freshwater aquifer located at depths of <700 feet below the surface. This aquifer is unconfined and recharged by rainfall and is used for domestic, agricultural, and industrial purposes in the county.

A secondary source of drinking water occurs within the [REDACTED] minor confined [REDACTED] [REDACTED]. It

recharges primarily from rainfall and transfers from adjacent aquifers. It primarily produces brackish hard water and has [REDACTED]. Due to inferior water quality compared to [REDACTED], it is generally not utilized for water production in western Loving County.



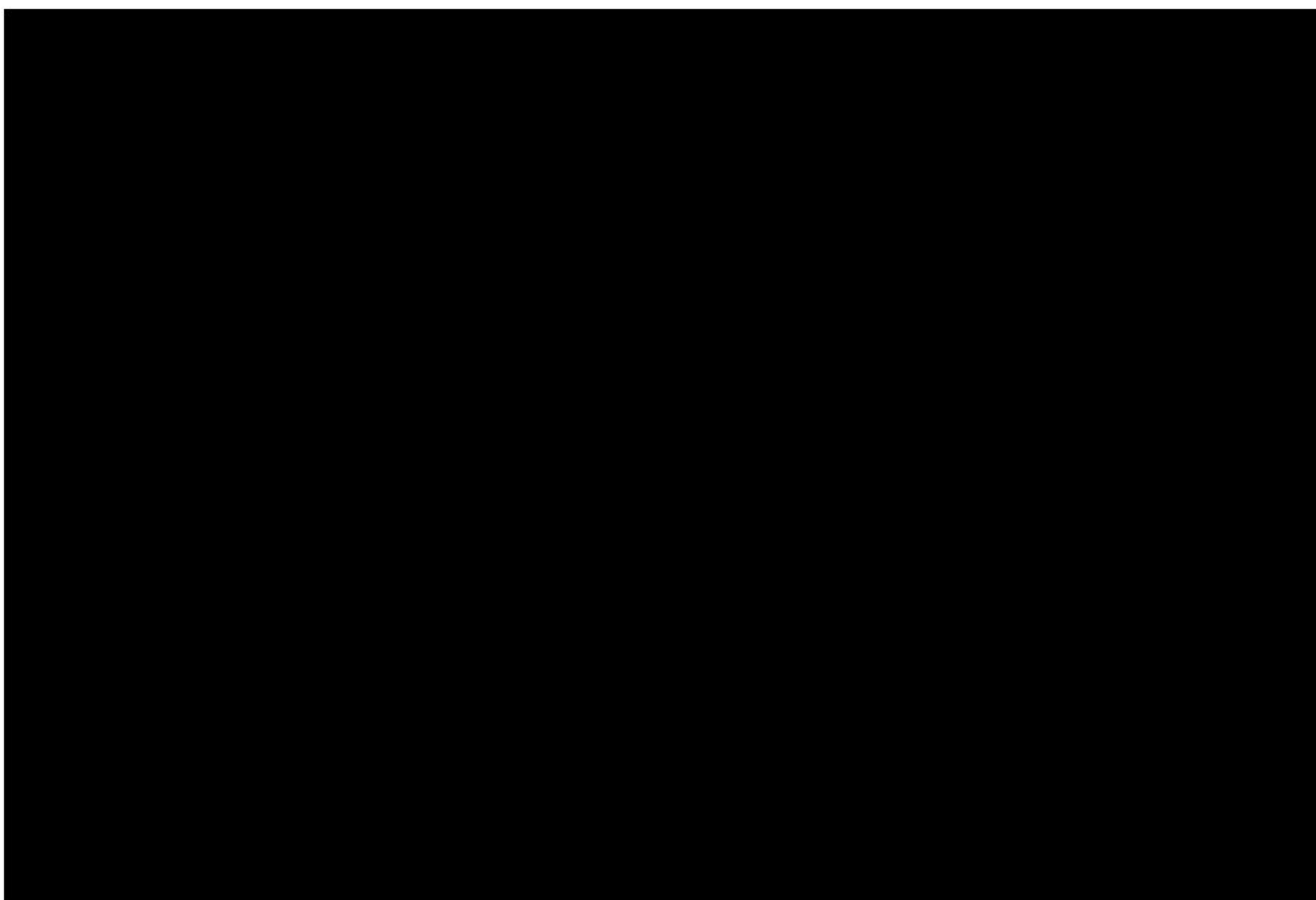
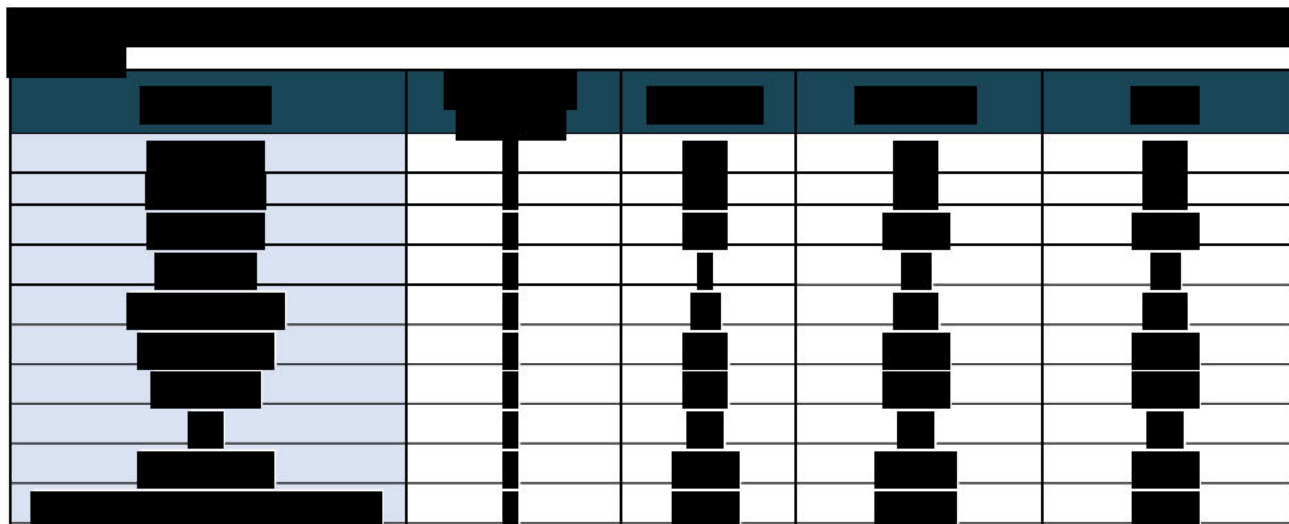
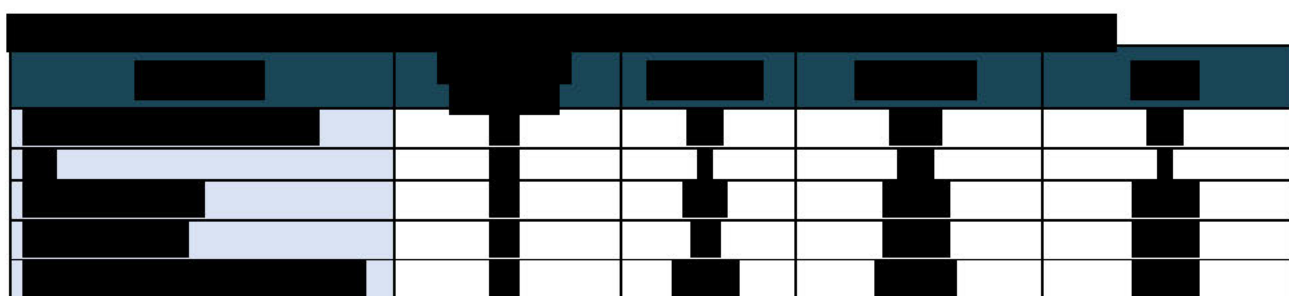
1.4.1 [REDACTED]

[REDACTED]

[REDACTED] is comprised of unconfined Cenozoic alluvial and aeolian deposits filling several structural basins, the largest of which are the [REDACTED]

[REDACTED]. Thickness of the alluvial and aeolian fill reaches [REDACTED] and freshwater saturated thickness averages about [REDACTED]. The aquifer is primarily recharged by rainfall in the summer months. (TWDB Report 2016).

The water quality of the [REDACTED] is highly variable, the water being typically hard, and generally [REDACTED]



More than 80 percent of groundwater pumped from the aquifer is used for irrigation, and the rest is withdrawn for municipal supplies, industrial use, and power generation. Localized water level declines in south-central Reeves and northwest Pecos counties have moderated since the late 1970s as irrigation pumping has decreased. In Loving County, the water level is shown to be relatively flat with a change of [REDACTED]

[REDACTED]

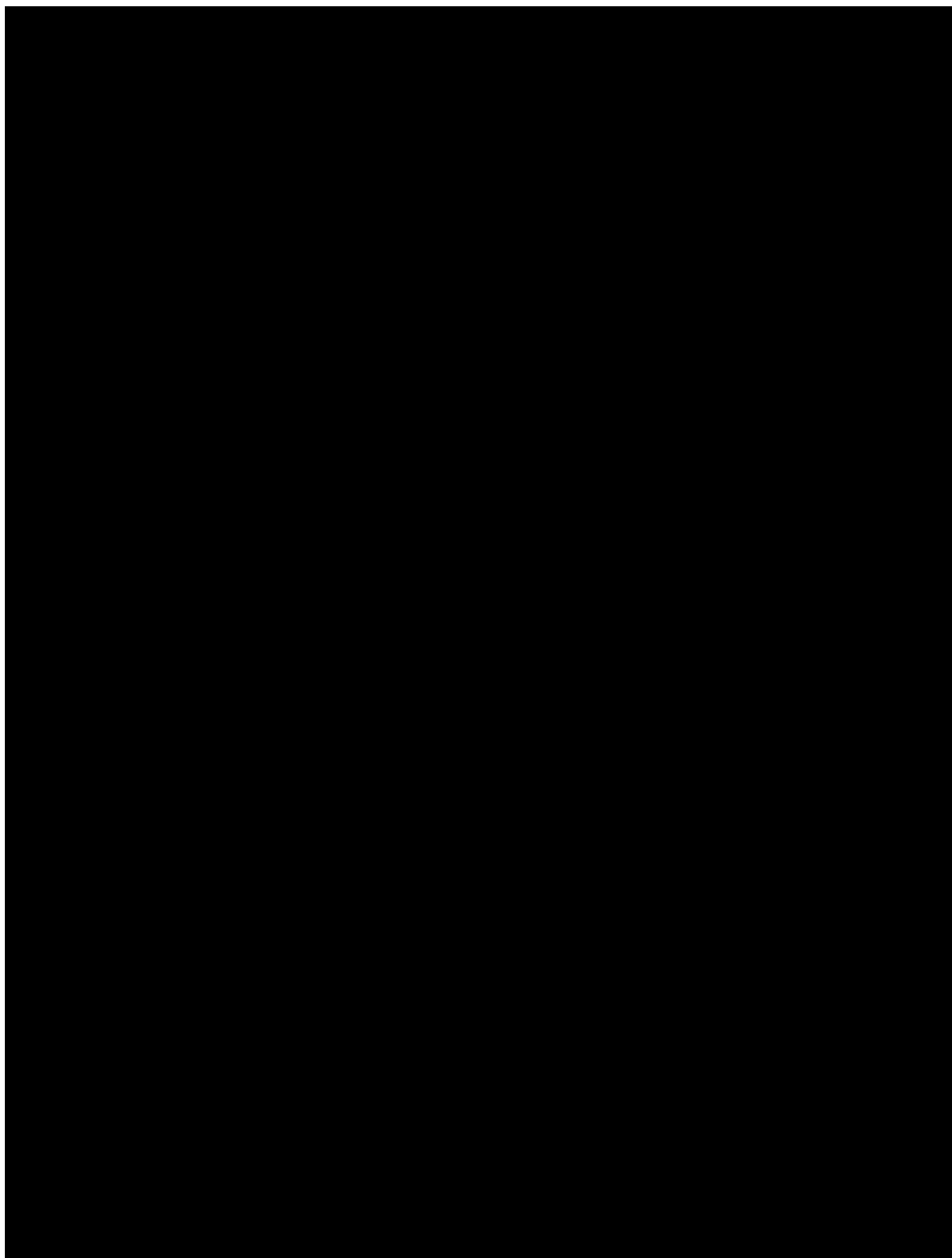
Total storage of the [REDACTED] is estimated to be more than [REDACTED], with recoverable storage estimated between [REDACTED]. The hydraulic conductivity in central Loving County in the [REDACTED] is reported as [REDACTED]

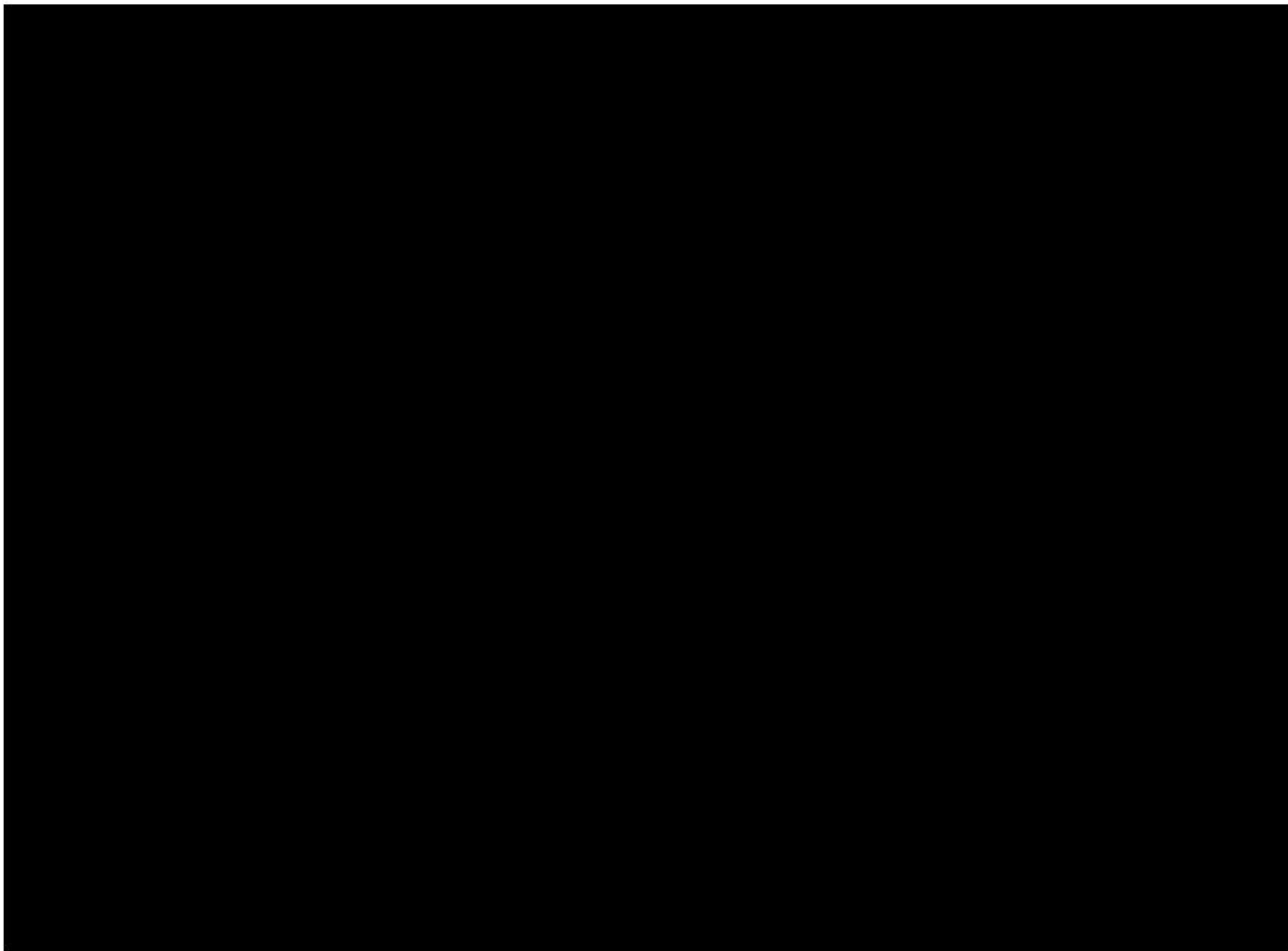
[REDACTED]

[REDACTED]

[REDACTED]







A distribution of water wells showing percent penetration into the [REDACTED] is shown in **Figure 1-15** (next page). Wells colored green and yellow near the AoR, due to the expanded aquifer thickness, [REDACTED]

The area around the AoR appears to have a regionally thicker [REDACTED]

[REDACTED] . The study indicates alluvium filling this local thickening of the aquifer from all directions. [REDACTED]

[REDACTED]

[REDACTED]

[REDACTED]

[REDACTED]

Recharge takes place by cross-formational flow from adjacent aquifers and percolation of surface water through the outcrop west of the [REDACTED]. Discharge is predominantly from wells and cross formational flow into overlying aquifers such as [REDACTED]

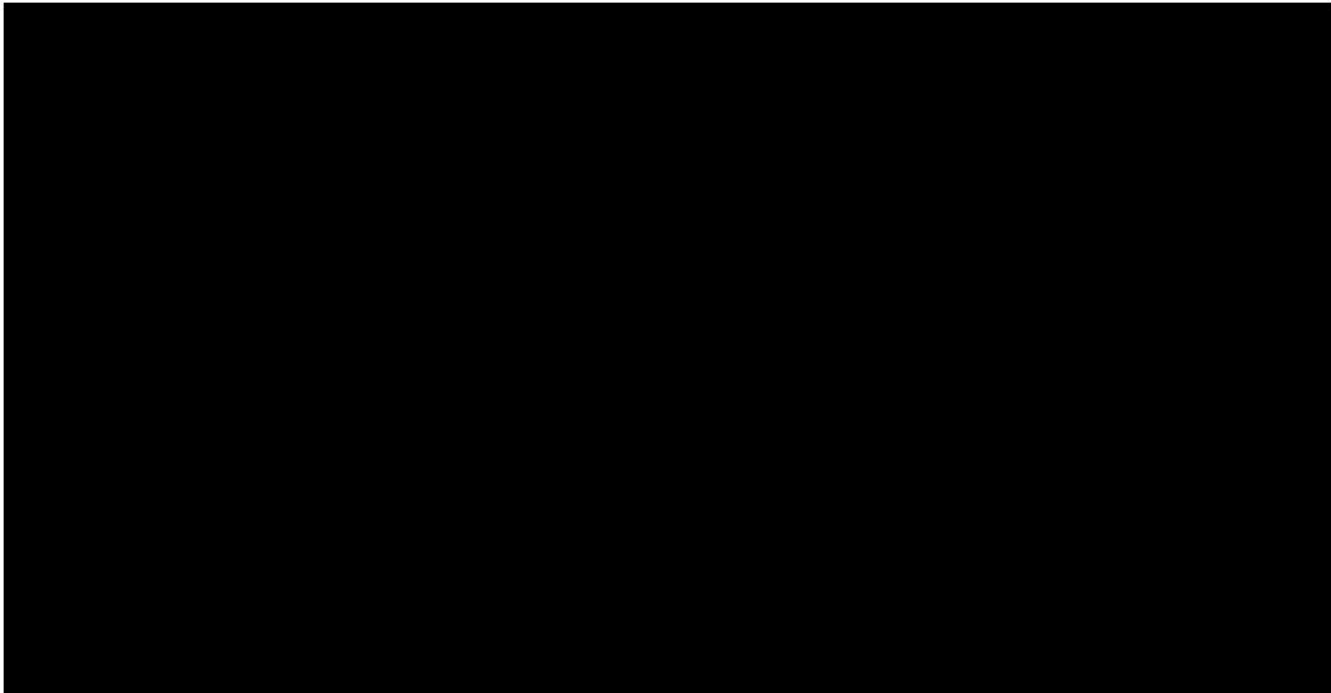
[REDACTED]

The formation yields moderate to large quantities of fresh to brackish water primarily from solution openings in its upper section. [REDACTED]

According to [REDACTED] the median horizontal hydraulic conductivity in the area around Loving and Ward Counties is [REDACTED], the median vertical hydraulic conductivity is [REDACTED] and the specific storage is [REDACTED]. Aquifer permeability and porosity are expected to be low except where it has been enhanced by fracturing or dissolution. [REDACTED]

According to the TWDB, [REDACTED]





Water-level data for the [REDACTED] is very sparse. Historically, no more than [REDACTED] have been measured throughout the aquifer in any given year. The areal distribution of the wells with water-level measurements made it impossible to contour an aquiferwide potentiometric surface map.

[REDACTED]

[REDACTED]

The potentiometric and water flow diagrams from [REDACTED] show flow generally to the south from [REDACTED] and point to an increasing depth of water level in an [REDACTED] Data on water flow in the [REDACTED] is not available

[REDACTED]

[REDACTED]

[REDACTED]



#### 1.4.3 RRC GAU Determinations

The Texas Railroad Commission (RRC) Ground Water Advisory Unit (GAU) determination of the base of underground sources of drinking water (USDW), [REDACTED]

[REDACTED] These determinations hold within 200 ft laterally to the proposed well locations. The RRC determines a *minimum depth of vertical isolation* that is deeper than the depth of USDW. It is a standard industry practice to set pipe approximately 150-200 feet below this *minimum depth of vertical isolation*. Milestone well construction details are found in permit **Section 3**.

The RRC determined that injection, into the Injection Interval defined in **Section 1.1**, will not endanger protected water strata at the proposed location(s) based on the information provided when submitting the GAU letter request.

#### 1.4.4 Springs in Loving County

There are [REDACTED] springs in Loving County:

[REDACTED] Records of water chemistry, rate or source-aquifer were not available from TWDB at the time of the application.

## 1.5 Regional Geology Background [40 CFR 146.82(a)(3)(vi)]

The proposed facility is located in the eastern portion of the Delaware Basin within the larger Permian Basin, as seen in **Figure 1-22**. The Delaware Basin is the major western structural subdivision of the Permian Basin and is contained by the Central Basin Platform to the east, the Capitan Reef/Northwest Shelf to the north, the Ouachita Fold Belt to the south, and the Diablo Platform/Guadalupe Mountains to the west.



**Note:** An extensive treatise on Permian geology and the deep Paleozoic formations of interest was published by Ruppel et al., 2008, 2019. These are included as an appendix item (permit **Section 13**). This section is meant to summarize the regional characteristics of Injection Interval formations or adjacent formations. For detailed local characteristics, see subsequent sections **Section 1.6** onward.



### 1.5.1 Stratigraphy

The proposed [REDACTED]

A generalized stratigraphic column for the Delaware is shown in **Figure 1-23** and **Figure 1-24** (2<sup>nd</sup> from left). Omitted from this column (since it is regional) are Cenozoic Pecos Valley and Rustler aquifers which are described in **Section 1.4** and are included in the USDW resources in the area. [REDACTED]

[REDACTED] Below the aquifer zones, and forming a no-flow boundary, are the Ochoan-aged Salado and Castille Formations. The Castille contains massive evaporites that cap and vertically seal the Guadalupian-aged Delaware Mountain Group (DMG). Below the Ochoan, the Guadalupian-aged DMG is found. The DMG is composed of three formations, the Bell Canyon, Cherry Canyon and Brushy Canyon.

Originally, these DMG sands produced oil and gas and were drilled from the 1930s until about 1960. In the modern era, since they are depleted of pressure, they are used to dispose of large amounts of produced brine from Wolfcamp and Bone Spring Formations.

Within the Leonardian-aged rock is the Bone Springs which is typically subdivided into the first, second and third carbonates and sands. The top of the Bone Springs is often called the Avalon Shale. It is not listed on the stratigraphic column; it is a subdivision of the Bone Springs first carbonate. It is the organic shale at the top of the Bone Springs that is a prolific producer in Lea County, New Mexico just north of the Facility.

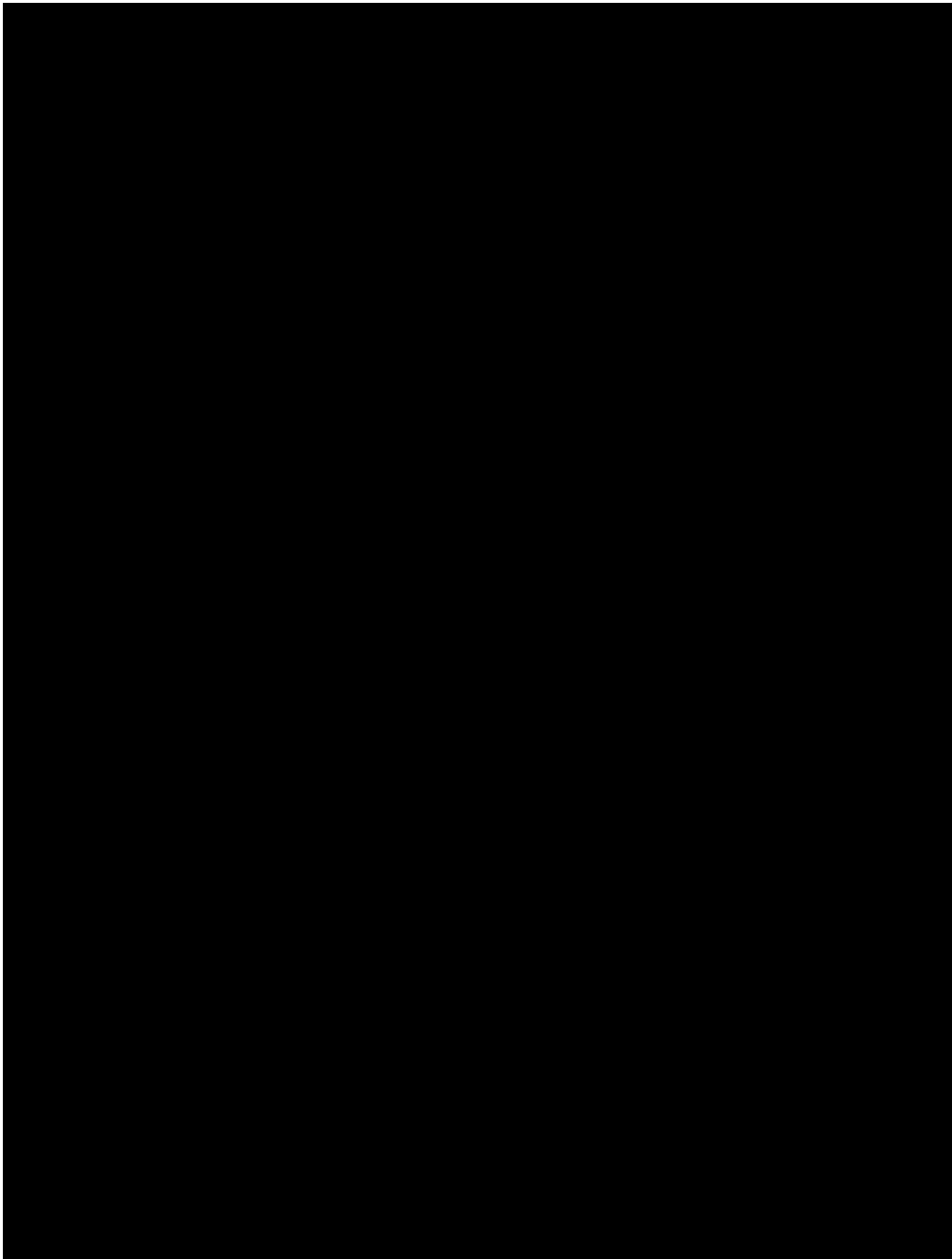
Below the Bone Springs, the Wolfcamp shale occurs. It is often broken into the following members, Wolfcamp X-Y, Wolfcamp A, Wolfcamp B, Wolfcamp C, Wolfcamp D. It is the last Permian-aged formation in the section. The Wolfcamp is a sequence of organic shales, sands and carbonates and is a prolific oil and gas producer in the region owing to its high thickness, porosity and organic content.

Below the Wolfcamp, starts the Pennsylvanian section of rock. The Pennsylvanian-aged Cisco and Canyon form a sequence of argillaceous shales and the Strawn and Atoka are predominantly carbonate benches. The Morrow sand may occur below the Atoka. It is often observed in eastern Loving County as part of ancient delta complex and is a gas producer. Following this, the Upper Mississippian Barnett Shale is present, which is equivalent to the Barnett Shale in the Fort Worth Basin. This is underlain by the Mississippian lime, a tight carbonate that overlays the organic Woodford Shale. [REDACTED]

Below the Woodford is an unconformity and undifferentiated Devonian section which is primarily packstone but is dolomitized in Lea County, NM. At the base of the Devonian is the Thirtyone Formation and then the Silurian Wristen Group. Below the Wristen Group is the Fusselman, the Montoya Formations and the argillaceous and organic Simpson Group which is expected to act as a secondary seal within the Injection Interval. Below the Simpson is [REDACTED] the Ellenburger Group which is a fractured dolomite that has undergone extensive periods of subaerial exposure and cave collapse (**Fig. 1-23, 1-24**).

Finally, at the base of the section, right above basement, is the Cambrian Wilberns and Bliss sand. [REDACTED]





The Atoka Shale is expected to occur directly above the Barnett Shale [REDACTED]. In parts of eastern Loving County, the Morrow sand is found between the Atoka and the Barnett Shale, [REDACTED]. The interval of Mississippian-aged rock with high gamma ray is referred to as the Barnett Formation (see type log in **Section 1.9**). The Barnett Shale sits above a section of low gamma ray which is unnamed but referred to colloquially as the "Mississippian Lime" which is in turn underlain by the Woodford Shale (**Fig. 1-23**) in most parts of the Delaware Basin (Ruppel et al., 2008).

The Barnett Formation of the Delaware Basin comprises two end-member lithologies: a carbonate dominated section in Northern Lea and Eddy County, NM and a siliciclastic-rich shale section in Southern Lea and Eddy and also the Texas portion of the Delaware Basin. Underlain by a basal carbonate (Ruppel et al., 2008).

The Mississippian system is one of the most poorly known depositional successions in the Permian Basin. This is largely due to the fact that only small volumes of oil and gas have been produced from these rocks and there has thus been little interest in collecting data to interpret them. This has recently changed due to the successful development of the Barnett Formation in the nearby Fort Worth Basin as a reservoir of natural gas [REDACTED]. A contributing factor to poor understanding of the Mississippian section is the abundance of washouts on well logs due to smectite rich clays.

The total Mississippian thickness varies widely across the Permian Basin area. A maximum thickness of more than 2,200 feet was reported by Craig and Connor (1979) in parts of Reeves and Ward Counties, Texas. The Mississippian section can be <500 feet thick in areas of New Mexico where it transitions to a carbonate facies. There are no Barnett Shale pinchouts in Loving County (**Fig.1-25**).

The mineralogy of the Barnett Shale is primarily quartz, calcite, smectite, and illite in roughly equal abundance. Higher gamma ray intervals increase clay and quartz minerals at the expense of carbonate minerals. Organic matter is present and indicated by intervals of high gamma ray and lower density. The shales are generally very fine-grained with nearly no distinguishable grains without the aid of electron microscopes.

The Barnett Shale in the Delaware Basin is additionally characterized by extreme overpressure. Mud weights while drilling through the Barnett Shale often exceed 17 lb/gal (Bethancourt, 1977). Additional discussion is found in **Section 1.10**. [REDACTED]

In the Delaware Basin, the Barnett Shale is often broken up into the Upper Barnett Shale (Sometimes referred to simply as Barnett Shale) and the Lower Barnett Shale. The Upper Barnett is characterized by medium high gamma ray, low resistivity (1 to 2 ohm-m) and extensive washouts on porosity logging tools. The Lower Barnett is characterized by higher gamma ray, higher resistivity (20-30 ohm-m), lower thorium counts and higher organic matter. [REDACTED]

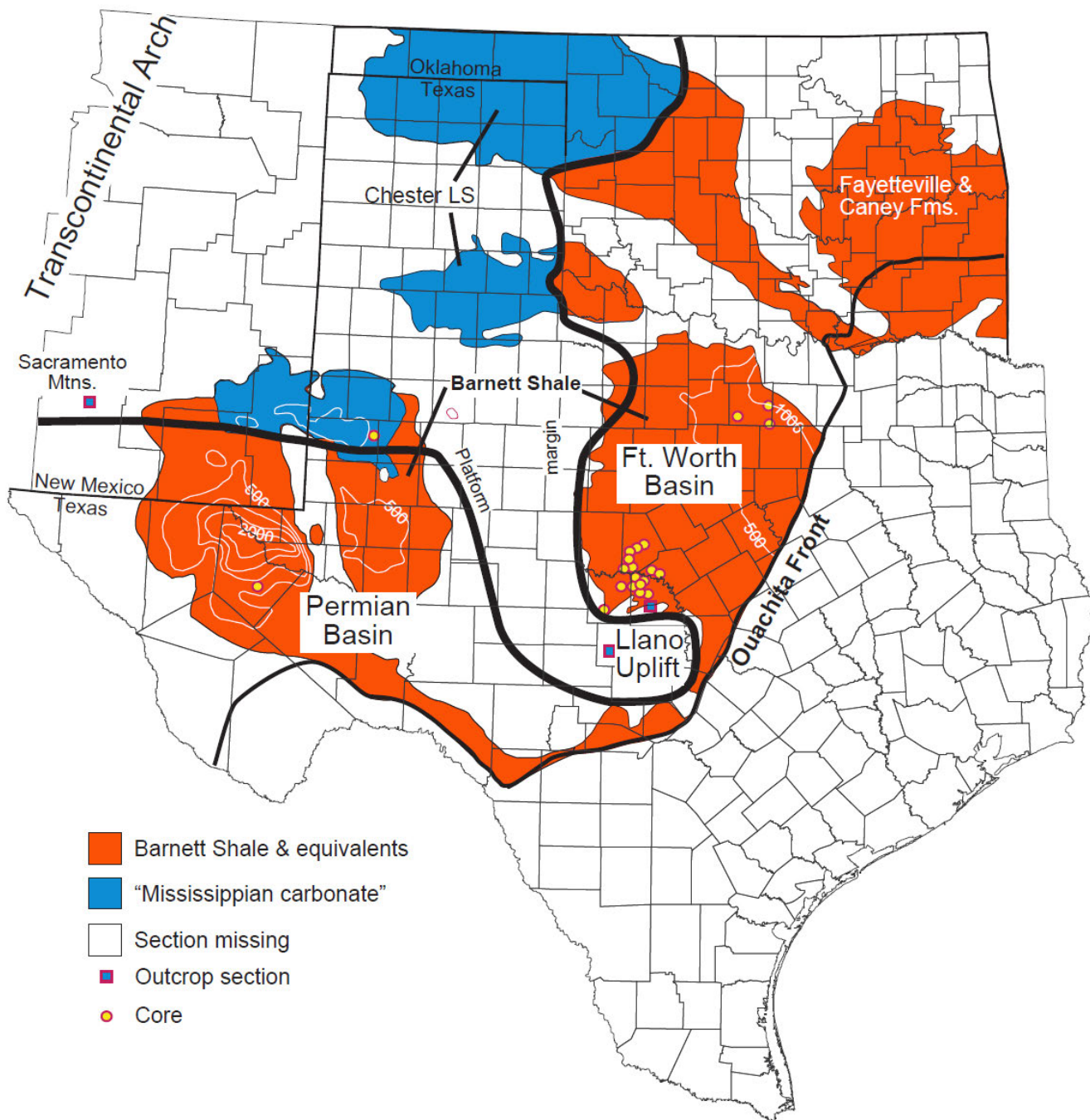


Figure 1-25: Regional Map of the Mississippian noting facies changes (Ruppel et al., 2008)

### 1.5.3.1 Mississippian Limestone

The unnamed Mississippian-aged Limestone, called the “Miss Lime,” is regionally continuous and found below the Barnett Shale and above the Woodford Shale. Although there is debate on the exact ages, the upper section is Osagean age, sometimes referred to as the Lake Valley Formation. The lower section is Kinderhookian age, sometimes referred to as the Caballero Formation (Broadhead, 2009).

In Loving County, the Miss Lime exhibits very low gamma ray in the Upper Osagean section and is composed of >90% calcite and generally very high resistivity. The Lower Kinderhookian section is characterized by pulses of higher gamma ray and up to 40% illite. There are generally sharp contacts at both the top and bottom of the Miss Lime, several authors have reported these as unconformities (Ellison, 1950, Comer, 1991).

Cores from Gaines County exhibit dark gray to black mudstones that are massive to locally laminated or burrowed. The dark color of these rocks, the absence of megafauna, and limited evidence of infauna indicates they were deposited in a low energy anoxic to dysoxic setting (Ruppel et al., 2008).

It is unknown whether the Mississippian Lime contains natural fractures. If present, they are expected to terminate at the Barnett Shale contact due to the substantial change in pore pressure at the contact. Also, if present, it may be necessary to alter the placement of the packer.

### 1.5.3.2 Woodford Shale

In the Delaware Basin, lithologic, electric log, and sparse faunal data define the Woodford Shale as an Upper Devonian organic shale bounded by unconformities at the top and the base (Comer, 1991). The Woodford Shale exists below the Miss Lime and above the undifferentiated Devonian packstones or dolomites. The unconformity at the base of the Woodford Shale is a major regional unconformity.

Ellison (1950) divided the Woodford Formation into three units using radioactivity, log response, and lithology. The Upper Woodford Shale is defined as brownish-black pyritic fissile shale with few resinous spores and abundant chert. It generally has medium gamma ray response and lower organic matter and clay content. The Middle Woodford Shale is characterized by the highest readings of gamma ray and the most abundant spores. It is generally high in clay and organic matter. The middle unit is also the most widespread unit of the Woodford Shale. The Lower Woodford Shale is characterized as a siliceous shale with few spores, medium chert content, lowest gamma ray and the highest resistivity of the three units (Fig.1-26).

The composition of the Woodford Shale primarily consists of organic matter and illite, and the silt-sized fraction consists of mostly dolomite, quartz, pyrite, mica, feldspar, glauconite, biogenic pellets, spores, and radiolarians. Other types of fossils, including conodonts, brachiopods, trilobites, sponge spicules, and vertebrate debris, were found locally, but only rarely. Organic carbon content in core samples ranges from 1.4 to 11.6 weight percent total organic carbon (TOC), (mean = 4.5 ± 2.6 wt % TOC for 72 samples), or from roughly 4 to 35 volume percent organic matter (Comer, 1991) (Haecker, 2016).

In terms of texture, parallel laminae are the most characteristic feature of black shale. Other distinguishing features include abundant pyrite, fine grain size, black color, and high radioactivity. The black color is caused by high concentrations of pyrite (as much as 13 vol %) and organic carbon (up to 35% by volume). High radioactivity is caused by tetravalent uranium bound in organic matter (R. Comer, 1991), (Haecker, 2016).

The Woodford Shale is a regionally continuous formation extending to all parts of the Permian Basin, with the exception of the Matador Uplift. It ranges from depths of as low as 2,000 feet on the Central Basin Platform to as deep as 21,000 feet below sea level in the Val Verde Basin (Comer, 1991).

Thickness of the Woodford Shale reaches its maximum of 661 feet in the Delaware Basin structural low in western Winkler County (Fig. 1-27). The Woodford Shale has been reported greater than 600 feet thick in southeastern Loving County. The Woodford thickness changes abruptly at large regional faults.

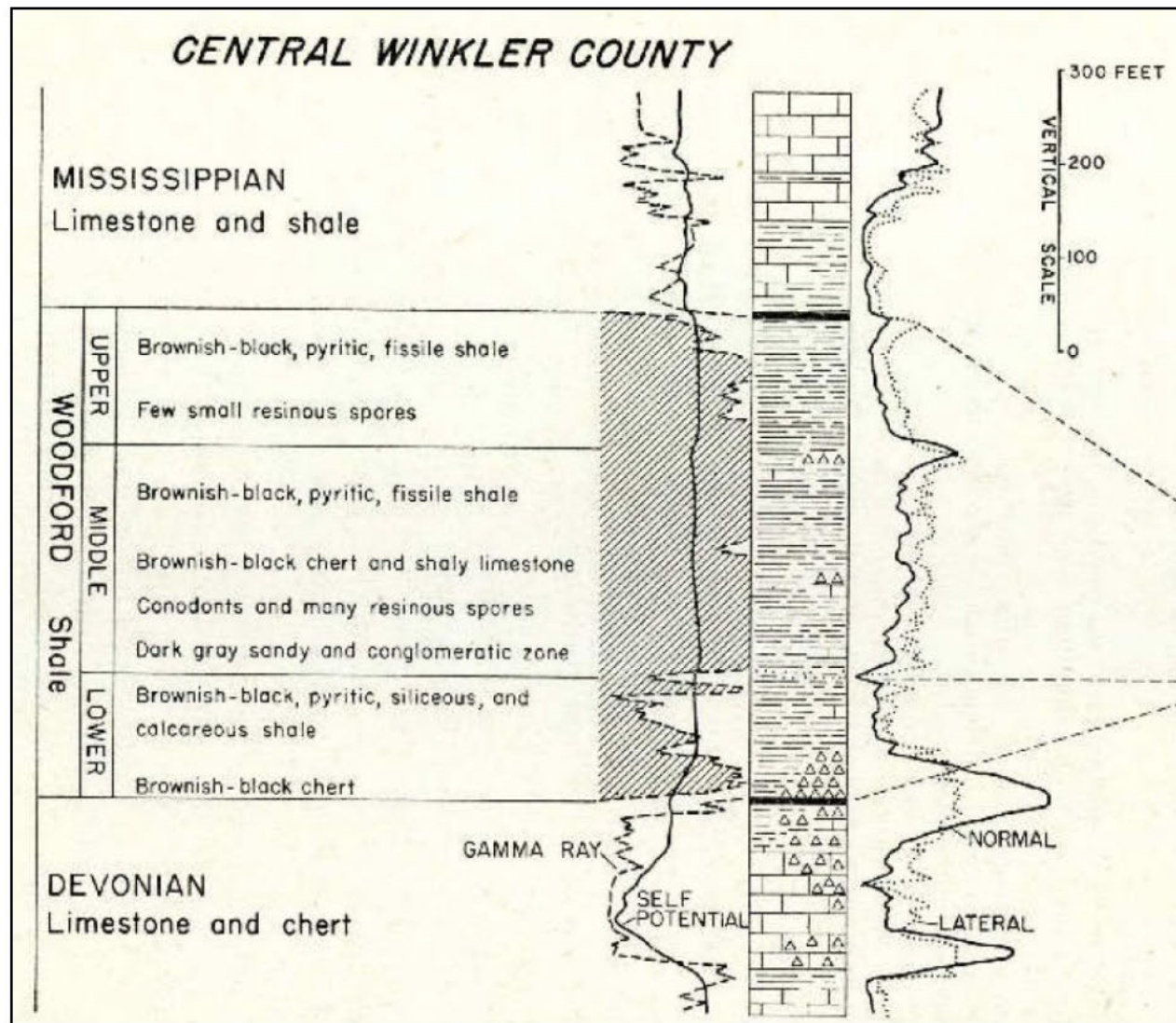
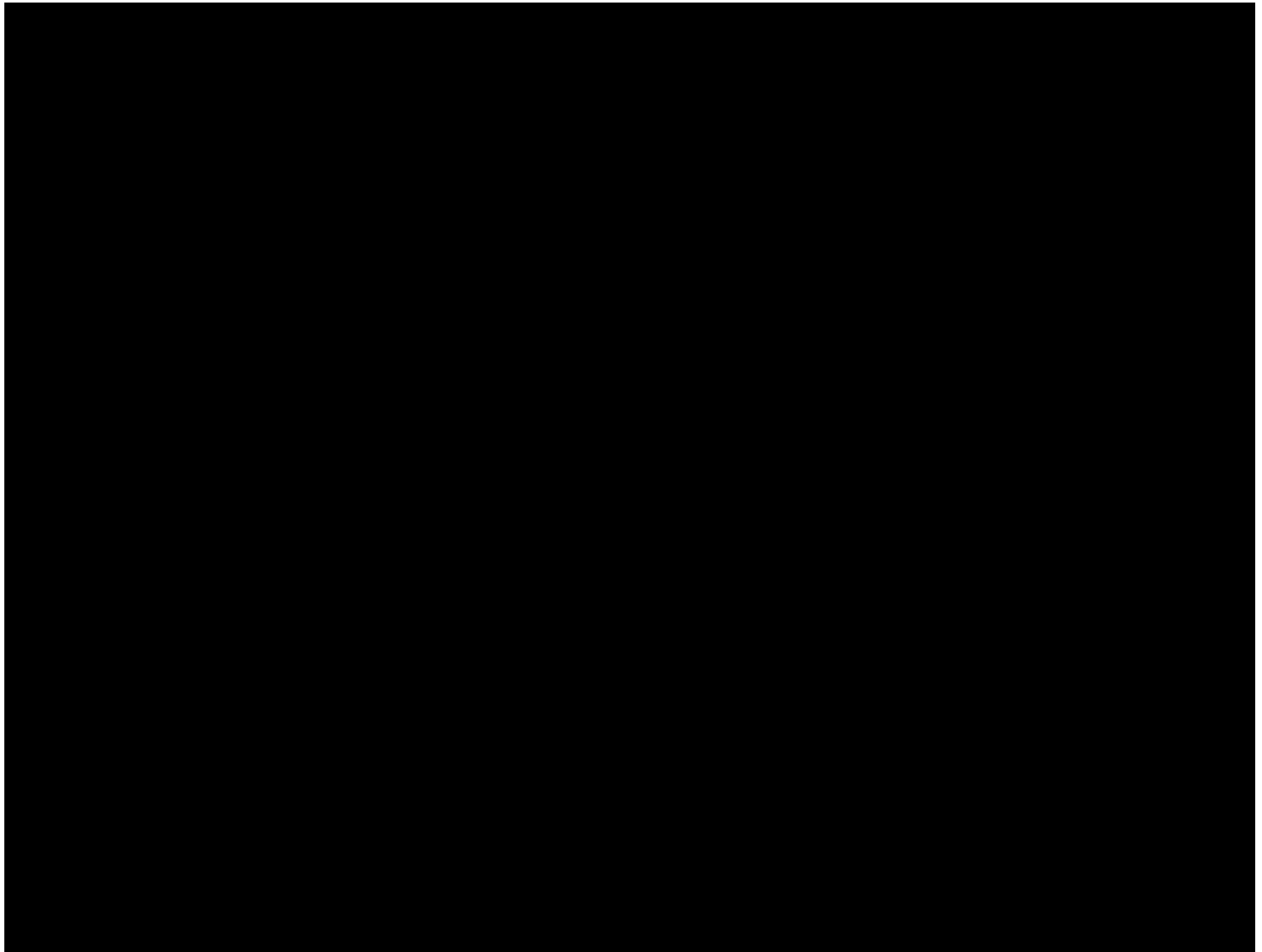


Figure 1-26: Woodford Upper, Middle and Lower definitions (Ellison, 1950)



### 1.5.4.1 Siluro-Devonian Carbonates

The interval defined as the Siluro-Devonian Carbonates extend from the regional unconformity at the base of the Woodford Shale to the top of the Fusselman Formation. This includes the undifferentiated Devonian, the Thirtyone Formation, and the Wristen Group (Fig.1-23, 1-24). The Siluro-Devonian Carbonates are expected to be the first interval in the injection unit that has enough permeability for gas to enter the formation (Fig. 1-24).

Siluro-Devonian-aged undifferentiated packstones, dolomites and cherts are often referred to as "Siluro-Devonian Carbonates" or simply "Siluro-Devonian" in the remainder of this document. The Woodford is not included in this lithologic grouping even though the Woodford is also Devonian in age because it is an organic shale. The unconformity at the base of the Woodford is used as a boundary.

Throughout most of the Permian Basin, Siluro-Devonian rocks comprise three distinct facies: 1) skeletal carbonates, primarily pelmatozoan packstones and grainstones; 2) bedded, commonly spiculitic, chert; and, 3) shallow water ramp carbonates that contain abundant dolomite (modified from Ruppel and Holtz, 1994) (Fig.1-27).

Mineralogy of the Siluro-Devonian is primarily quartz in the chert intervals; calcite in the packstone intervals with some illite present; and dolomite in dolomite intervals. In parts of southeastern New Mexico and near Fort Stockton, Texas, packstone dolomite exist in a continuum with minority calcite in the interval. The Silurian Wristen Group is generally finer grained, argillaceous and has small volumes of organic matter. Within the Wristen Group, the Frame and Wink Members are present in the southern Permian Basin and the carbonate rich Fasken Member present in the northern Permian Basin (Ruppel et al., 2008). Based on offset logs, the facies within the Aor is expected to be calcite dominated packstone with minimal dolomite or chert. The Wristen Group is expected to be primarily the Frame and Wink Formations and may have up to 35% clay with the remainder being made up of calcite (Fig. 1-28).

Open and closed fractures are common in both chert and carbonate facies; however, cherts at Three Bar Field contain two to six times as many fractures as associated limestones. In addition, fractures are more abundant close to identified fault zones (Ruppel and Hovorka, 1995).

Siluro-Devonian Carbonates are regionally continuous across the Permian Basin but as noted above undergo several facies changes. The Siluro-Devonian eventually subcrops in the northern part of Lea County, NM. The Thirtyone Formation attains a maximum thickness of 1,000 feet in Crane County, TX and the Wristen Group attains a maximum thickness of 1,500 feet in Lea County, NM.

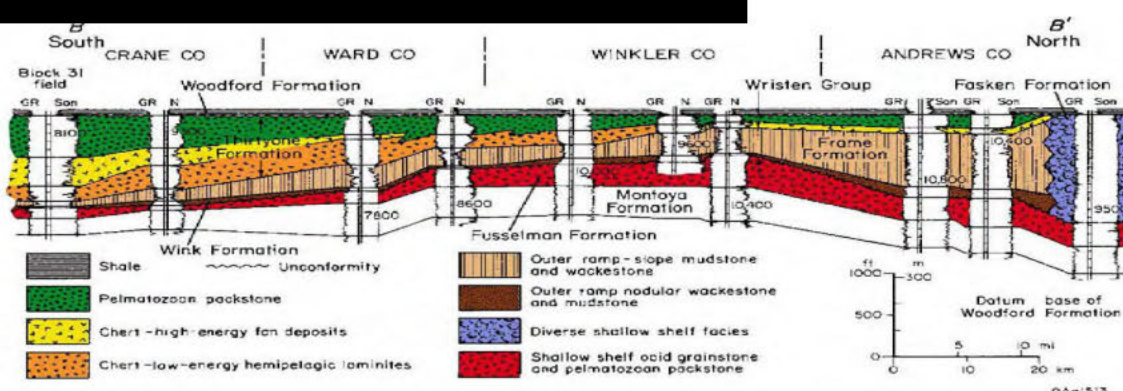


Figure 1-28: South-to-North (B-B') Cross-section of Wristen Group and Facies (Ruppel et al., 2008)

#### 1.5.4.2 Fusselman Dolomite

The Fusselman Dolomite Formation occurs below the Wristen Group and above the Montoya Group. It is a late Ordovician to early Silurian-aged dolomite that was deposited in shallow waters along the southern margin of the Laurentian paleocontinent. The contact of the Fusselman and Wristen Group is unconformable (Ruppel et al., 2008).

The Fusselman is regionally extensive, extending to all parts of the Permian Basin. It was deposited on an open marine carbonate platform that extended across much of present-day west Texas and New Mexico. No pinchouts are expected in Loving County or within the AoR.

The Fusselman is composed of a diverse succession of shallow water carbonate facies. The upper portion is primarily made up of pelmatozoan packstones and grainstones, while the lower section is composed of ooid packstones and grainstones (Ruppel et al., 2008).

The Fusselman was originally deposited as shallow water calcite; subsequent sea level fall dolomitized the formation in present day New Mexico and Delaware Basin. The Midland Basin is primarily still made up of original calcite (Ruppel et al., 2008). The Fusselman under the AoR is expected to be over 80% dolomite by volume.

Voids and vugs are common in the Fusselman due to secondary dissolution. In some cases, multiple dissolution events crosscut each other (Figure 1-29). The Fusselman also exhibits brecciation from cave collapse and past karsting which creates chaotic fractures. Dissolution of fractures and breccias has also been reported in several cores (Ruppel et al., 2008). Porosity and permeability are expected to be a function of vugs and fractures, which are regionally extensive. The majority of the injectate flowing into the Siluro-Devonian unit is expected to be within the Fusselman.

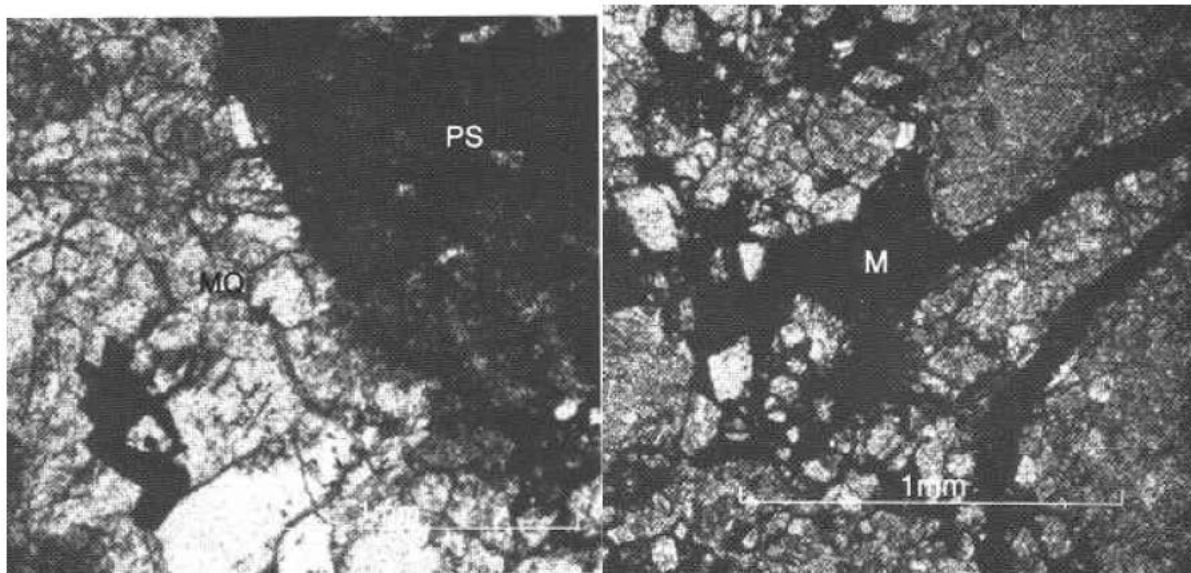


Figure 1-29: Thin Section Photo of Fusselman Dolomite Breccias from outcrop (Young et al., 1994)

#### 1.5.4.3 Montoya Group

The Ordovician-aged Montoya Group occurs below the Fusselman and above the Simpson Group. [REDACTED]

[REDACTED] The Montoya Group and Fusselman share many reservoir characteristics and have historically been grouped together.

The Montoya Group contains the coarse grained Upham, the cherty Aleman and the bioturbated Cutter Formations, from oldest to youngest. The boundary between the Fusselman and the Montoya is easy to discern based on either the Sylvan Shale at top or a lithologic change. The boundary in Loving County can be seen by a lithologic change from dolomite (Fusselman) to limestone (Montoya) (Ruppel et al., 2008).

Deposited on a shallow marine carbonate platform, the Montoya is composed of interbedded carbonate and chert with bioturbated fossiliferous wackestones and packstones. Lithology is highly dependent on which formation is present. Varying fossils, minerals and textures are present in each formation (see Ruppel et al., 2008 for extensive information on facies in each formation).

Porosities up to 8.4% have been reported in the Montoya Group but the porosity in Loving County is expected to be low, <3%. Permeability is expected to be very low as well unless fracturing is present. Fracturing has often been reported in the chertier intervals such as the Aleman Formation (Ruppel et al., 2008).

The Montoya Group reaches a maximum thickness of 700 feet in Loving, Pecos, Ward and Winkler Counties. It has a minimum of approximately 50ft in the eastern Midland Basin in Glasscock and Reagan Counties.

[REDACTED]

#### 1.5.5 [REDACTED]

The Simpson Group is a low permeability group of Ordovician shales and siltstones [REDACTED]. It is characterized by multiple formations. It has three (3) siltstone formations and three (3) shale formations, alternating in sequence. Shale is present on top and then a corresponding siltstone, it then repeats the sequence. The three siltstone members of the Simpson Group—the Connell, Waddell, and McKee—occur at the base of the Oil Creek, McLish, and Tulip Creek Formations, respectively, from oldest to youngest.

Gamma ray is often used to identify the formation boundaries with sharp contacts at maximum flooding surfaces at the base of shales. Shales exhibit >80 API. Siltstones represent lowstand or early transgressive deposits and typically have lenticular bedding with <30 API in clean intervals. Siltstones make up approximately 5 percent of the total thickness of the Simpson Group in west Texas and southeastern New Mexico. Not all siltstones are likely present in all areas owing to their depositional setting facies changes up-dip and down-dip (Ruppel et al., 2008).

Little-to-no fracturing is expected within the shale members of the Simpson Group forming an effective intrazonal seal of low vertical permeability rock. Further, the siltstone members are also expected to have little-to-no porosity and permeability, they are defined by their quartz mineralogy, not their porosity.

[REDACTED]

[REDACTED]

1.5.6

The Ellenburger Group of the Permian Basin is typically defined as part of a Lower Ordovician carbonate platform sequence that covers a large area of the United States (Kerans, 1990). It is well known for being one of the largest shallow-water carbonate platforms in the geologic record (covering thousands of square miles (sq. mi) and as much as 500 mi wide in west Texas. Extensive cave collapse features (karsting) led to pervasive fracturing that occurred shortly after deposition. This fracturing enhanced the permeability of the group.

There are multiple unconformities within the Ellenburger Group. Unconformities are known to exist at the top of the Ellenburger, between the different Ellenburger formations, and then again at the base of the Ellenburger. This leads to dynamic changes in thickness across Loving and the Permian Basin.

The Ellenburger is extensively fractured due to three stages of karsting that occurred repeatedly for millions of years as sea level rose and fell over an area that covered the entire Permian Basin. When sea level was lower than the carbonate platform, karst features would form. **Figure 1-30** shows the various stages of cave collapse. First water infiltrates and dissolves carbonate, after a void is created, the ceiling above collapses into the void due to gravity and weight. Finally, the entire chamber collapses and is compacted. These features are called cave collapse breccias or simply breccias and the process is referred to as brecciation. This process happened shortly after deposition and then the rock was subsequently dolomitized (Loucks, 2023).

The process of dolomitization favors preserving open fractures and pores because it is mechanically and chemically more stable than limestone. Pores within dolomites are commonly preserved to deeper burial depths and higher temperatures than those of pores in limestone. Also, limestone breccia clasts tend to undergo extensive pressure solution at their boundaries and lose all interclast pores (Loucks and Handford, 1993), whereas dolomite breccia clasts are chemically and mechanically stable with burial (R. Loucks, 2007, 2023). Thus, even at extreme depths, pores and fractures are expected to be open and prevalent.

The pore networks in the Ellenburger are complex because of the amount of dolomitization, brecciation, and fracturing associated with karsting and regional tectonic deformation. Pore networks can consist of any combination of the following pore types, depending on depth of burial: 1) matrix, 2) cavernous, 3) interclast, 4) crackle-/mosaic-breccia fractures, or 5) tectonic-related fractures (**Fig.1-31, 1-32, and 1-33**) (Loucks, 2019, 2023).

The Ellenburger's mineralogy is primarily composed of dolomite (>80% dolomite) but it may contain calcite, anhydrite, chert, gypsum and other minerals in small quantities at a core scale. Many minerals occur in minor quantities related to evaporite deposition or other chemical processes. Over 99% of the non-dolomite mineralogy is contained within the pervasive fractures. The mineralogy is highly variable, and this makes porosity prediction difficult from triple combo logs (see type-log in **Sec. 1.9**).

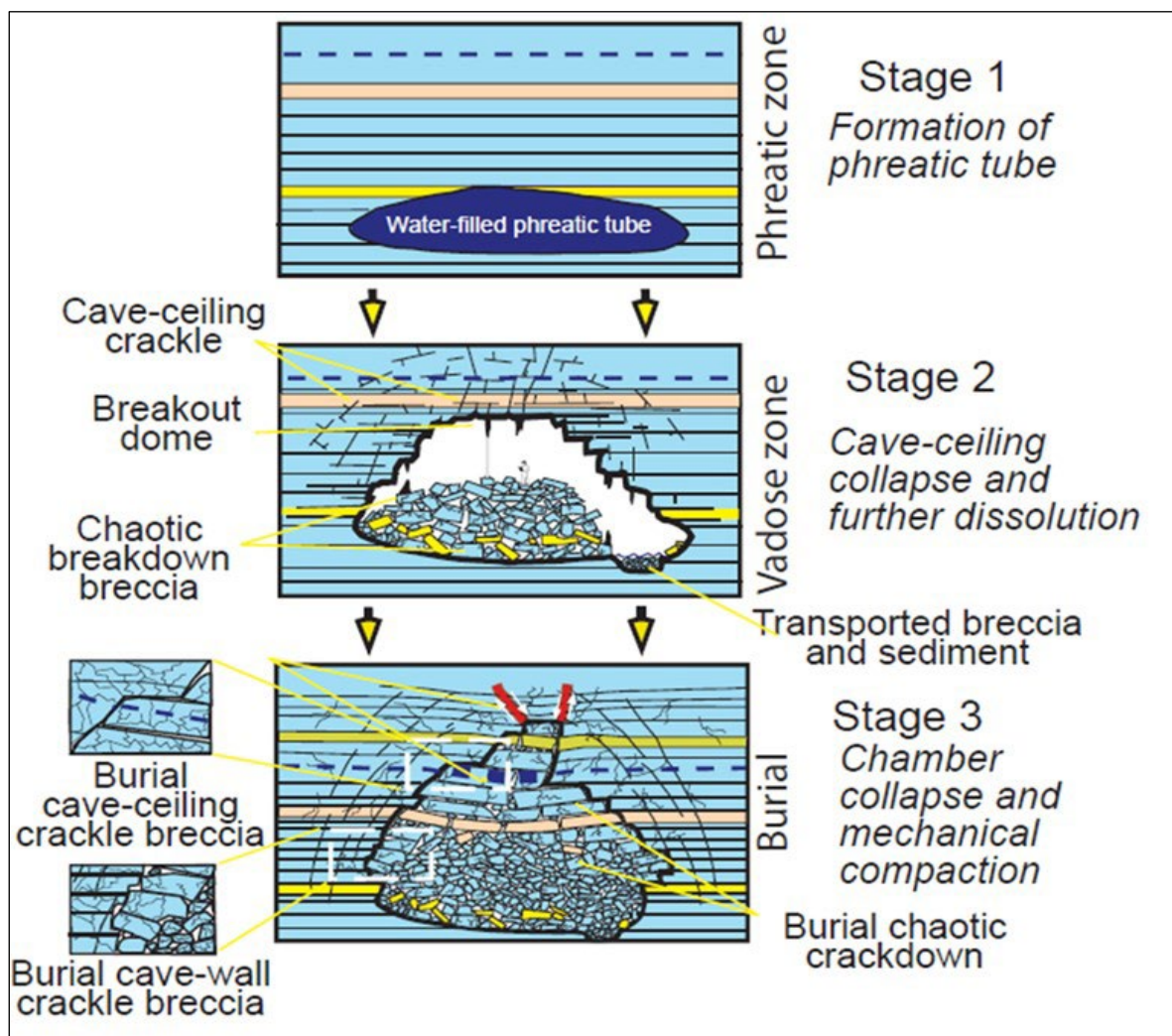


Figure 1-30: Cave Collapse Schematic (Loucks, 2023)

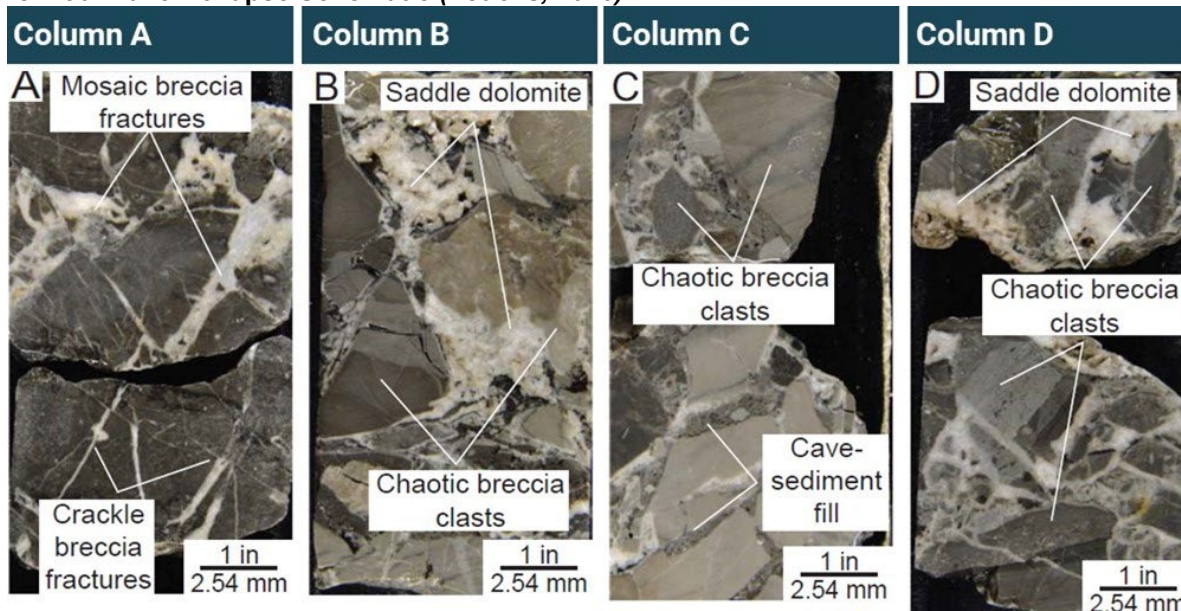


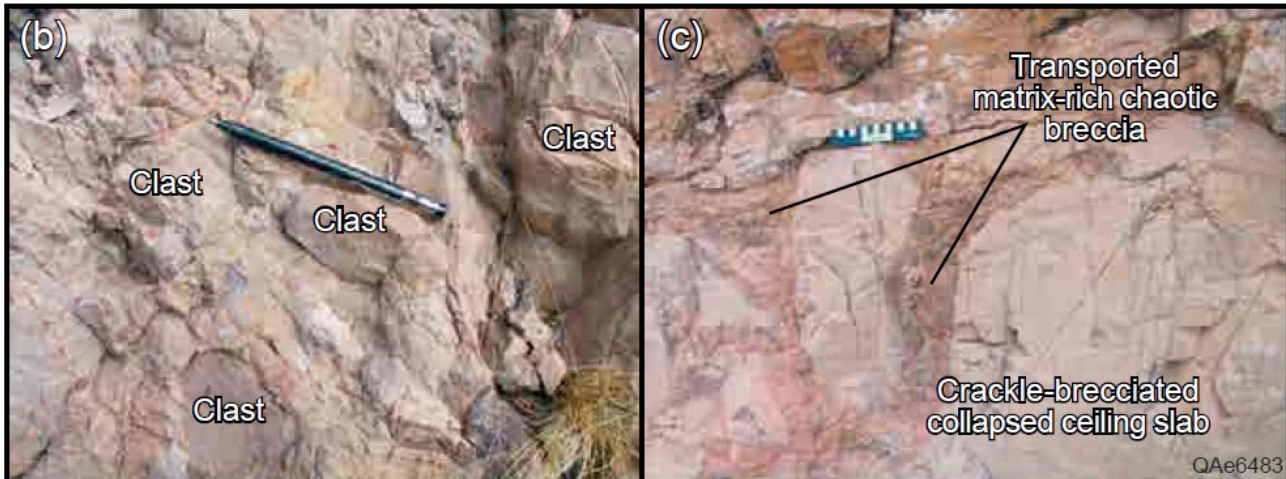
Figure 1-31: Meteoric karst breccias McElroy #1 Crane County, Texas.

Meteoric karst breccias from McElroy #1 core in Crane County, Texas. (Loucks, 2023)

Cave Facies	Interpretation	Description	Pore System/ Reservoir Quality
Undisturbed strata	Undisturbed host rock	Excellent bedding continuity for hundreds to thousands of feet.	Minor matrix and fracture pores. $\emptyset < 3\%$ to 5% $K <$ few millidarcys
Disturbed strata	Disturbed host rock	Bedding continuity is high but folded and offset by small faults. Commonly overprinted with crackle and mosaic brecciation.	Minor matrix pores and crackle to mosaic fracture pores. $\emptyset < 5\%$ $K$ is as much as tens of millidarcys
Highly disturbed Strata	Collapsed host rock (cave-roof and cave-wall rock) over passages	Highly disturbed, very discontinuously bedded strata with pockets and layers of chaotic breccia. Small-scale folding and faulting are common. Commonly overprinted with crackle and mosaic brecciation.	Localized pockets or layers of breccia might have porosities in the range of 5% to 15% and permeabilities in the tens to hundreds of millidarcys.
Coarse chaotic breccia	Collapsed-breccia cavern fill	Mass of very poorly sorted, granule- to boulder-sized chaotic breccia clasts 1 to 10 ft long. Commonly clast supported but can contain matrix material. Ribbon- to tabular-shaped body as much as 45 ft across and hundreds of meters long.	Abundant interclast pores. Porosity can exceed 20%, and permeability can be in the darcys.
Fine chaotic breccia	Transported-breccia cavern fill	Mass of clast-supported, moderately sorted, granule- to cobble-sized clasts with varying amounts of matrix. Clasts can be imbricated or graded. Ribbon- to tabular-shaped body as much as 45 ft across and hundreds of feet long.	Abundant interclast pores. Porosity can exceed 20%, and permeability can be in the darcys.
Sediment fill	Cave-sediment cavern fill	Carbonate and/or siliciclastic debris commonly with sedimentary structures.	Siliciclastic fill is commonly tight. Carbonate fill might be permeable.

**Figure 1-32: Ellenburger Formation Core Facies**

Identified facies from core in the Ellenburger Formation. After R. Loucks 2007, 2023

**Figure 1-33: Ellenburger Breccias in outcrops near El Paso, TX (Loucks, 2019)**

### 1.5.7 Lower Confining Layer – Cambrian and/or Precambrian Basement

An unconformity exists between the Ellenburger and Precambrian basement that may have eroded the lower Ellenburger, the Cambrian-aged Wilberns sand or the Cambrian-aged Bliss sand from the geologic section. It is unknown whether the Cambrian Bliss or Cambrian Wilberns sands will be present at the base of the Ellenburger due to lack of well penetration. It is expected to be discontinuous if it is present. The crystalline basement below the Cambrian section has been well studied and is primarily granite and rhyolite in Loving County.

Loving County resides over the western extension of the Abeline Gravity Minimum (AGM) which is a large regional granitic and rhyolite bearing batholith (**Fig. 1-34**) (Ewing et al., 2019) (Adams and Keller, 1996). The age of the batholith is not known except that is cut by the Llano Deformation front and therefore occurred prior to it. Samples taken near Abilene, TX yielded an age of 1078 +/- 23 MA from U-Pb dating. This batholith is likely related to the large, unusually deep low-gravity anomaly that straddles the Texas-New Mexico border and is partially within Loving County (Ewing et al., 2019).

### 1.5.8 Major Geologic Features and Description on Tectonic History

The Permian Basin initially developed as the ancient Tobosa Basin, a 350-mile-wide sag from the Texas Arch to the Diablo arch that formed in the middle Ordovician. In the Mississippian and Pennsylvanian, the basin was deformed by the Central Basin Platform rising and the Ouchita-Marathon (OM) thrust belt and the basin has mostly stayed the same ever since. The Tobosa Basin ceased to exist with the formation of the Central Basin Platform (CBP), Delaware and Midland Basin.

The Permian Basin is composed of several sub-basins, each with its own unique characteristics. The Delaware Basin is located in the western part of the Permian Basin and is known for its fault systems that are oriented east-west and rotate towards major tectonic features. The Midland Basin is located in the eastern part of the Permian Basin and is characterized by its long periods of regional subsidence and north-south trending faults (Fig.1-36) (Ruppel, 2019). The Delaware Basin is nearly twice as deep as the Midland Basin.

The Central Basin Platform is a heavily faulted relatively flat area that separates the Delaware and Midland Basins and contains many north-south trending faults. The Northwest Shelf is the northernmost portion of the Permian Basin and has relatively few faults, while the Ouchita thrust belt is located in the southern part of the Delaware basin and is heavily faulted by east west faults.

Hills (1970) developed a system of crustal blocks that define the different tectonic regions of the Permian Basin. Hills' primary objective was to determine the direction of tectonic forces responsible for regional deformation.

Hills interpreted two tectonic systems. The first consists of folds and faults possessing orientations of N35W (folds) and N55-80E (right lateral faults), and N50-65 W (left lateral faults). The age of this deformation is thought to be early Late Mississippian to late Middle Pennsylvanian. There also are a series of NNW-trending faults that appear to be right lateral systems with larger displacement that formed synchronous with the other faults. It is this system of conjugate faults that has been interpreted to control the jagged geometry of the Central Basin Platform, especially along its eastern margin (Fig. 1-35) (T. Hoak et al. 1998). The Andrews Shear zone correlates with the Abeline Gravity Minimum.

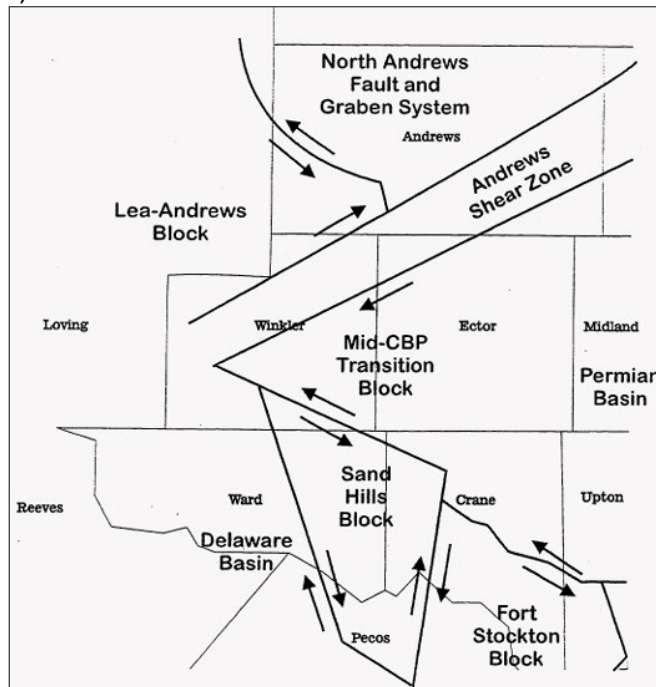
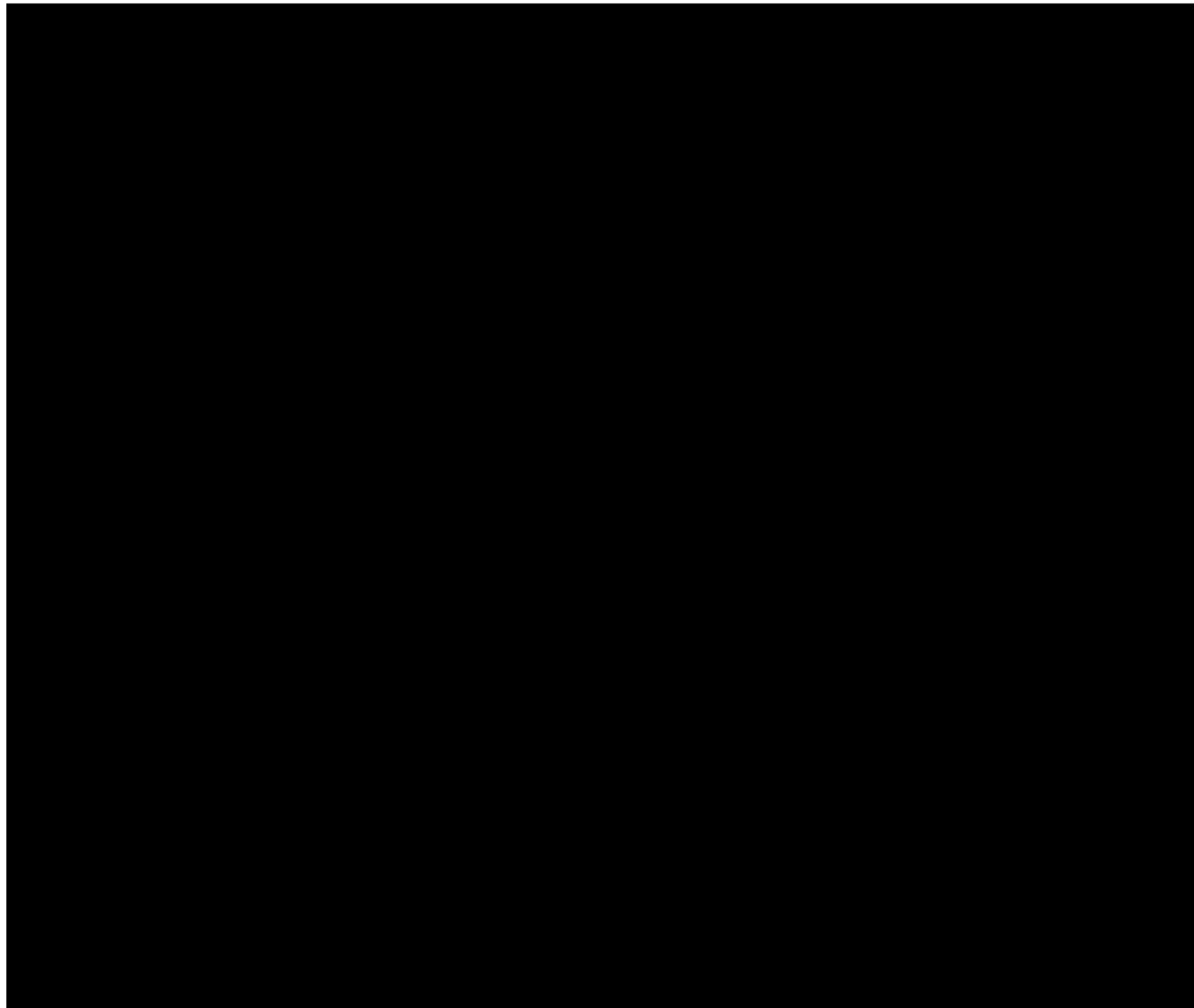
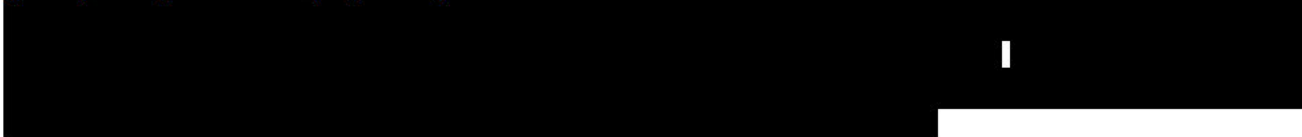


Figure 1-35: Interpreted crustal blocks (T. Hoak et al. 1998)

A second, later deformation phase as interpreted by Hills (1970), is marked by the relaxation of stress and normal fault motion due to reactivation of older fault systems. The timing of this deformation is interpreted to be middle-to-late Permian in age and fault displacements are relatively minor. Finally, during the Tertiary, the western margin of the Permian Basin was uplifted, and Basin-and-Range tectonism commenced in this area. This deformation has apparently been restricted to the western Delaware Basin and the basin margin (T. Hoak et al. 1998). One of the results of these two stages of Paleozoic tectonism can be seen in seismic cross-sections where faults terminate at the base of the Barnett Shale, making the Barnett an excellent seal due to its lack of cross cutting faults.

Recent work by Horne et al. (2022) resulted in generation of a new fault map for the Delaware Basin and Central Basin Platform using an integrated dataset of 3-D seismic, well steering data, INSAR and gravity- magnetic data (Fig. 1-36).



Horne et al., (2022) reported the principal tectonic elements that define the modern greater Permian Basin formed as a result of the diachronous collision between the northwest-verging Ancestral Rocky Mountain (ARM) orogeny and northeast-verging Ouachita-Marathon orogeny.

Subsequent Mesozoic and Cenozoic events are interpreted to have been influenced by the accumulated tectonic fabrics generated by these Paleozoic events; many of the structures exhibit characteristics of reactivation and transferred strain. These events include the Laramide orogeny, basin-range extension and the Rio Grande rifting. The post-Permian tectonic events control much of the western Delaware basin and rotations in stress orientation found there.

A diagram of the age of different orogenies can be found in **Figure 1-37**. The type log shown in the diagram is from eastern Loving County and is a good representation of the stratigraphy at the Facility except shallower. Take note of the large time gap between orogenies between the Ordovician and the Pennsylvanian, and then again in the Permian.

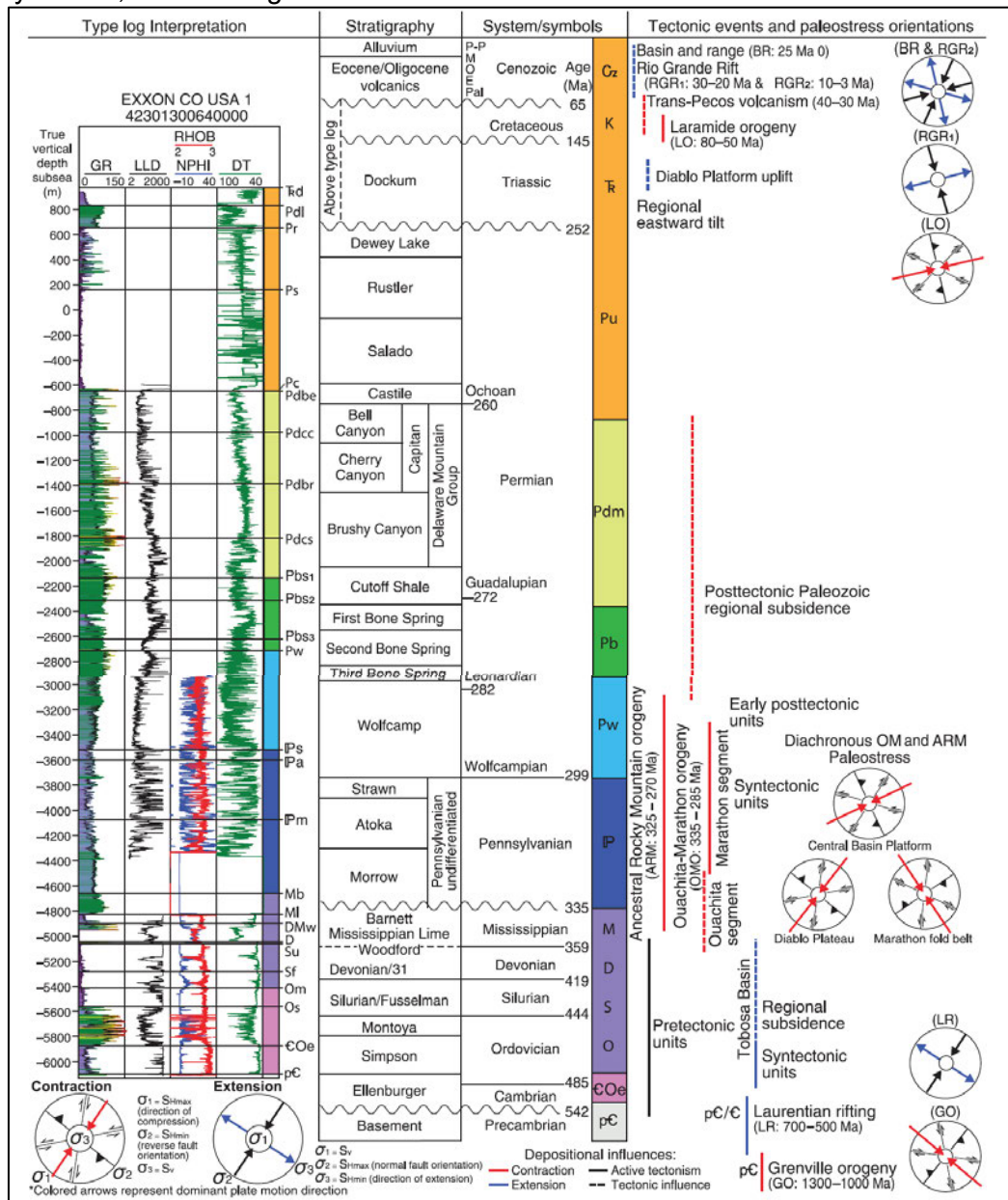


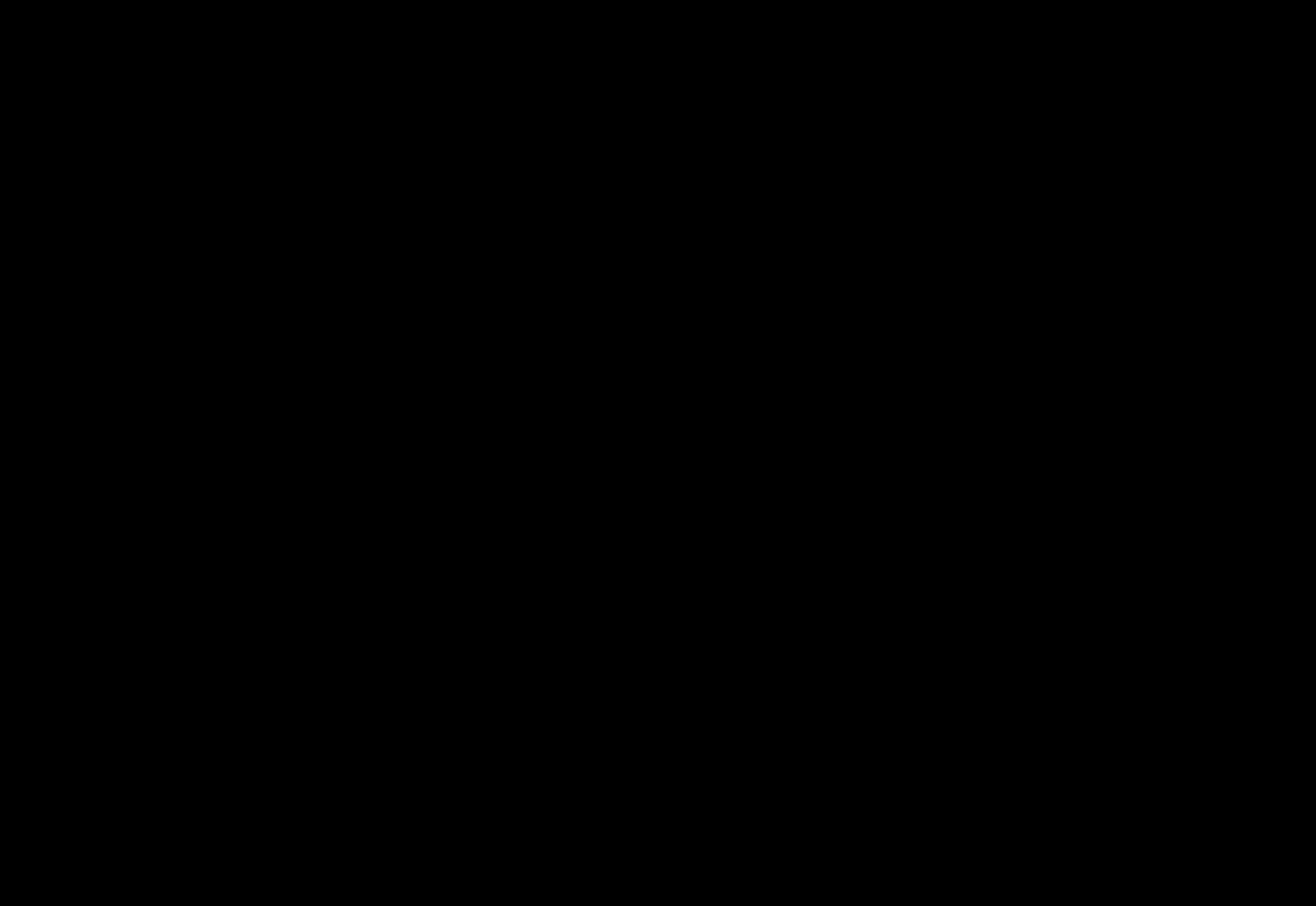
**Figure 1-37: Horne Delaware Basin Orogenic History with Type-log and Strat. (Horne et al., 2022)**

## 1.6 Local Geology Introduction

The following **Sections 1.7 through 1.12** discuss the local geology around the proposed Facility.

- Section 1.7 – Structural Geology - Thickness, Lithology
- Section 1.8 – Faults and Fractures – Faults and Fractures, Seismic History, Regional Stress
- Section 1.9 – Petrophysical Characterization – Porosity, Permeability, Salinity, Cap Pressure
- Section 1.10 – Geomechanics – Stress Magnitude, Orientation, Strength, Ductility, Pressure
- Section 1.11 – Geochemistry – Brine-CO<sub>2</sub> Interactions, Mineral-CO<sub>2</sub> interactions
- Section 1.12 – Mineral Resources – Petroleum production from Ellenburger or Siluro-Devonian

The local geology in the area of the proposed Facility includes



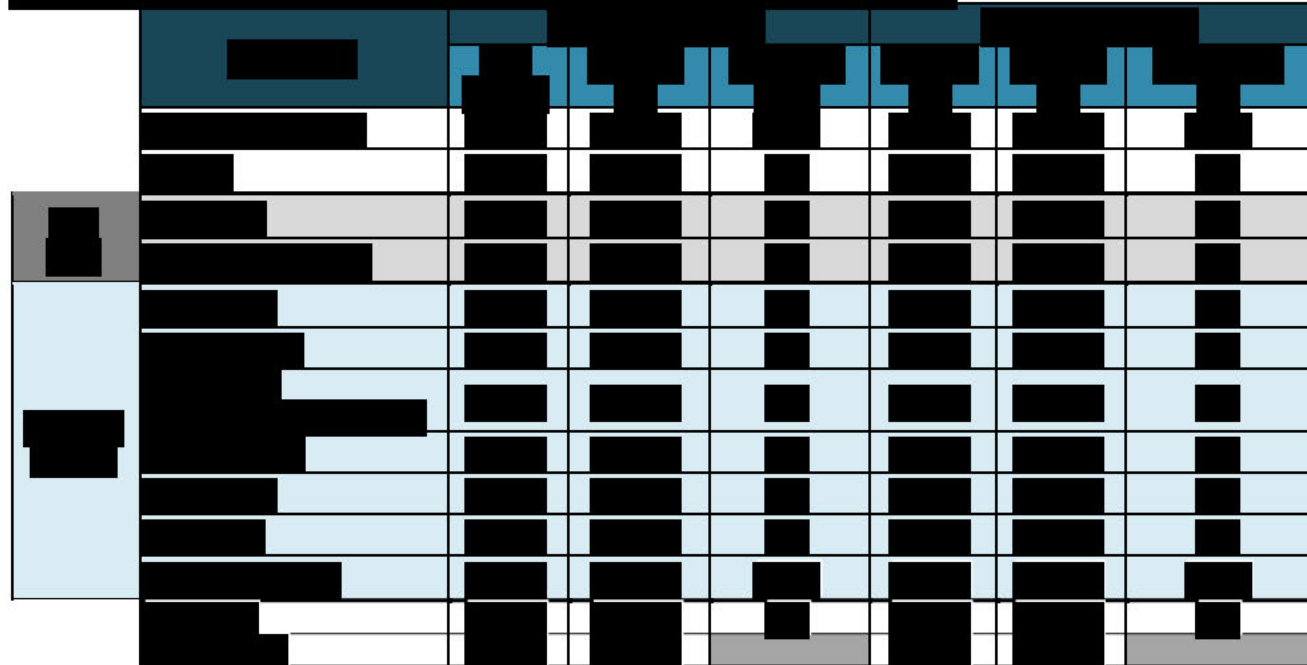
## 1.7 Structural Geology [40 CFR 146.82 (a)(3)(iii)]

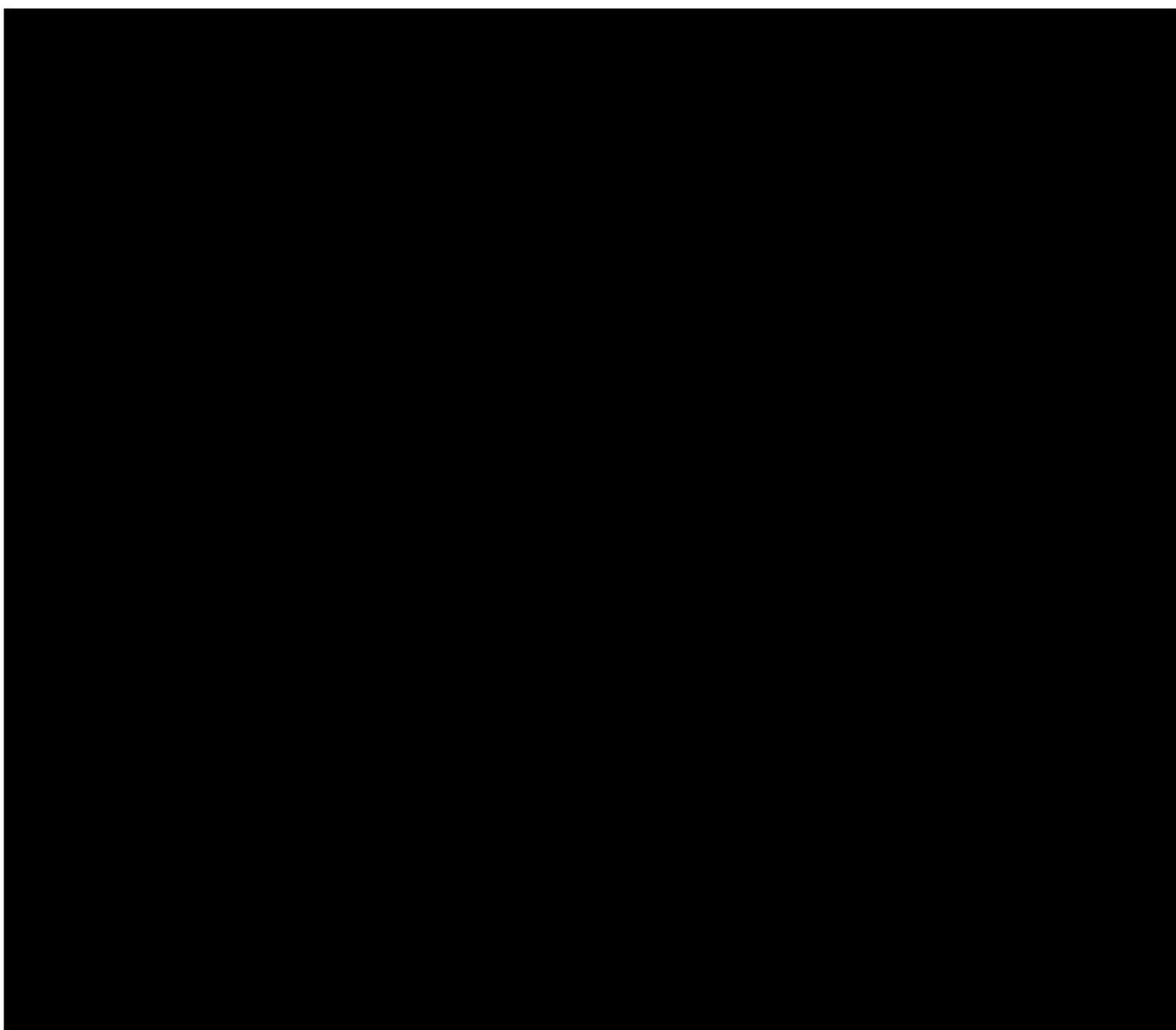
### 1.7.1 Structure

The purpose of **Section 1.7** is to demonstrate, that within the AoR, the structure of the Top Seal and Injection Interval is laterally continuous and predictable with very low dip (<5deg), limited faulting and properly characterized lithology. In this section, Milestone will present the depth, thickness, and lithology of the injection and confining zones.



All of the formations below the Wolfcamp Shale are regionally extensive, conformable and cover Loving County.



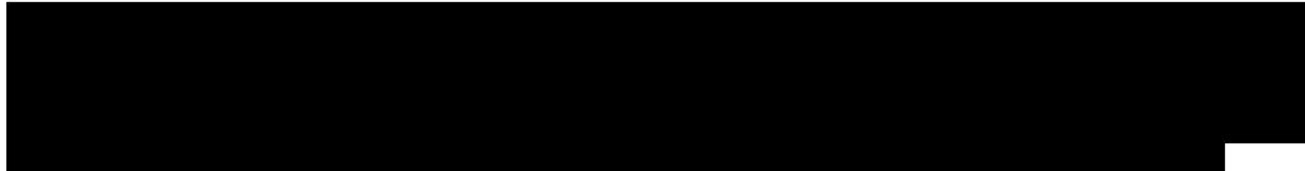
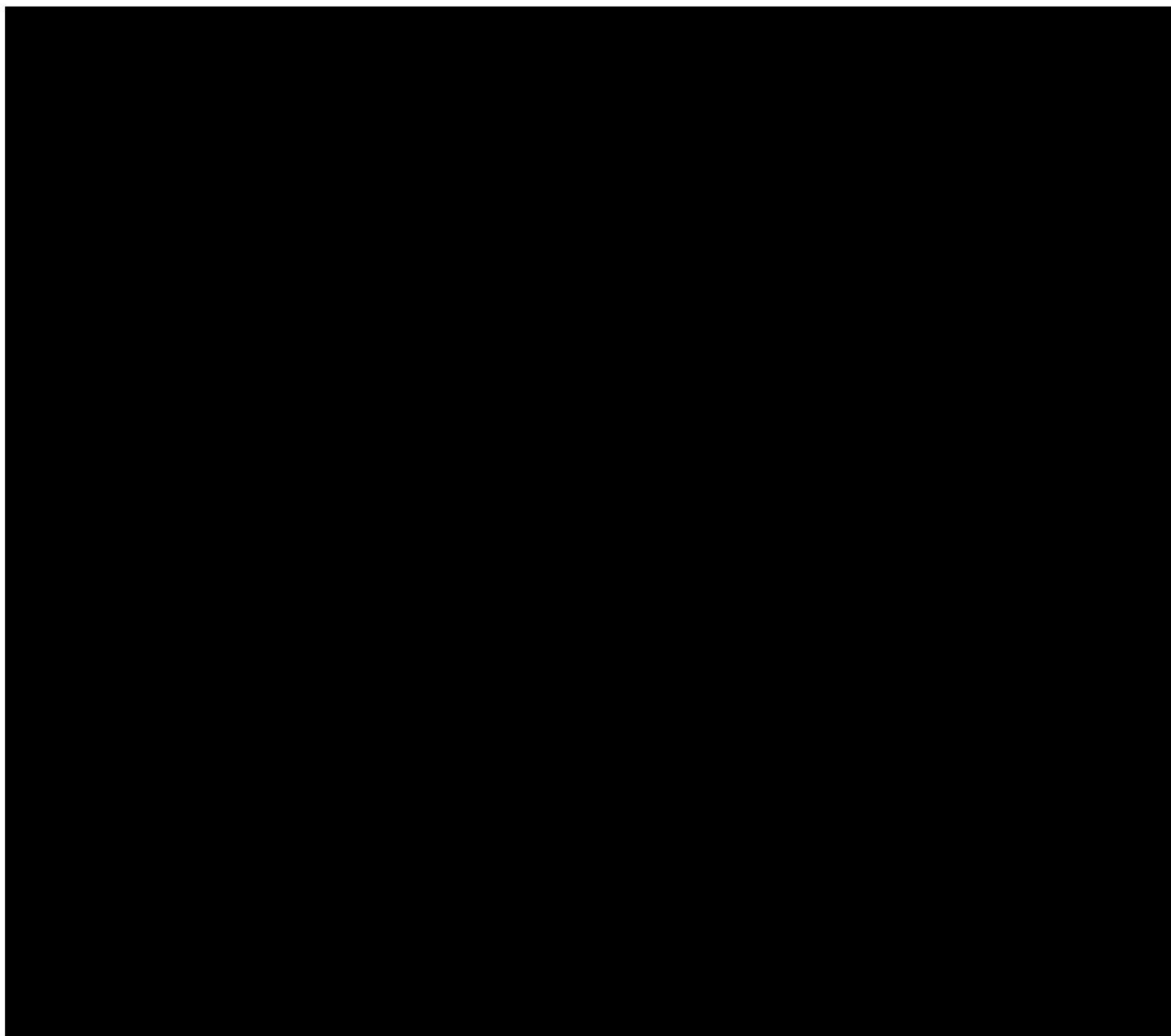


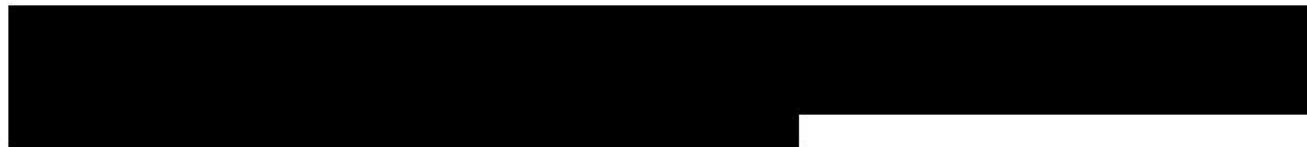
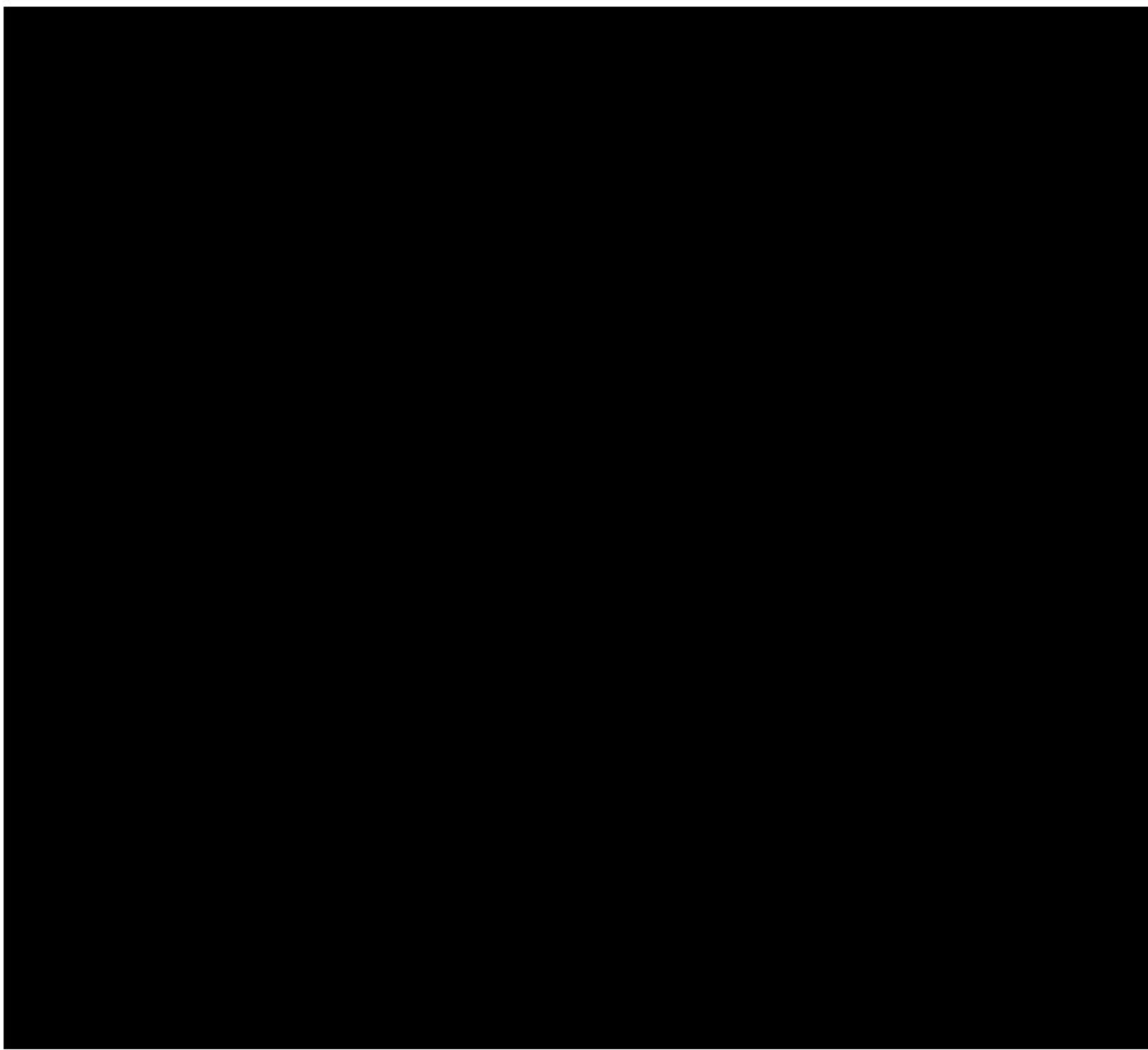


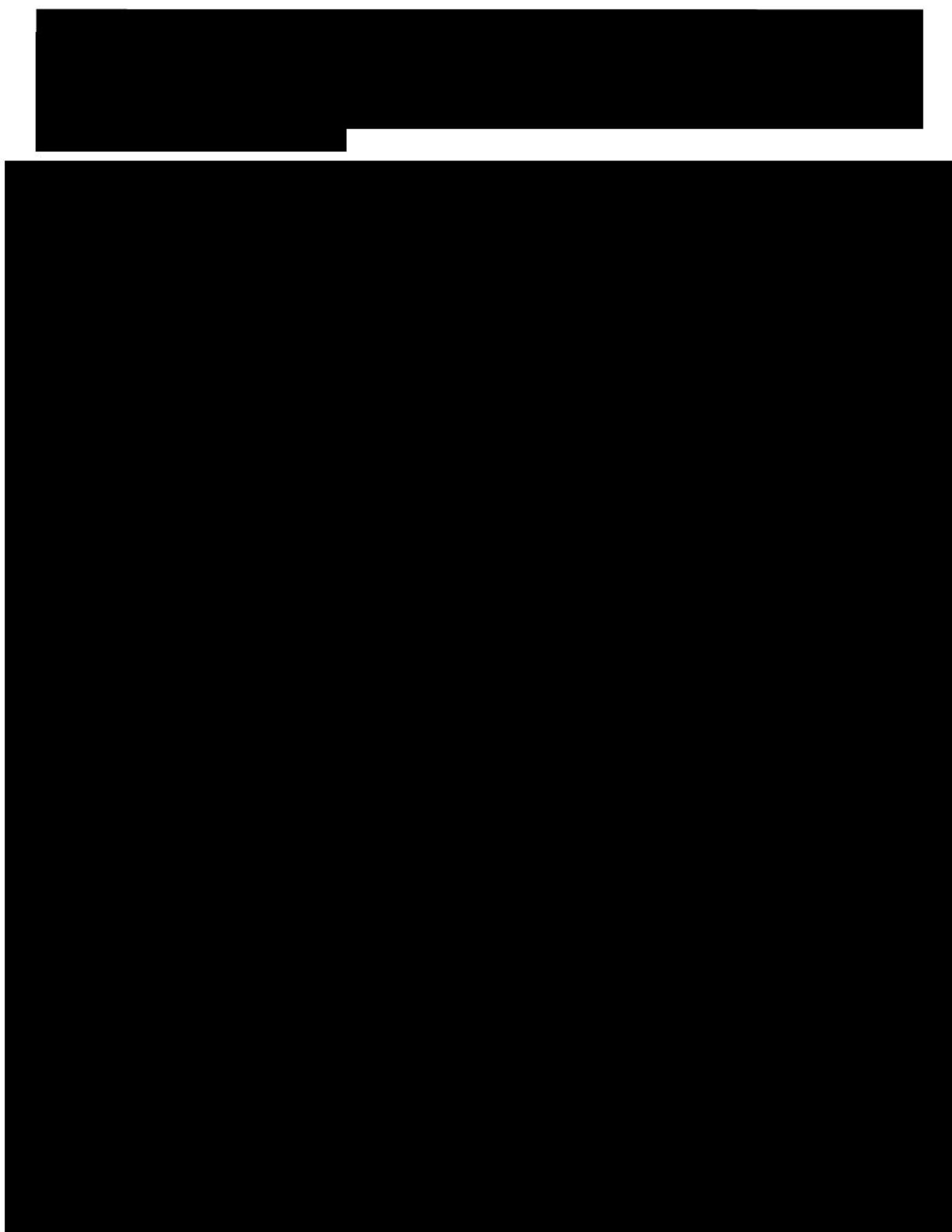


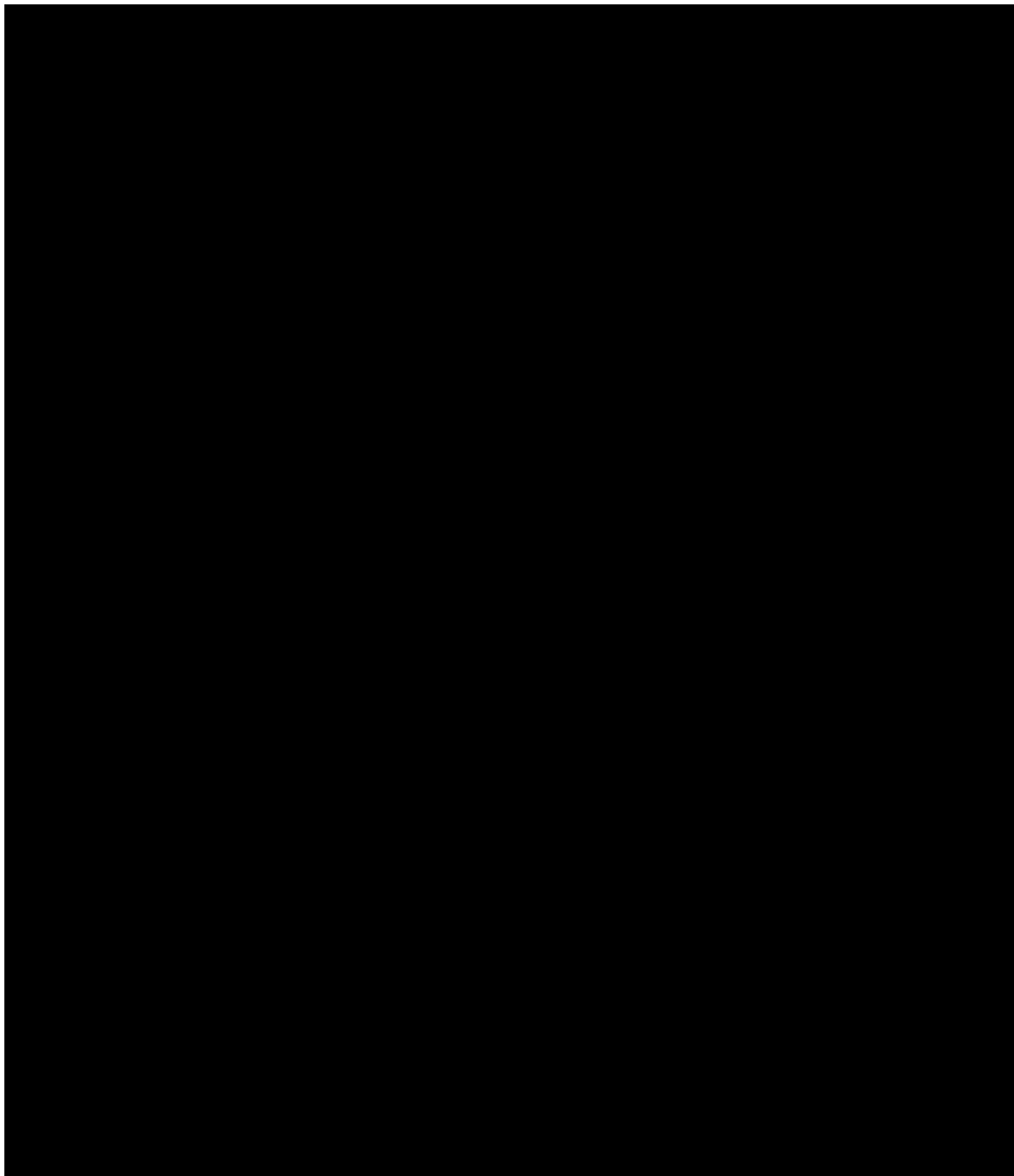








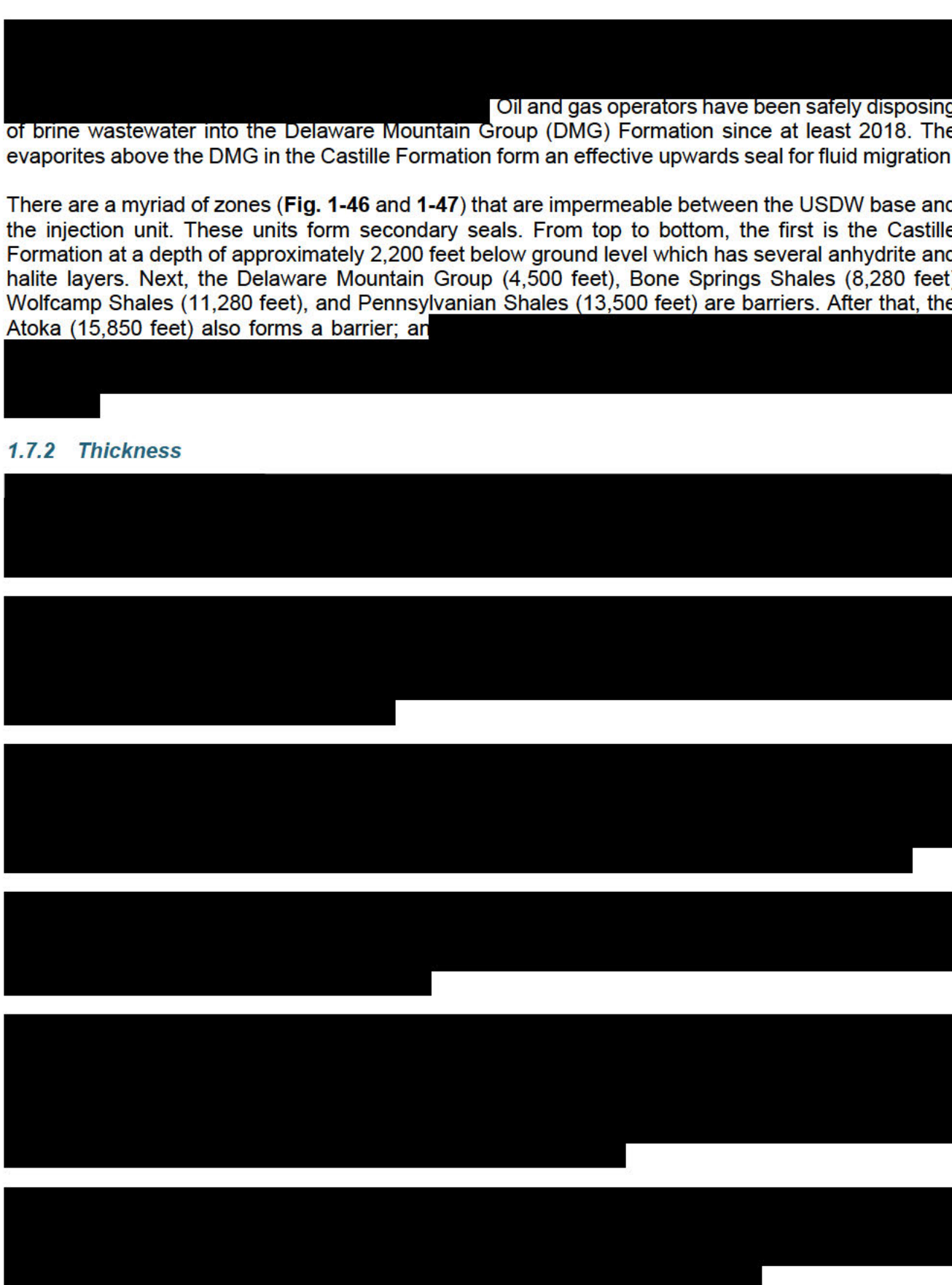




Oil and gas operators have been safely disposing of brine wastewater into the Delaware Mountain Group (DMG) Formation since at least 2018. The evaporites above the DMG in the Castille Formation form an effective upwards seal for fluid migration.

There are a myriad of zones (Fig. 1-46 and 1-47) that are impermeable between the USDW base and the injection unit. These units form secondary seals. From top to bottom, the first is the Castille Formation at a depth of approximately 2,200 feet below ground level which has several anhydrite and halite layers. Next, the Delaware Mountain Group (4,500 feet), Bone Springs Shales (8,280 feet) Wolfcamp Shales (11,280 feet), and Pennsylvanian Shales (13,500 feet) are barriers. After that, the Atoka (15,850 feet) also forms a barrier; an

### 1.7.2 Thickness







### 1.7.3 Cross-sections





[REDACTED]

[REDACTED]

[REDACTED]

[REDACTED]

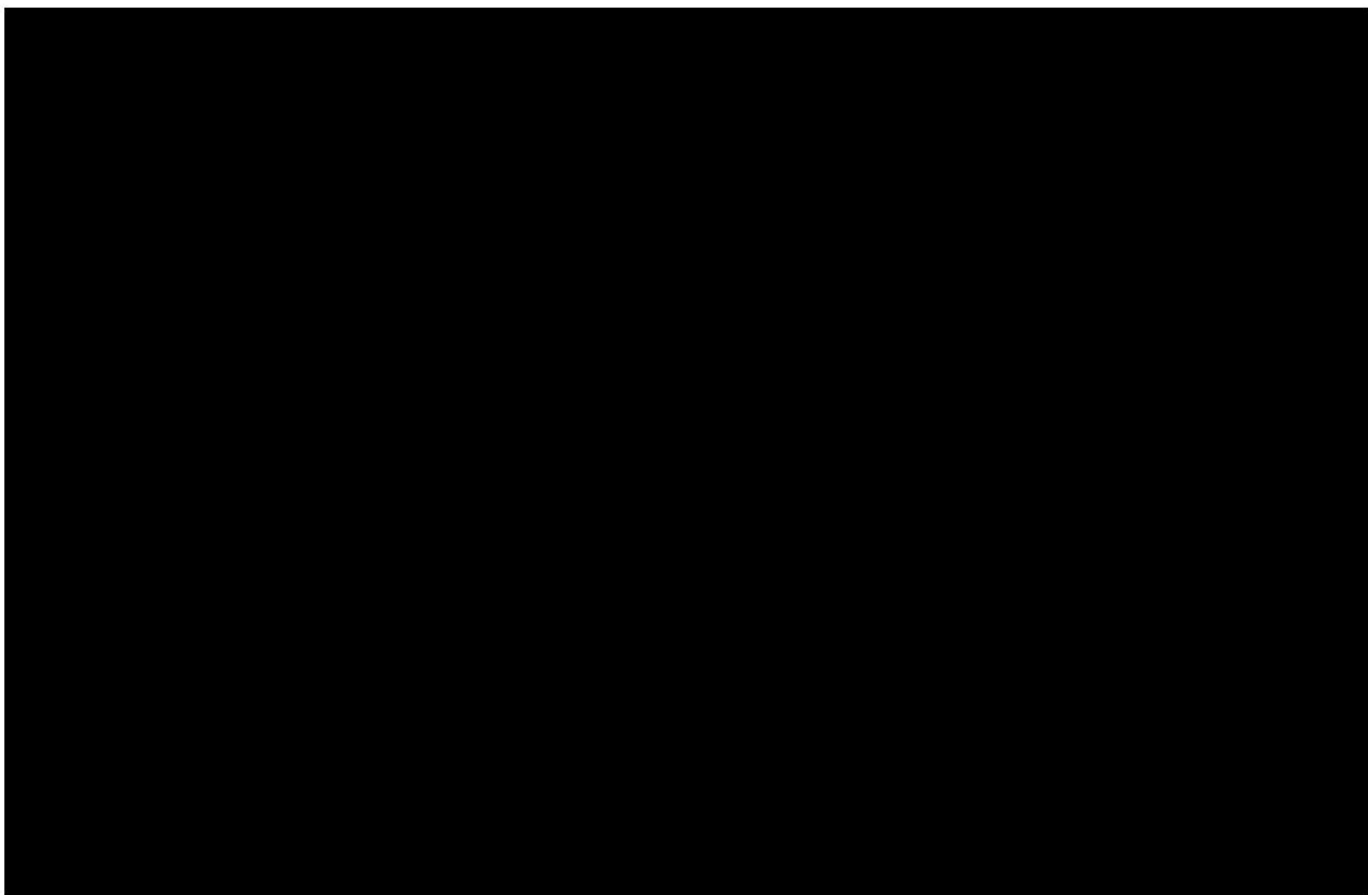
[REDACTED]

[REDACTED]

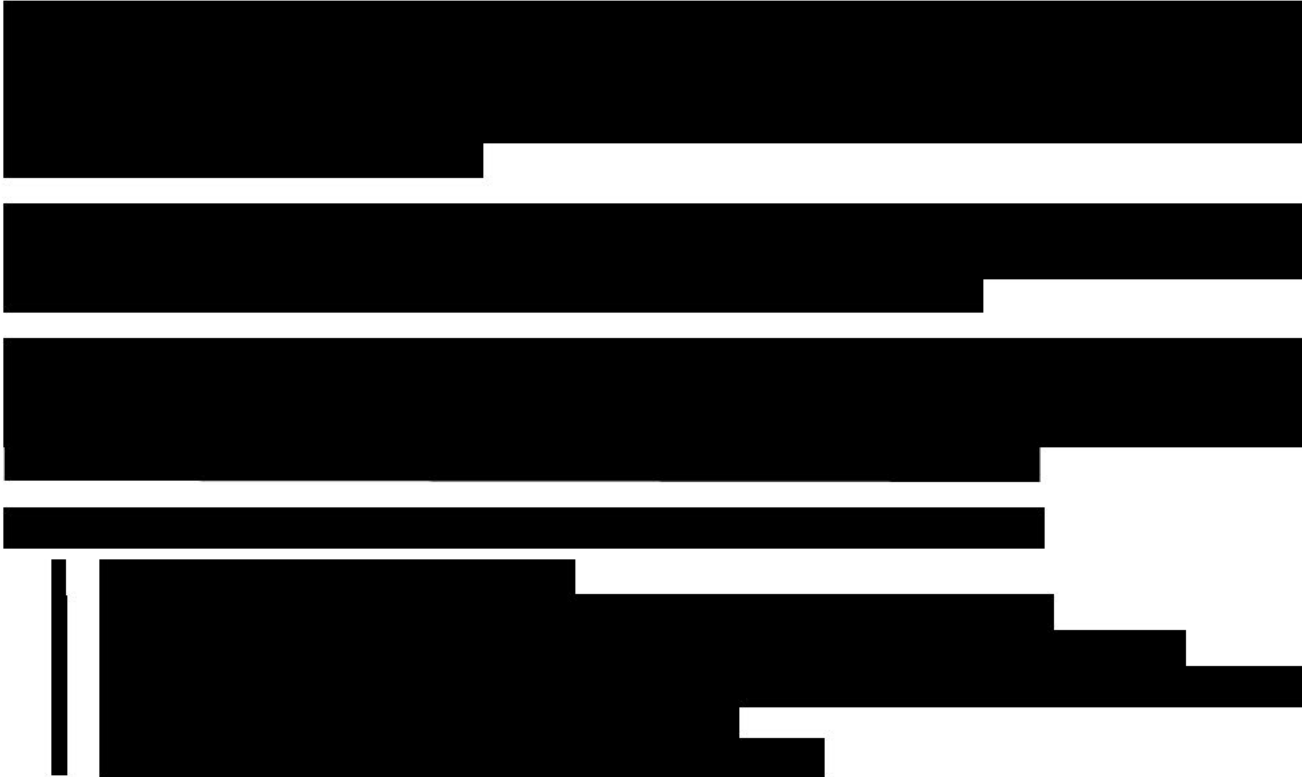
[REDACTED]

[REDACTED]





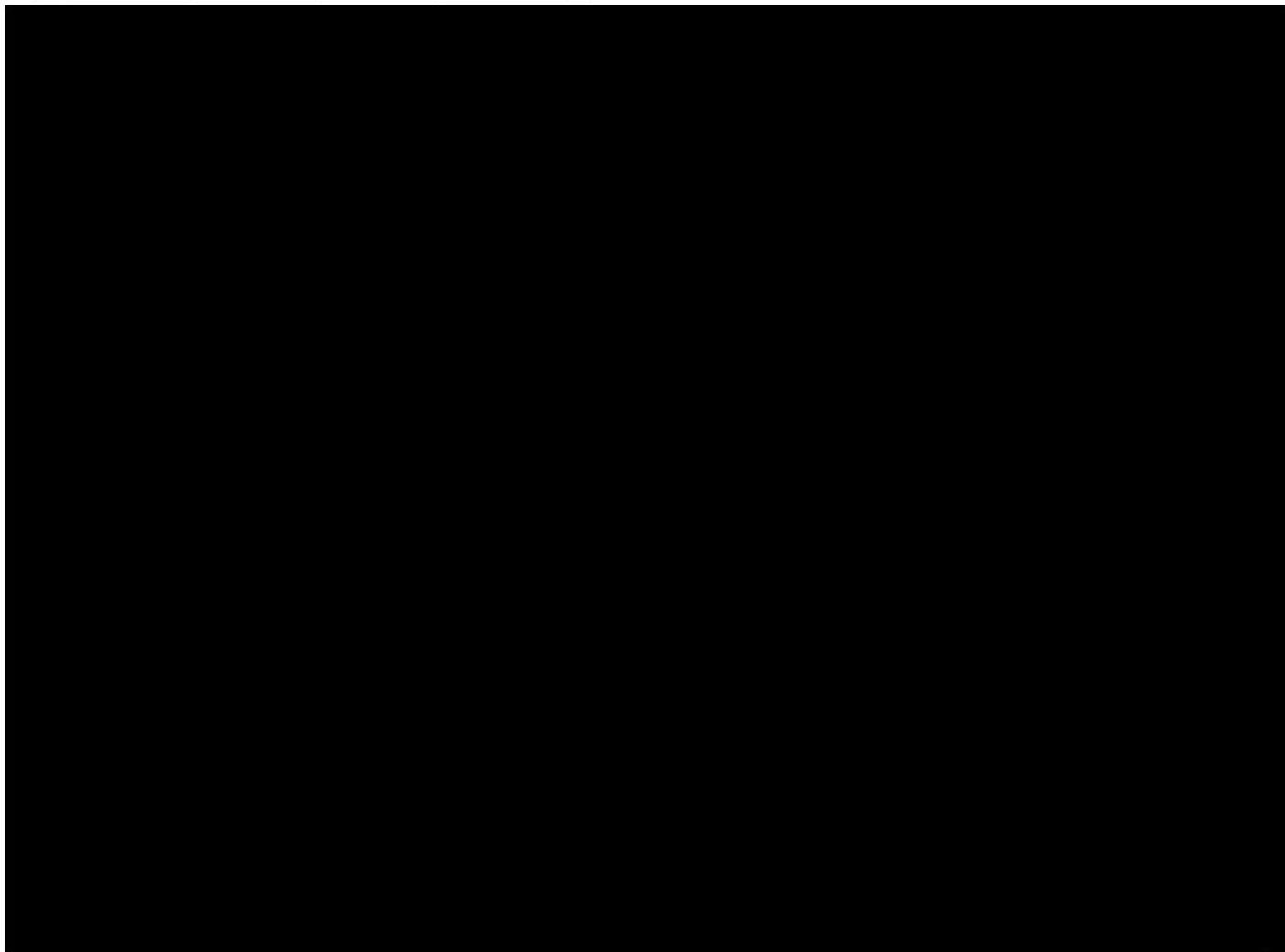
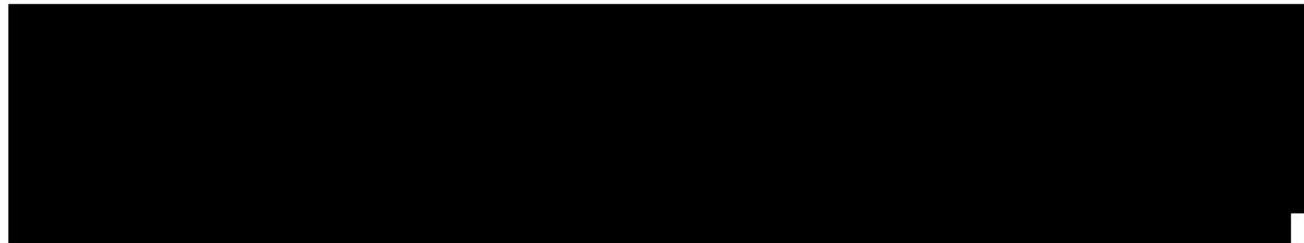
#### 1.7.4 *Lithology*

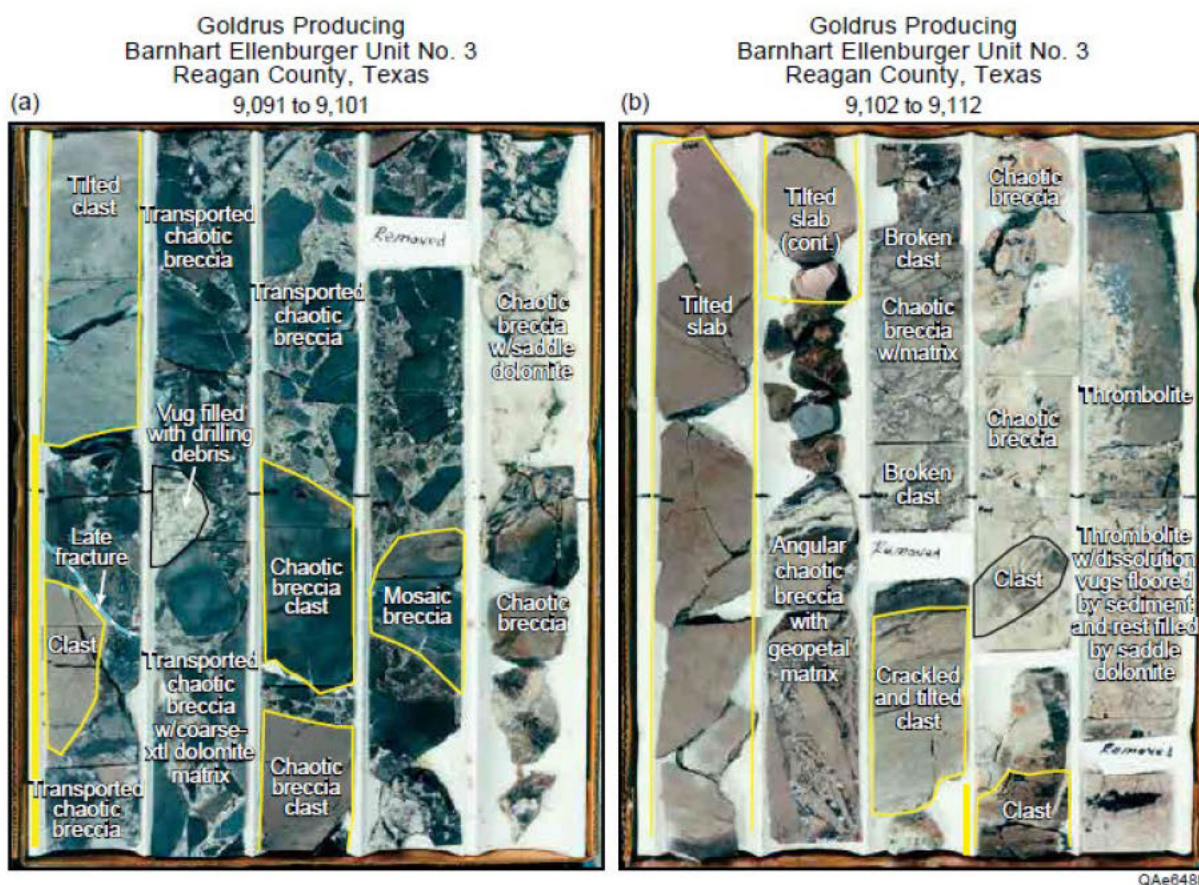


## 1.8 Faults and Fractures [40 CFR 146.82 (a)(3)(ii)]

This section addresses data regarding faults and fractures in the seals and injection units as well as the seismic history of the area. It further documents the regional stress field for the western Delaware Basin and shows fault slippage analyses for nearby faults.

### 1.8.1 *Fractures*

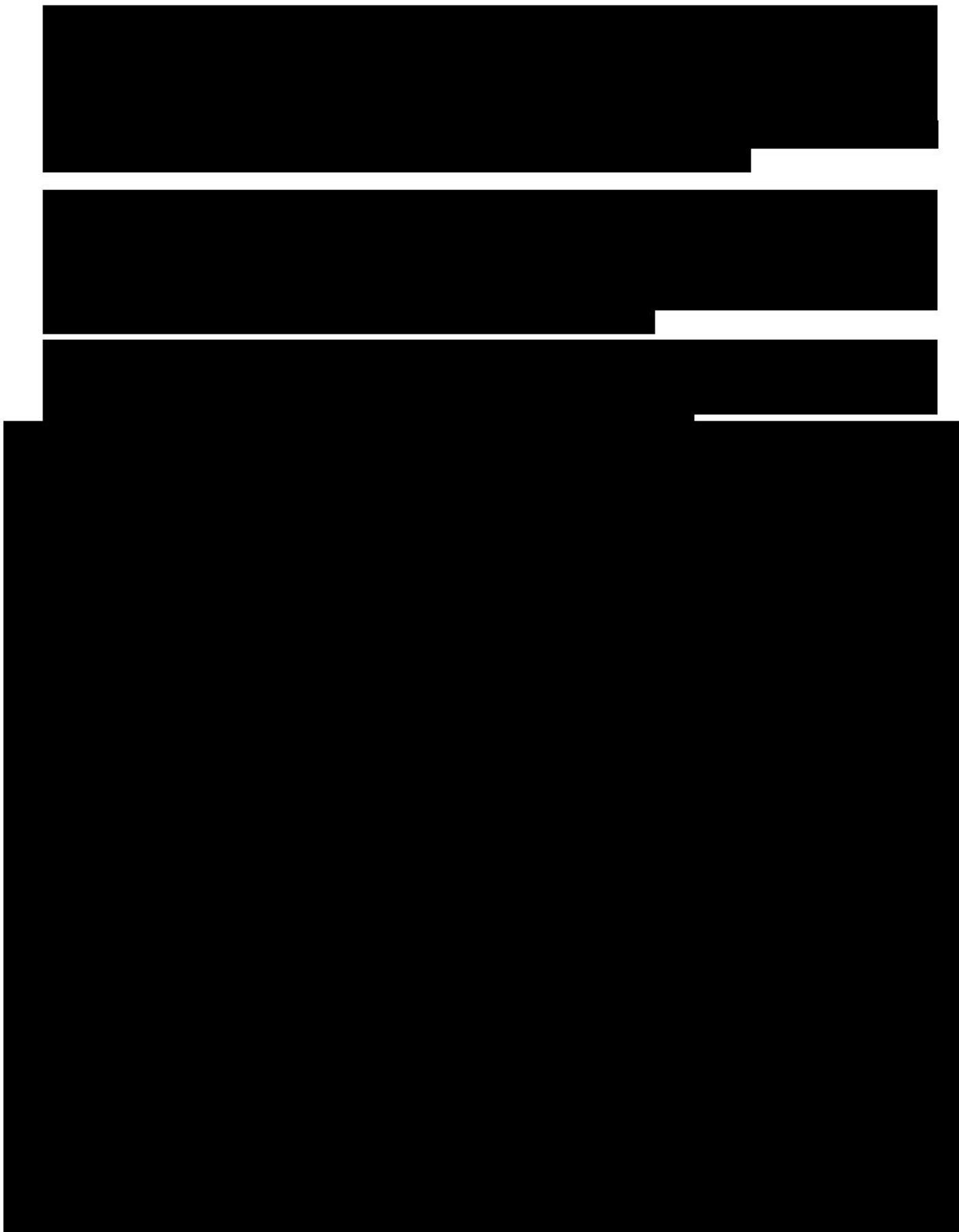


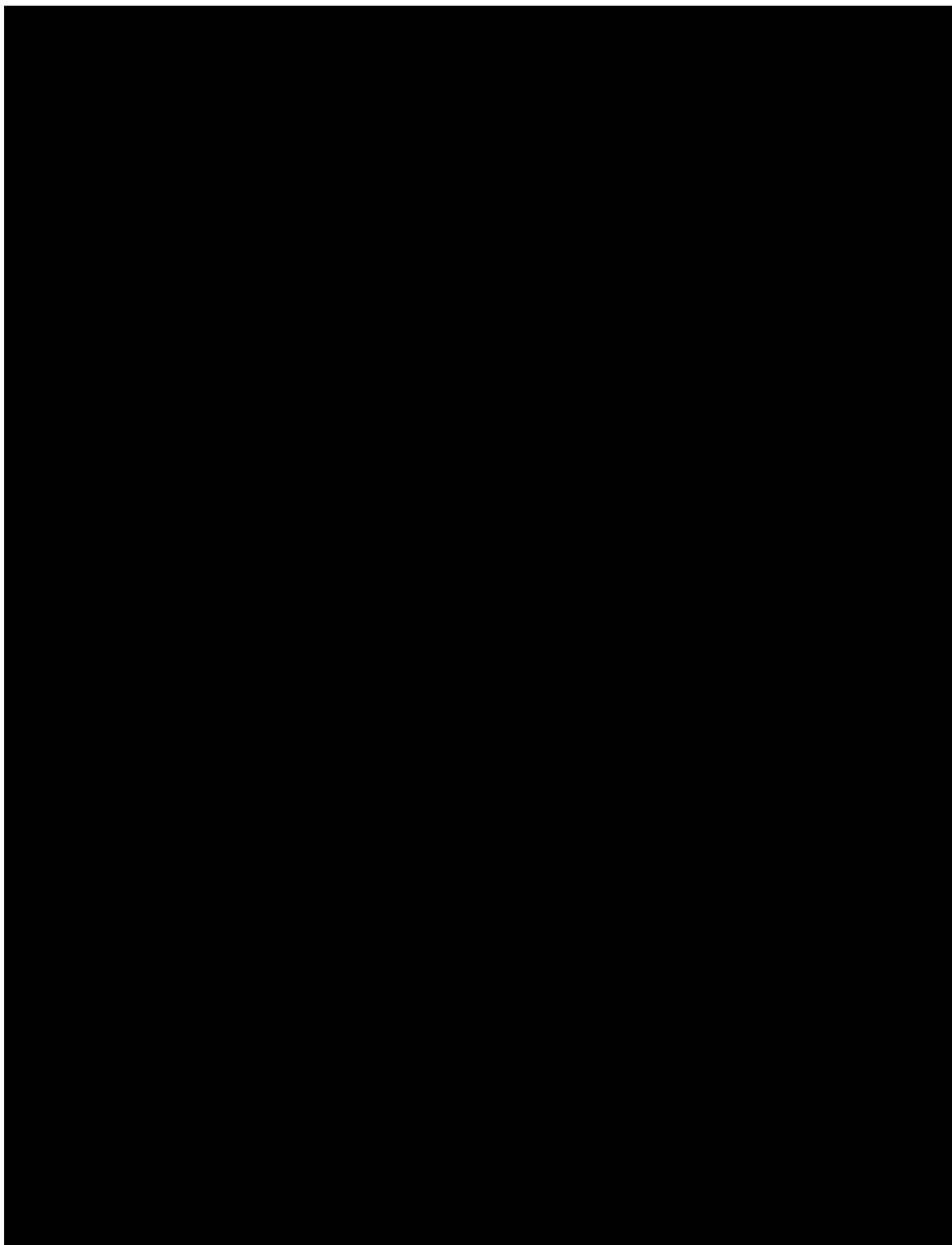


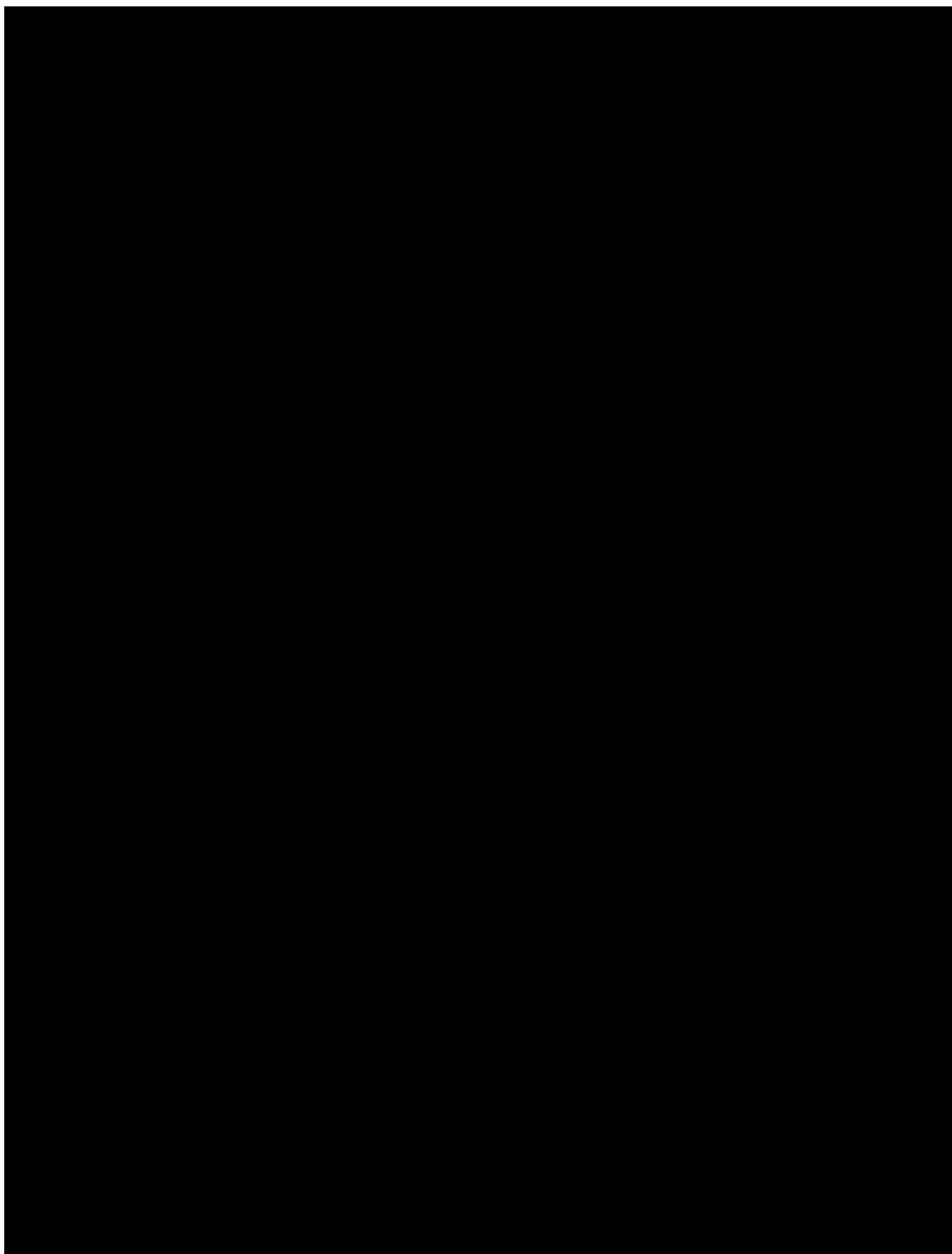
**Figure 1-59: Ellenburger Paleocave Facies**

Copied from Loucks and Kerans 2019, Example of several Ellenburger paleocave facies from Goldrus Producing Company Barnhart Ellenburger Unit No. 3 core in Reagan County, Texas. Larger clasts are outlined in yellow. (a) Debris-flow chaotic breccia in a paleocave passage. Notice that some clasts show crackle brecciation by compaction. (b) Large deformed blocks with crackle-breccia overprint at far-left column and far right









### 1.8.2 Faults





### 1.8.3 Seismic History [146.82 (a) (3) (v)]

An important consideration in the design and development of new injection well projects is the determination for the potential of injection activities to induce a seismic event. As shown in more detail below, there is a low probability, [REDACTED] of seismic events being induced or affecting the injection activities in the proposed Facility.

Studies completed by the United States Geological Survey (USGS) indicate there is a low probability of earthquake events occurring in the Delaware Basin of west Texas that would cause damage to infrastructure with only 4-10 damaging earthquake events predicted to occur over a 10,000-year time period (Fig. 1-67) (US Geological Survey Website, 2019).

Since 2020, there have been a number of earthquakes associated with oil and gas wastewater injection that may have not been contemplated in the below forecast. This will be addressed later in this section.

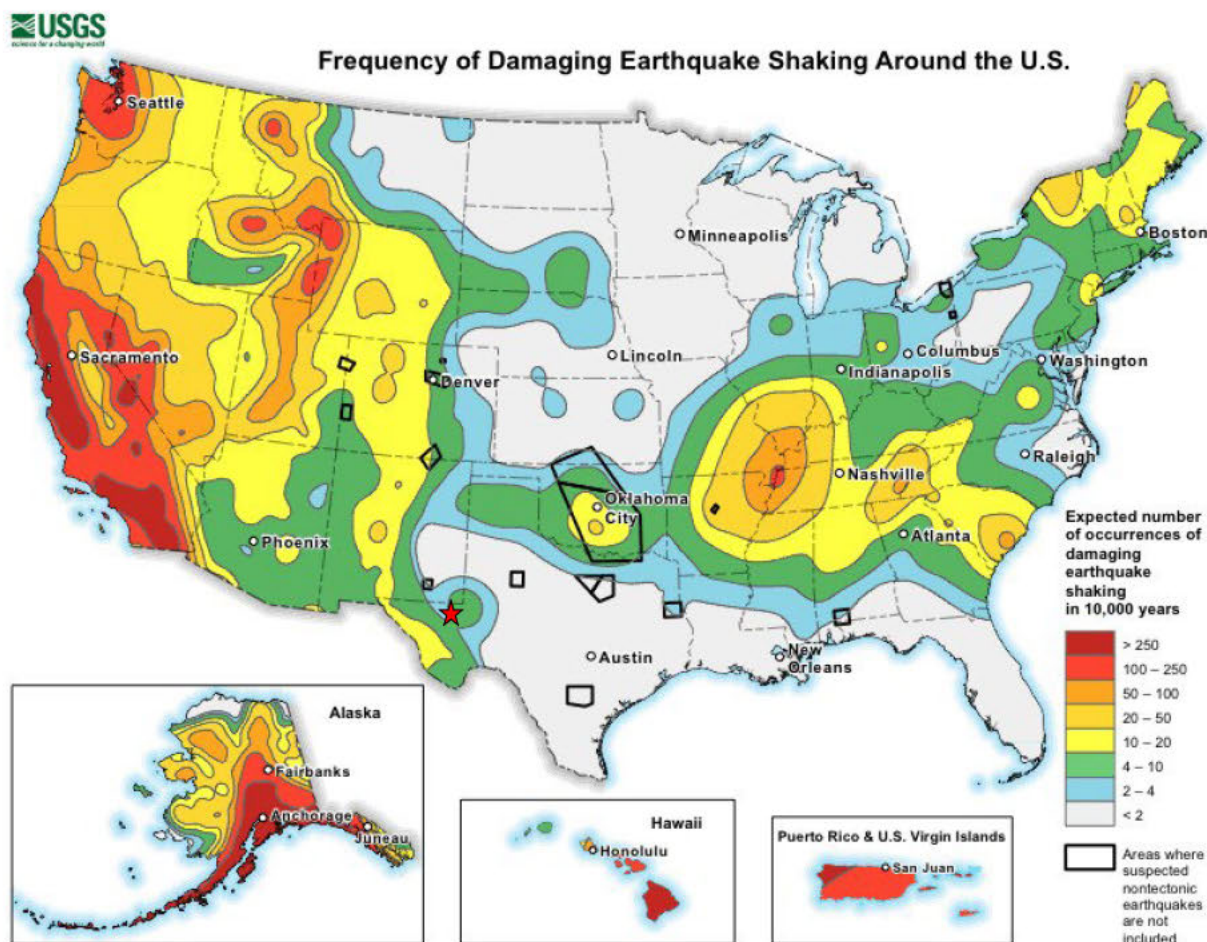


**Figure 1-67: Frequency of U.S. Damaging Earthquakes**

Probabilistic map showing how often scientists expect damaging earthquake shaking around the United States (U.S. Geological Survey Website, 2019). The map shows there is a low probability of damaging earthquake events occurring in West Texas area near the Delaware CCS #1 and CCS #2 well (red star).

Texas has several distinct structural regions, each with different fault orientations, ages and architecture (Fig. 1-68). The Central Loving Facility lies within the Delaware Basin, which can be considered part of the Basin and Range province of Texas, distinct from other regions such as the Gulf Coast.

The Basin and Range province of West Texas, in the center of the North American Craton, has fault systems related to past orogenic events and is currently being stressed by several mountain ranges to the west including the Franklin Mountains, the Guadalupe Mountains, the Sacramento Mountains and smaller ranges and the Ouachita-Marathon Thrust belt to the south. The Ouachita-Marathon thrust belt forms the northern terminus of the Balcones Fault Zone and is noted in purple. Mountain ranges are noted in red, yellow and lavender to the west of the facility (Fig. 1-66).

The current stress regime, based on earthquake moment tensor analysis, [REDACTED]

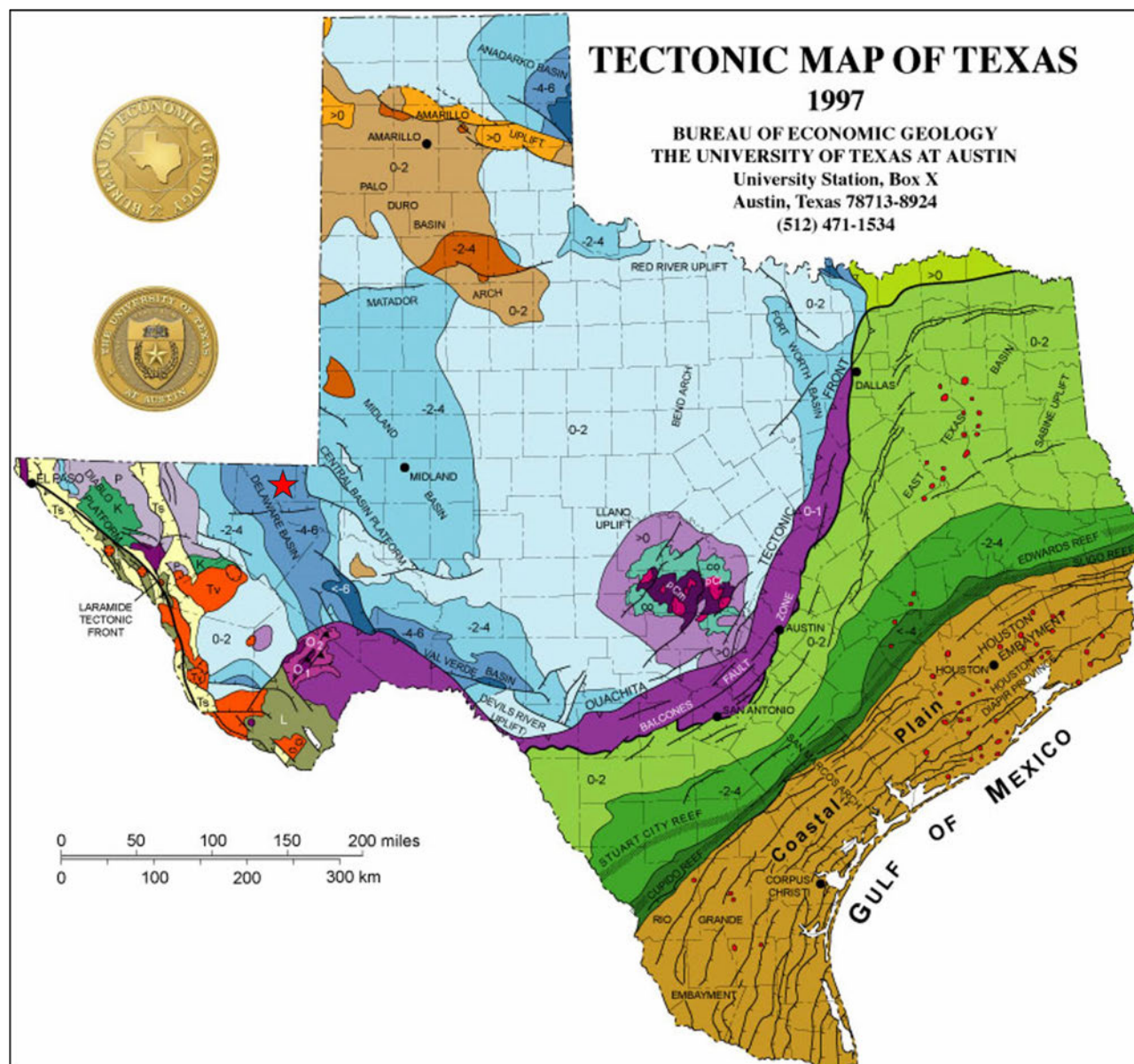
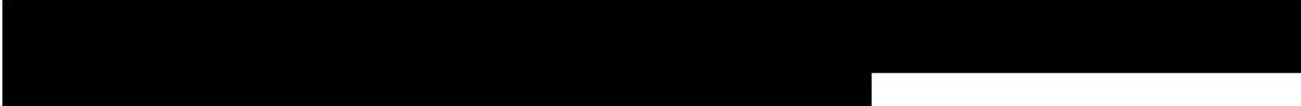


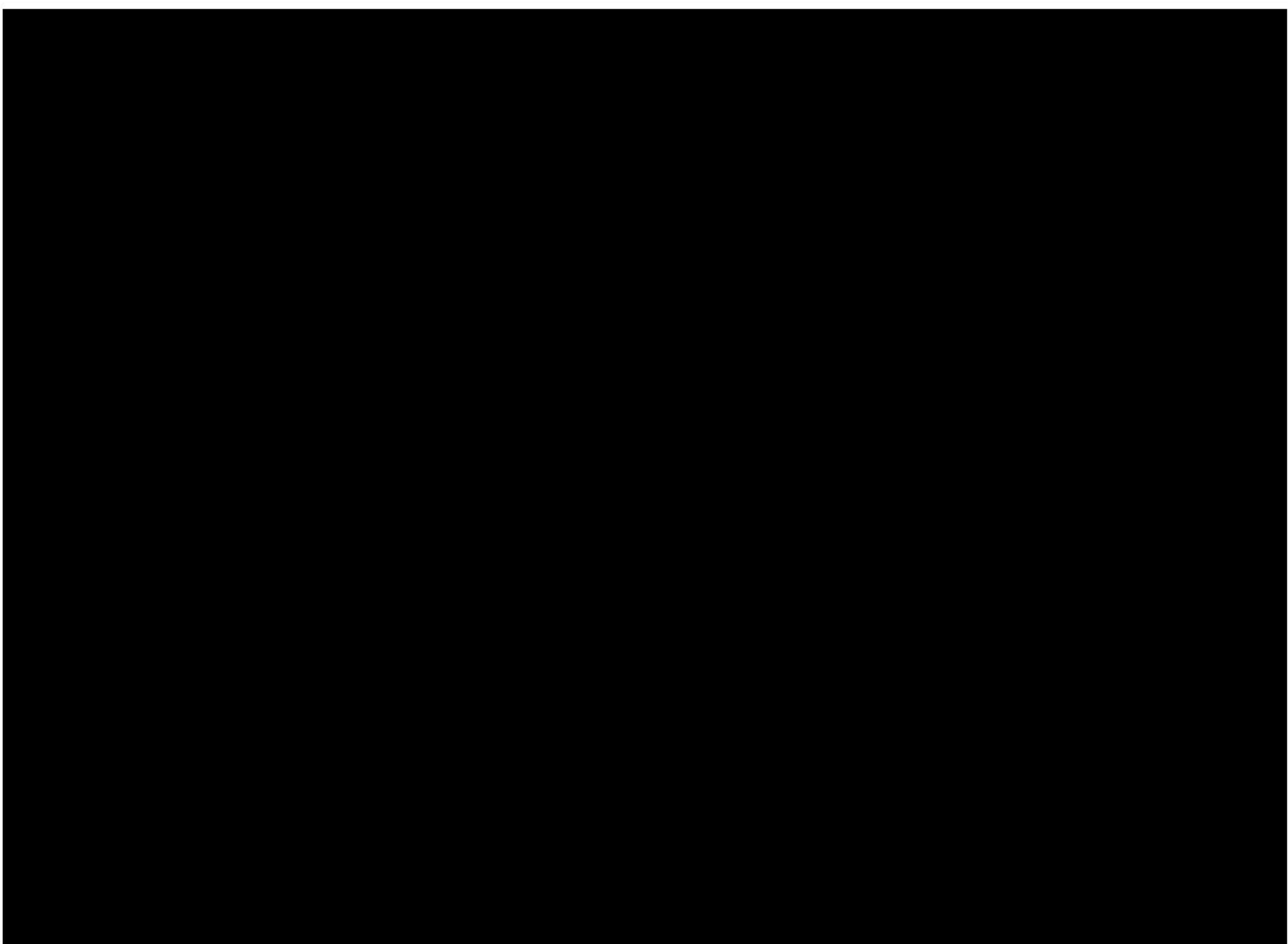
**Figure 1-68: Tectonic Map of Texas, Major Structural Features of the Lone Star State**  
 Tectonic map of Texas, BEG 1997 (Source: University of Texas Libraries Website)

The local region of the Delaware Basin has several distinct fault systems and earthquake swarms of note. The Culberson Mentone Earthquake Zone, the Grisham Fault Zone, East Loving Trend and the State Line Earthquake Trend (Fig. 1-69, 1-70).



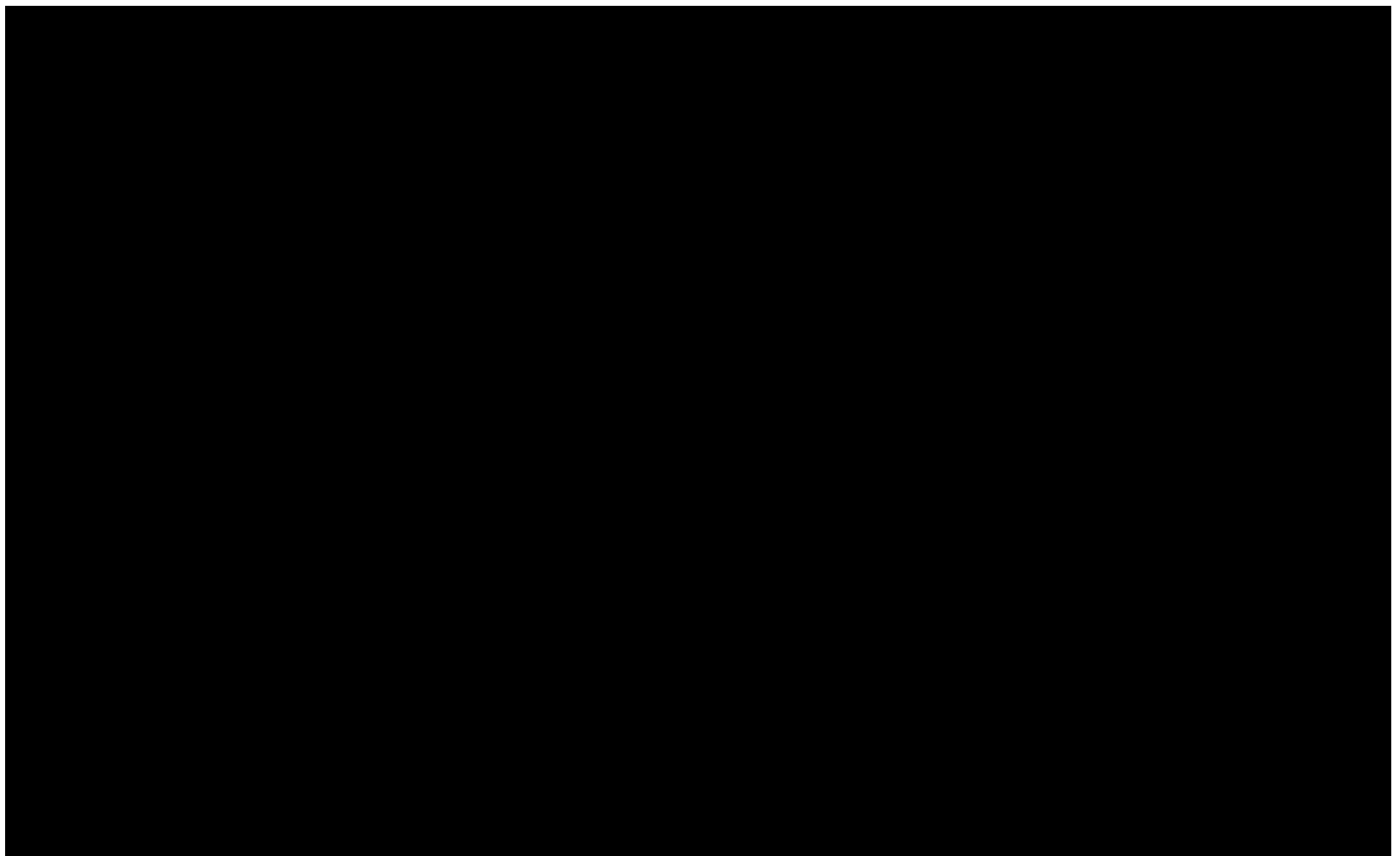
In general, moving from west to east there is a stress rotation towards either north or south, depending on the latitude.





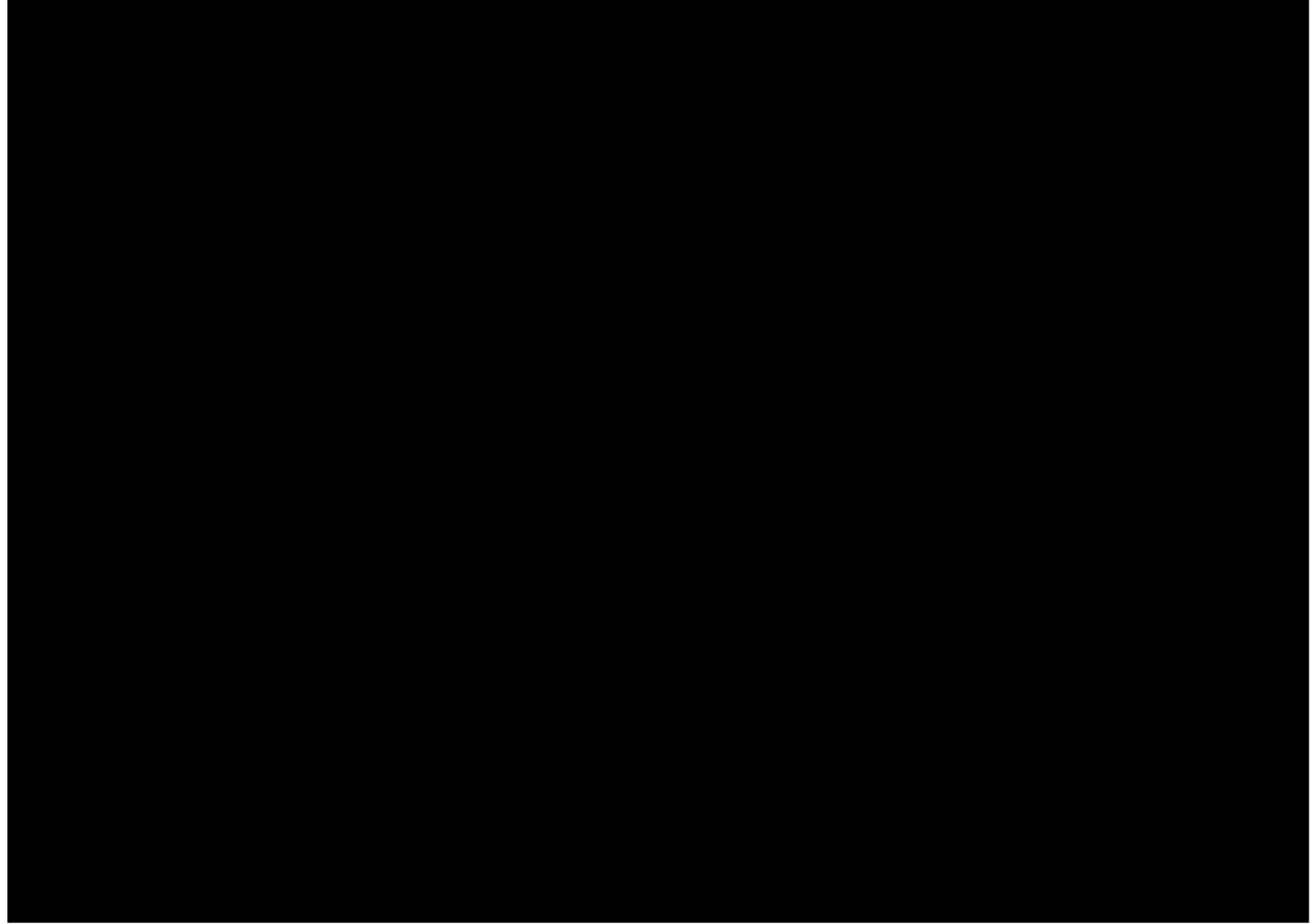
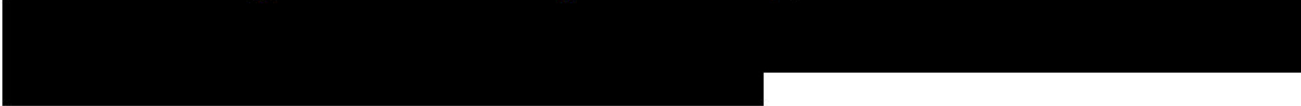
In the area within a 10-mile radius of the Central Loving Facility, the Texas Seismological Network and Seismology Research (TexNet) earthquake catalog and USGS Earthquake catalog shows little earthquake activity (Fig. 1-69, 1-70).

Despite extensive injection in shallower intervals in the area since 2016, Dvory and Zoback (2021) suggest that historical depletion of the Delaware Mountain Group (DMG) reservoirs has mollified effects of recent brine injection and reduced earthquakes. This, combined with deep [REDACTED] faults that likely have high coefficients of friction and are not prone to normal deformation, reduces the likelihood of earthquakes in the region.



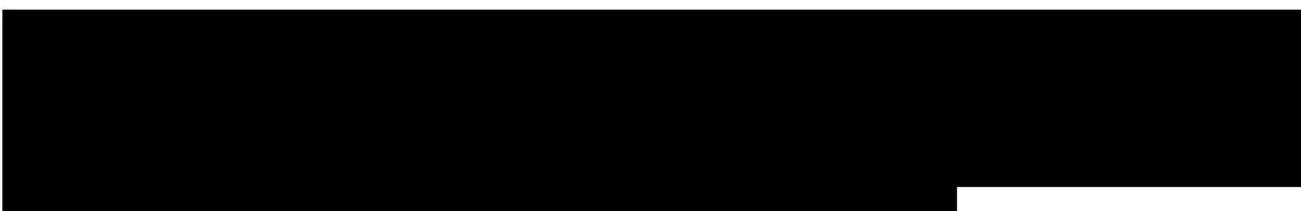
#### 1.8.4 Regional Stress

The stress regime and maximum horizontal stress orientation in the west Texas area are well-studied and understood. **Figure 1-71** shows the regional stress map.



#### 1.8.5 Fault Slippage Potential (FSP) Analysis

This section presents a fault slip potential (FSP) analysis to evaluate the likelihood of fault reactivation or slippage due to increased reservoir pressure from future CO<sub>2</sub> injection at the Central Loving Facility.

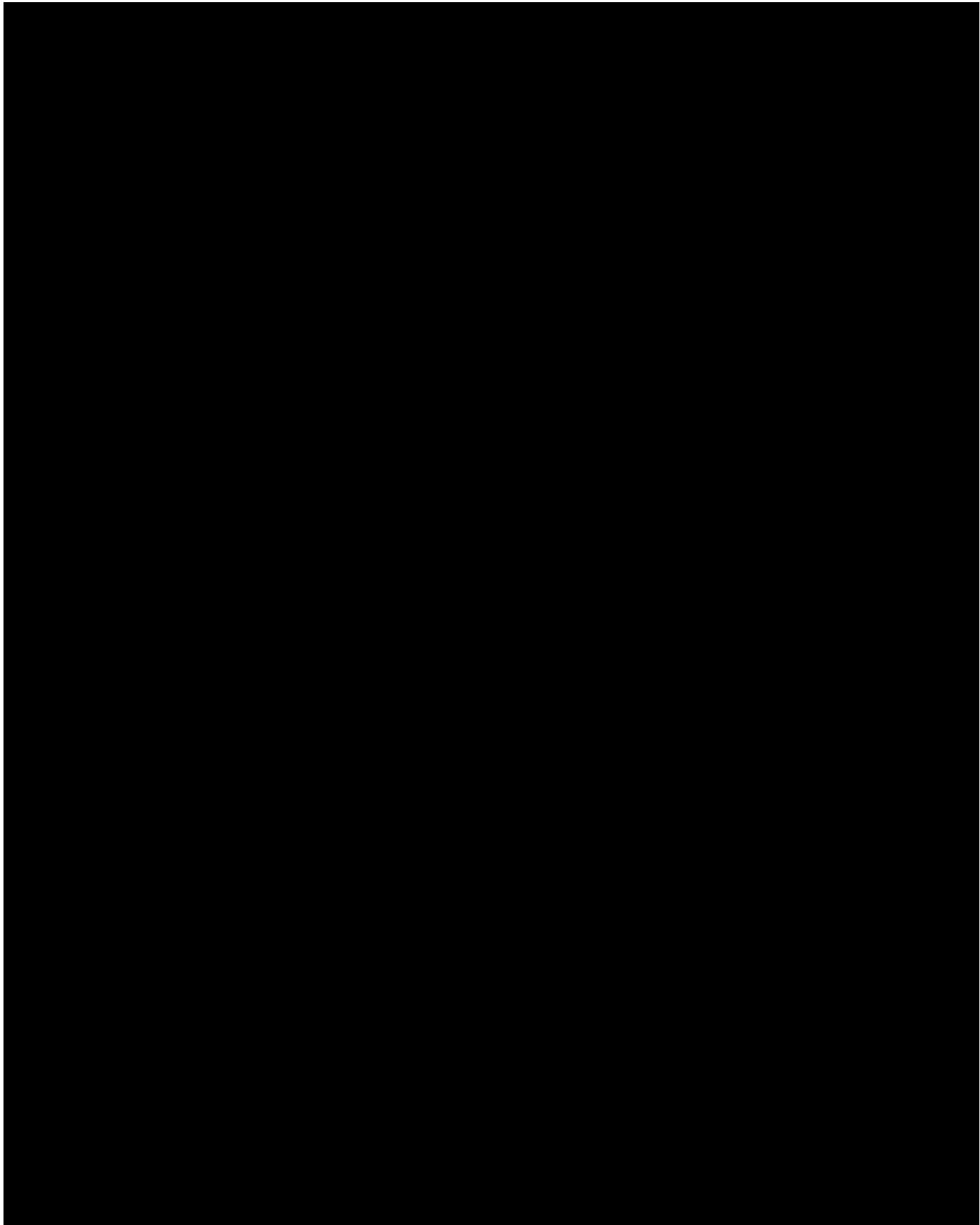














### 1.8.6 Summary



Results of USGS studies and the Fault Slip Potential (FSP) analysis indicate stable geologic conditions in the region surrounding the potential injection site. The low probability of induced seismicity due to distance away from faults and the low incremental pressure along faults with the small volume of CO<sub>2</sub> injected as part of this project suggest the probability that seismicity interfering with CO<sub>2</sub> containment is low.



## 1.9 Petrophysical Characterization [40 CFR 146.82(a)(3)(iii)] [40 CFR 146.82(a)(3)(iv)]

This section includes a petrophysical characterization of the injection and confining zones and includes discussion on porosity, permeability, salinity, capillary pressure and related properties. The petrophysical properties indicate the proposed Well location is suitable for the project due to it having sufficient storage (porosity), ability to inject (permeability) and the in-situ formation waters have a salinity that is significantly higher than the statutory lower limit of 10,000 parts per million (PPM) at an average salinity of [REDACTED]. Further, [REDACTED]

### 1.9.1 Type Log

The type log in Figure 1-78 is a penetration to the southeast of the facility. [REDACTED]





### 1.9.2 Porosity









### 1.9.3 Permeability

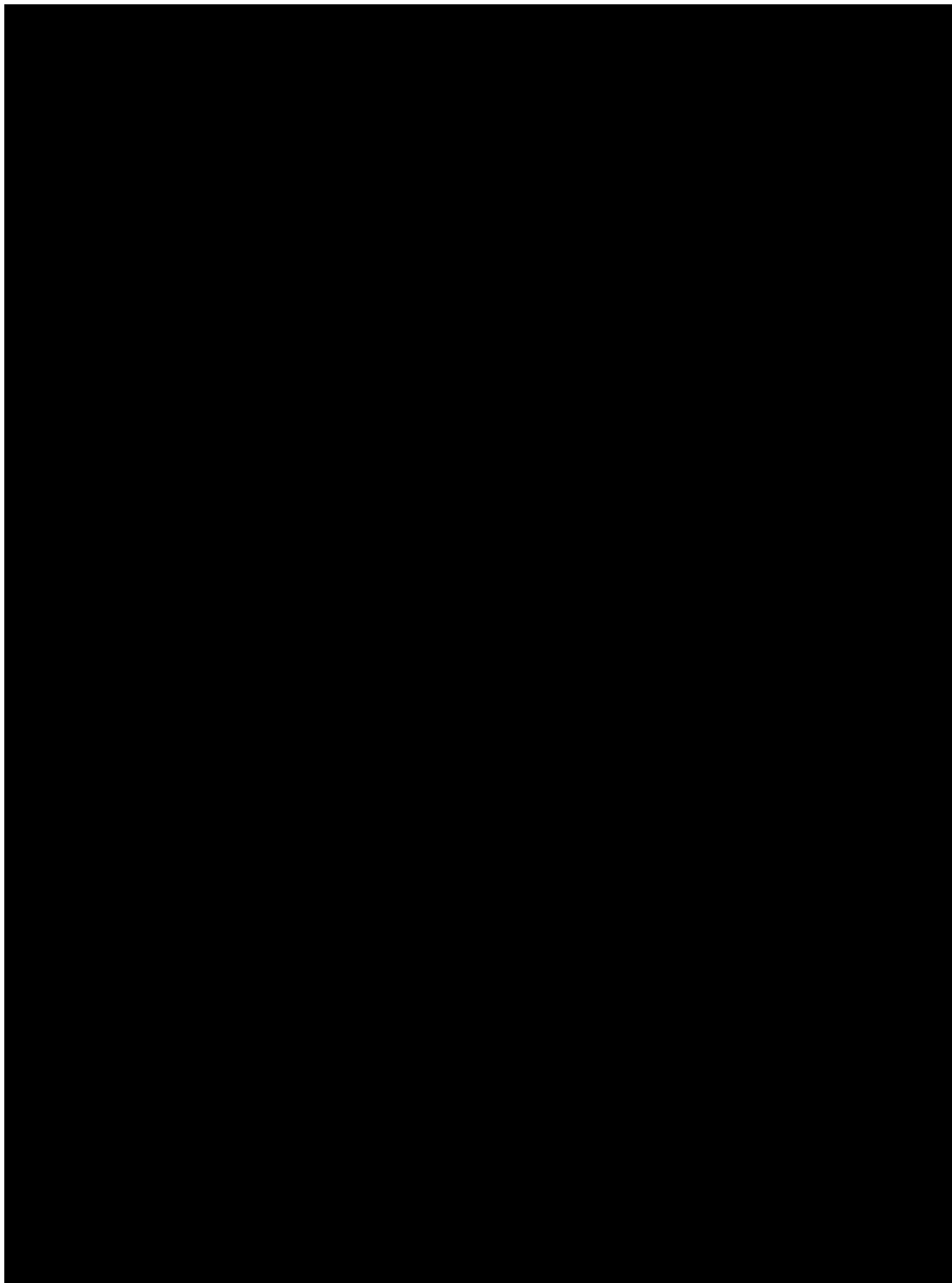
16. **What is the primary purpose of the *Journal of Clinical Endocrinology and Metabolism*?**

1. **What is the primary purpose of the proposed legislation?**

10. **What is the primary purpose of the *Journal of Clinical Endocrinology and Metabolism*?**

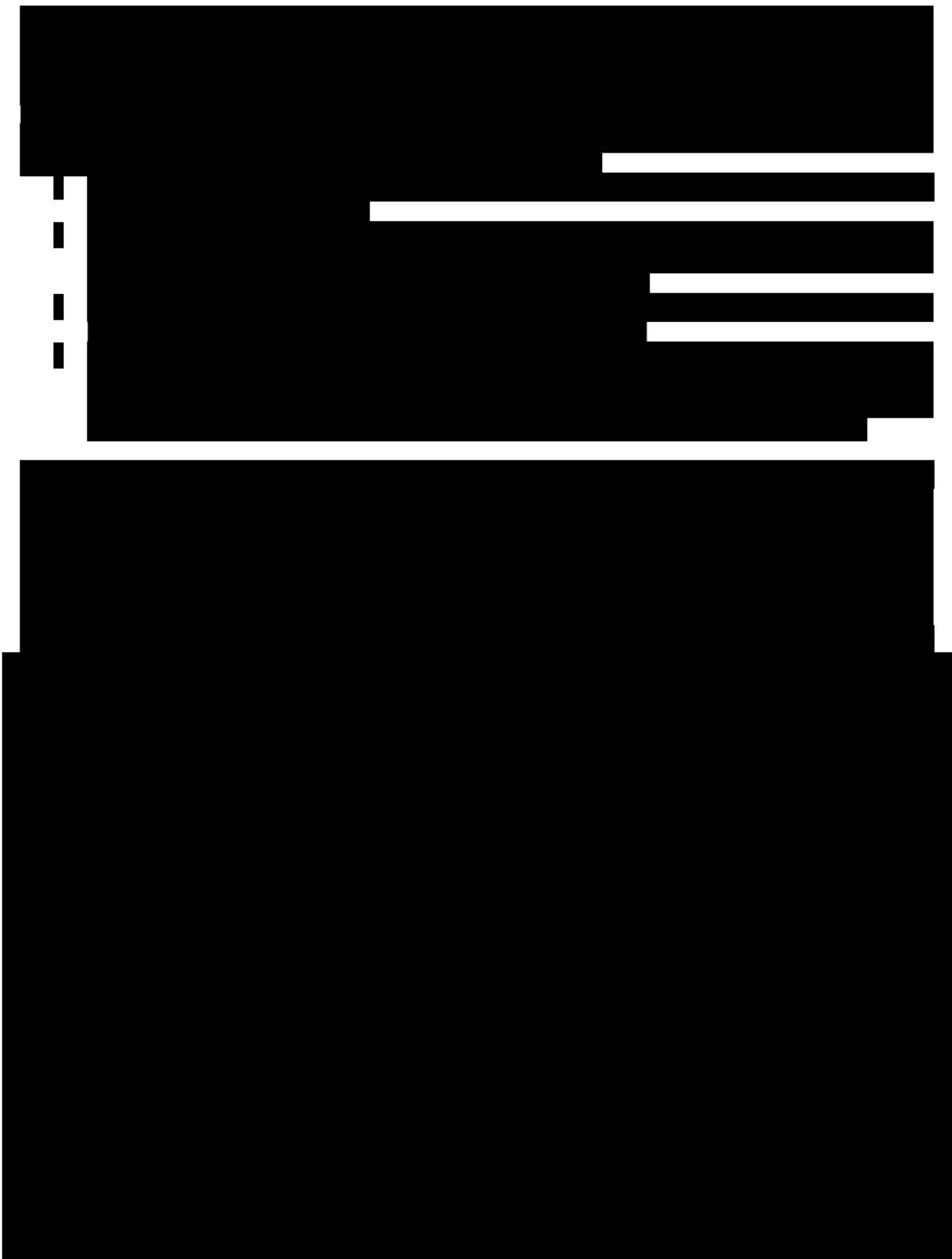
11. **What is the primary purpose of the *Journal of Clinical Endocrinology and Metabolism*?**







#### 1.9.4 Salinity







### 1.9.6 Capillary Pressure

Porosity and permeability data, but not full capillary pressure data, is available in the literature for Ellenburger and to a lesser extent the Siluro-Devonian. Milestone intends to thoroughly test the capillary pressure during pre-operational testing once core samples are retrieved. Therefore, this application will focus on the capillary pressure

[REDACTED]

Existing literature supports the idea that the incremental increased pressure from injection activity of [REDACTED] will not exceed the unconfined threshold entry pressure of the shales, 10,000 psi. Thus, the Barnett Shale provides an adequate Top Seal to the system. (See permit **Section 2** for additional information about pressure changes in the system.)

[REDACTED]

Sigal reported in his conclusions, "For all the [REDACTED] samples measured, significant mercury intrusion occurs only at pressures above 10,000 psi. This corresponds to a pore throat that is 18 nm in diameter."

[REDACTED]

The importance of capillary pressure data cannot be understated. Additional data points from core from the proposed Wells will be acquired when core samples are acquired.

[REDACTED]

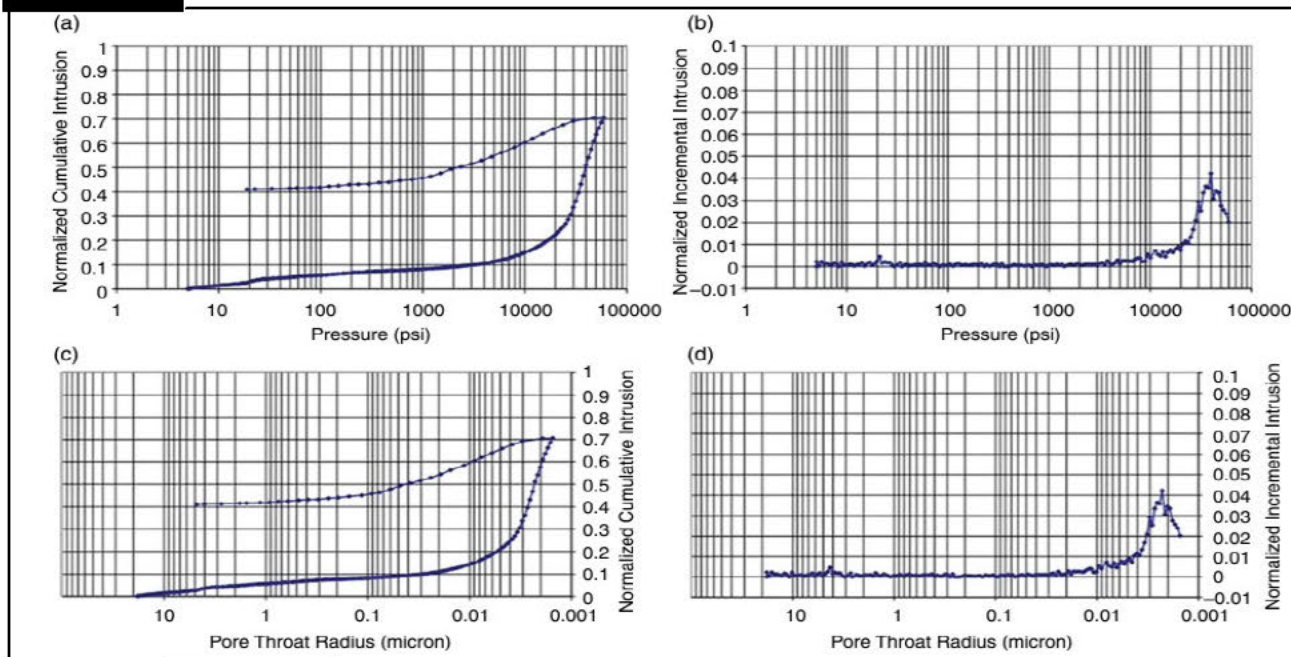


Figure 1-90: [REDACTED] Capillary Pressure Curves (Sigal, 2013)

## 1.10 Geomechanics [40 CFR 146.82(a)(3)(iv)]

This section discusses data for the upper confining zone, Siluro-Devonian and Ellenburger injection zones' related stress, ductility, rock strength, and initial pore pressures. At the proposed injection Well locations, 90% of the minimum horizontal stress is [REDACTED]

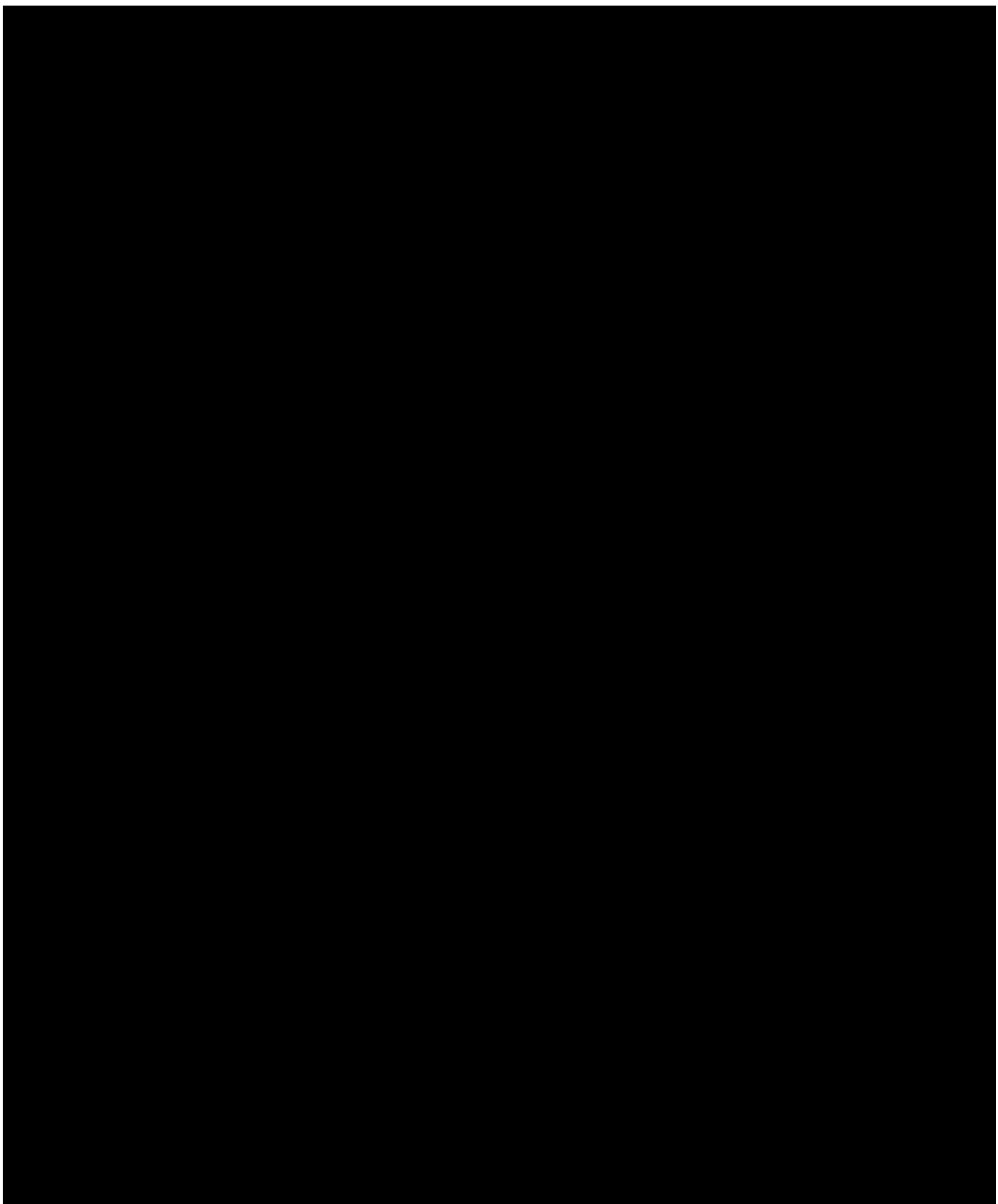
[REDACTED] Therefore, the hydraulic fracture pressure, even with an additional 10% tolerance, is still well in excess of the pressure during injection, showing this location and formation are suitable for permanent CO<sub>2</sub> sequestration. Further, USDWs will not be impacted by any CO<sub>2</sub> escaping via hydraulic fracturing.

### 1.10.1 Methods

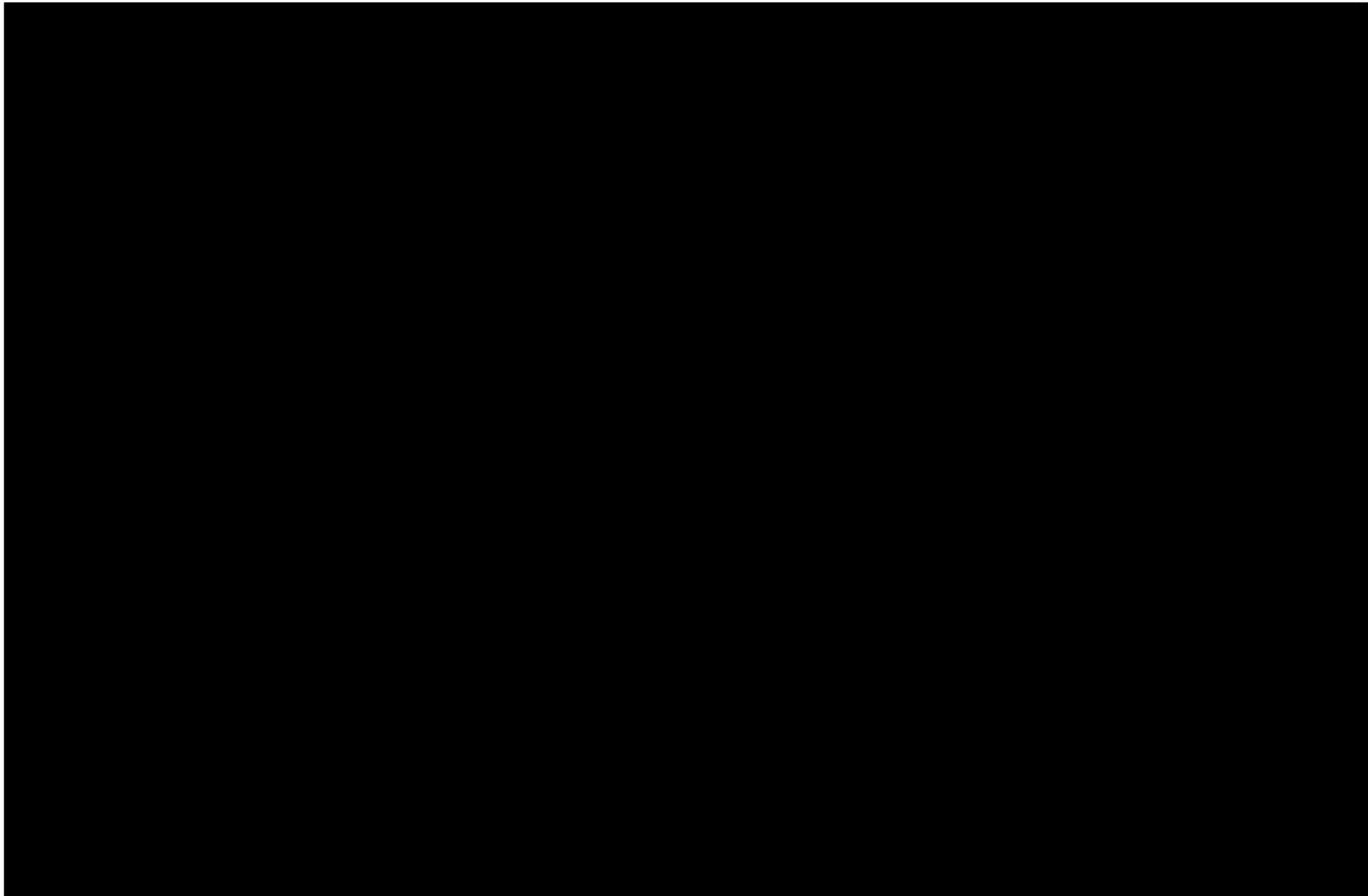
[REDACTED]

[REDACTED]

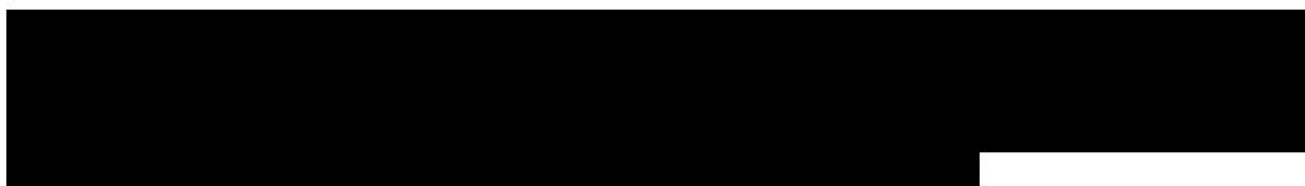
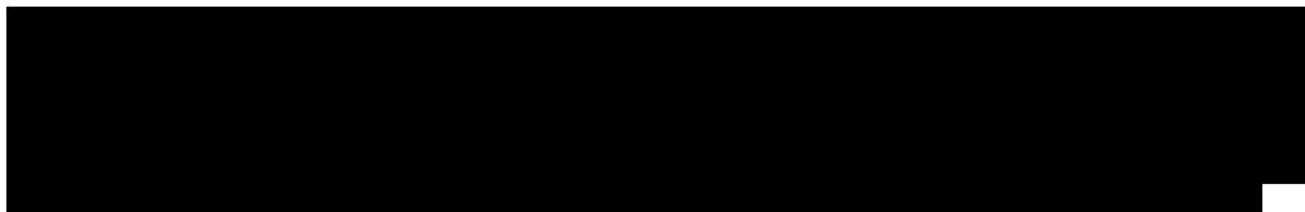
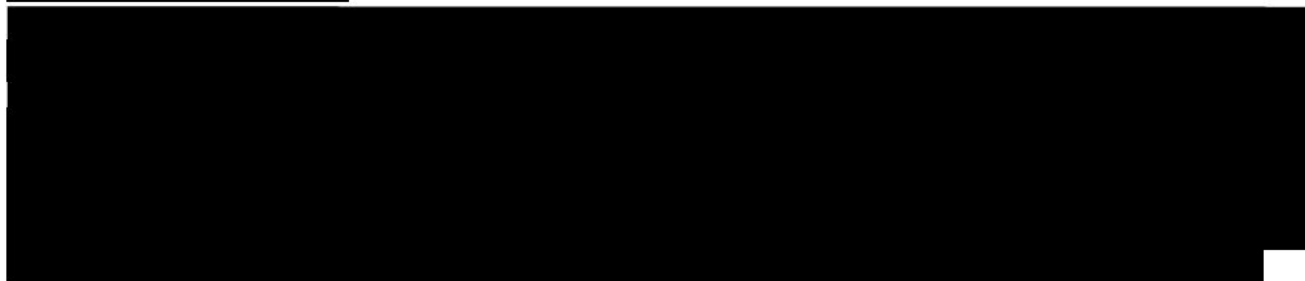
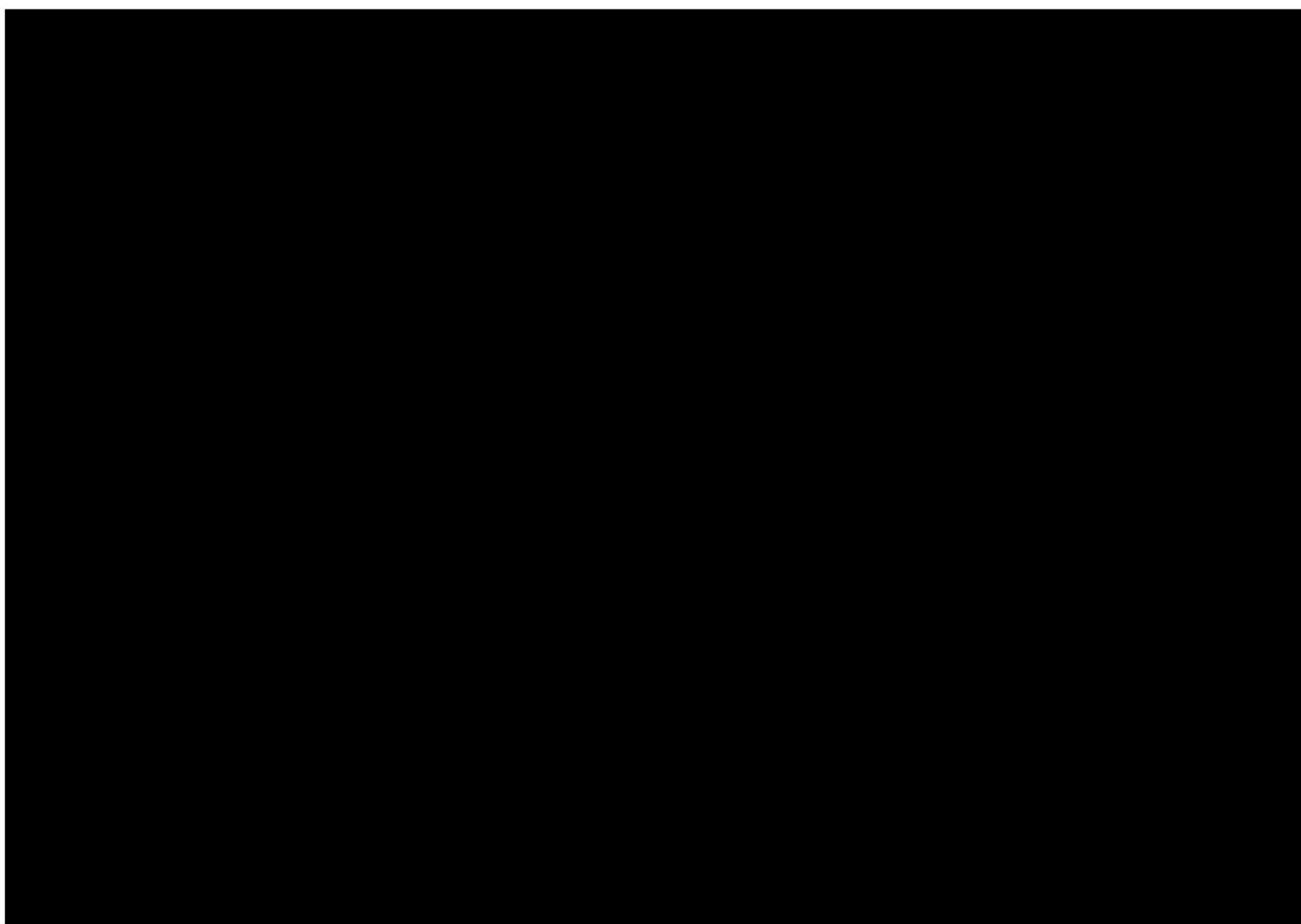
[REDACTED]



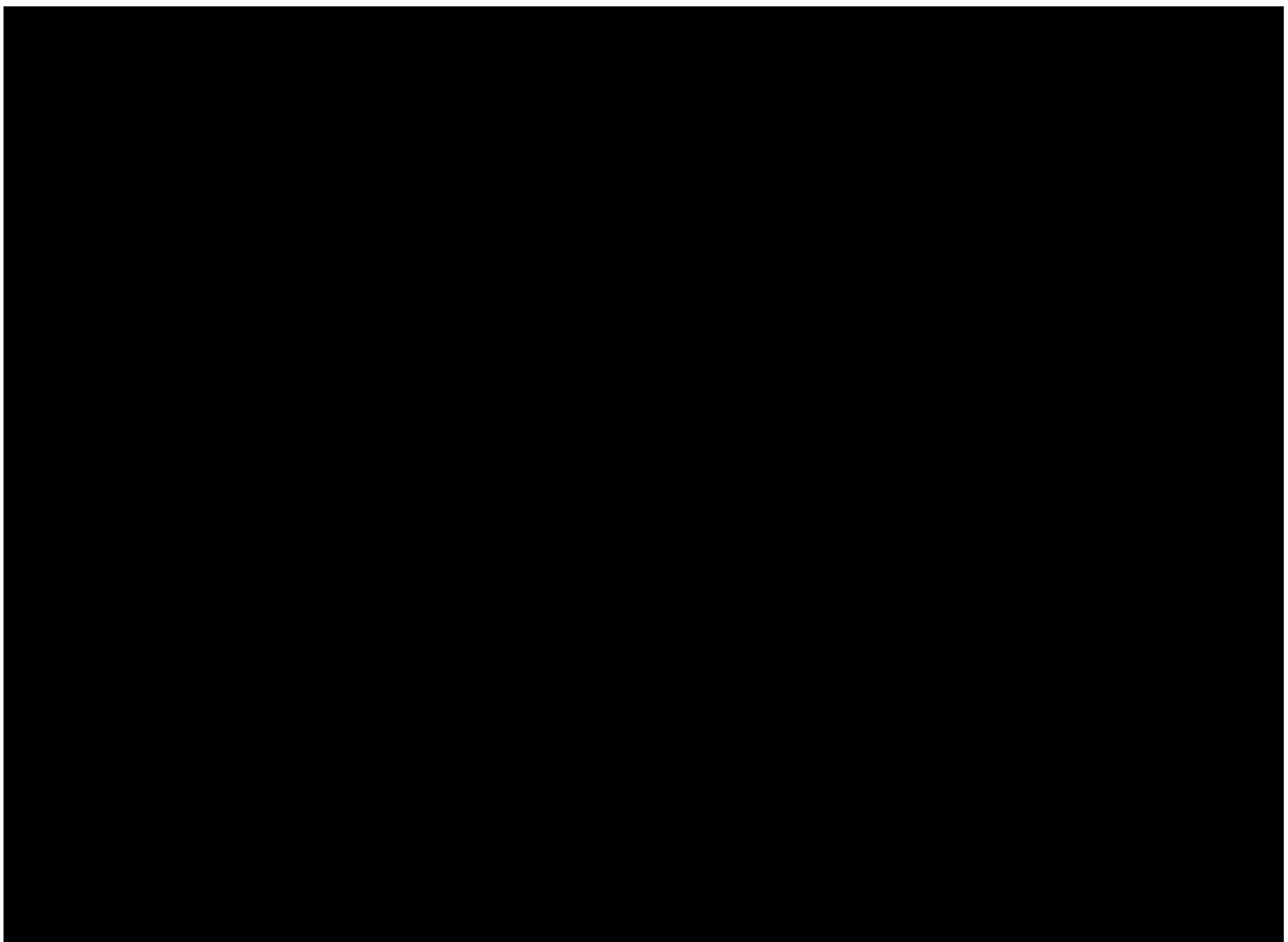
### 1.10.2 Pore Pressure











#### **1.10.4 Stress Orientation**

Maximum-principal-stress direction is observed to be nearly E-W in central Loving County. Most measurements put it at 75 from true north +/- 15 in a clockwise direction. World Stress Map data shown in **Figure 1-95** illustrates the consistent mostly E-W pattern of stress direction. This has been proven repeatedly by horizontal well development in the basin as well. There is some rotation of the stress field to the south of Loving County in southern Reeves County proximal to the Ouachita Thrust Belt and to the west in Culberson County near the Guadalupe and Davis Mountains. These rotations are far from the facility, over 25 miles, and not expected to affect injection. There is high confidence based on repeated tests that the max stress orientation is oriented 75 +/- 15° from true north in the central part of Loving County.

### 1.10.5 Rock Strength

[REDACTED]

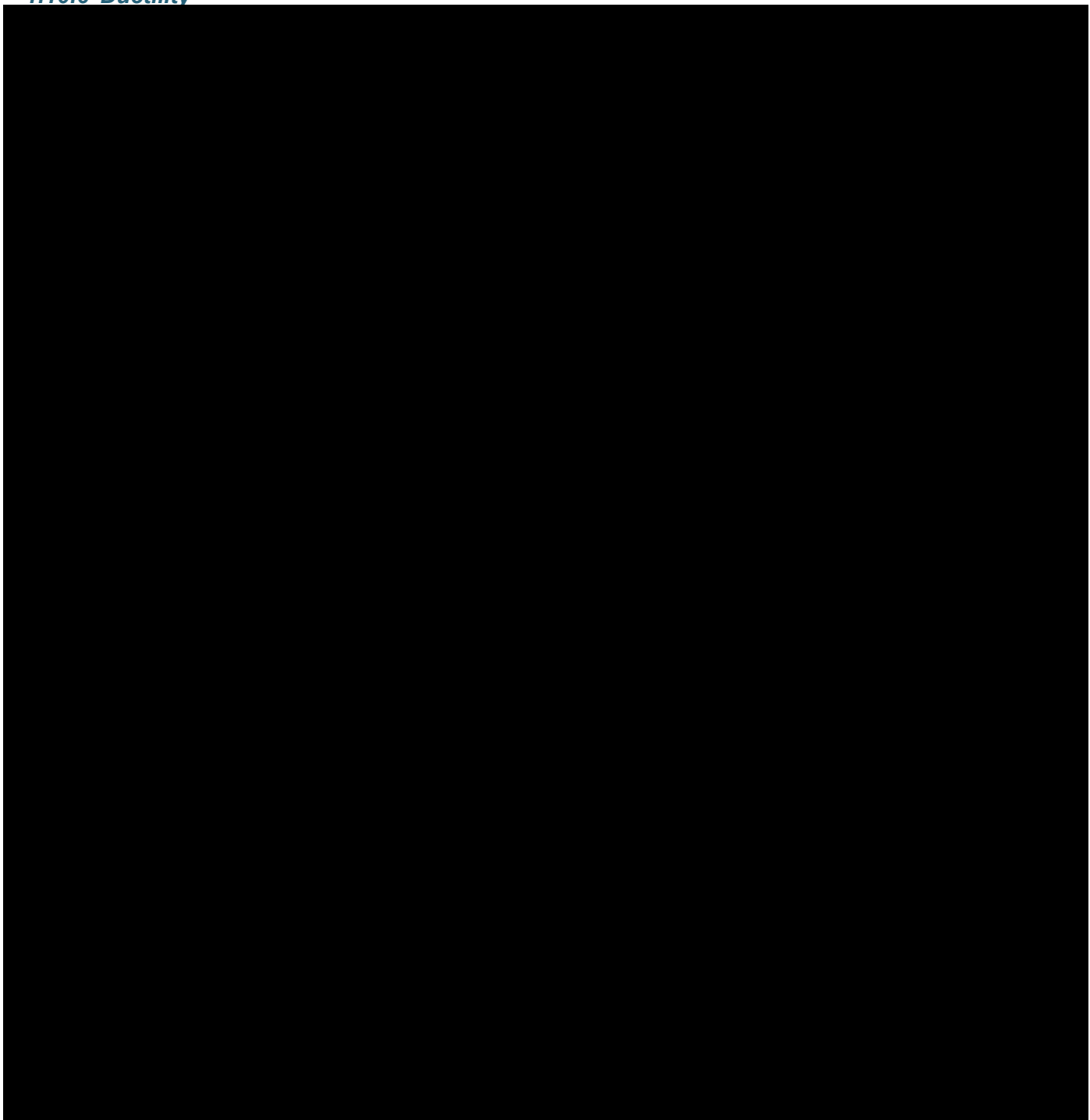
[REDACTED]

[REDACTED]

[REDACTED]

[REDACTED]

### 1.10.6 Ductility



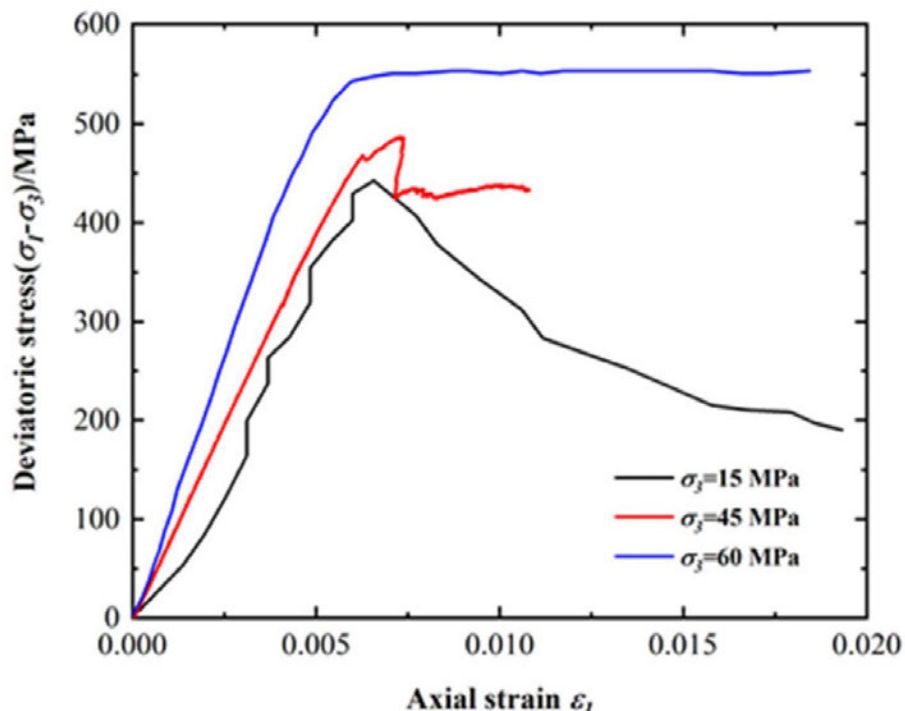
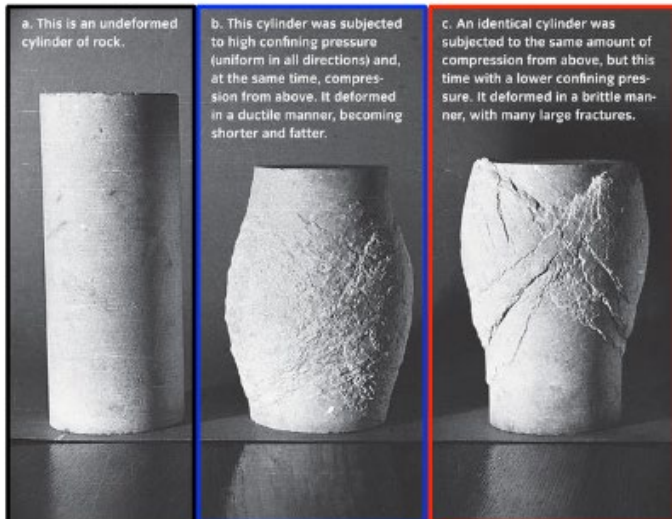


**Figure 1-96: Dolomite Triaxial Test from Analogous Low Porosity Dolomite**

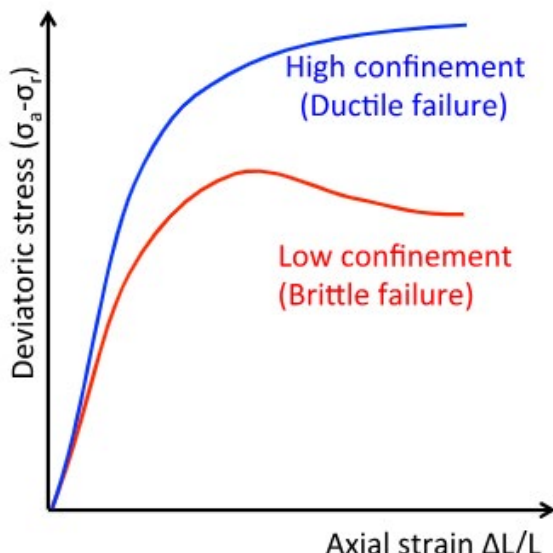
Dolomite triaxial test from analogous low porosity dolomite found in China. Exhibits brittle behavior at low confining stress and ductile behavior at high confining stress ( $\sigma_3$ ). blue line or 60



Visualizing Geology, WileyPlus

**Figure 1-97: Example of Brittle and Ductile behavior**

It is proposed that due to the extreme confining pressure, the Injection Interval may behave ductile, blue box/line (Source: <https://dnicolasespinoza.github.io/node/31.html>)



### 1.10.7 Additional Testing

Extensive additional geomechanics testing will be performed once core material is obtained from a stratigraphic test well. See permit **Section 5** – Preoperational testing for more discussion.

## 1.11 Geochemistry [40 CFR 146.82(a)(6)]

This section covers the fluid and solid-phase geochemistry of subsurface formations in the AoR and modeling of the mineral-brine-CO<sub>2</sub> system across the mineralogical facies associations present for the injection Wells.

Milestone Carbon, LLC (Milestone) has requested that Daniel B. Stephens & Associates, Inc. (DBS&A) perform geochemical modeling for a proposed carbon sequestration project in the Delaware Basin to help comprehend chemical reactions during carbon dioxide (CO<sub>2</sub>) storage in the Siluro-Devonian and the Ellenburger Formations. Information used to perform the modeling was obtained from Milestone's project narrative, the U.S. Geological survey (USGS), and the geologic literature, as well as other data provided by Milestone.

Geochemical modeling was conducted to evaluate the compatibility of the injectate with groundwater and rocks composing the aquifer system. The intent of the modeling is to identify the major potential reactions that may affect injection or containment (U.S. EPA, 2013).

Geochemical modeling using the PHREEQC (pH-REdox-Equilibrium) software was used to calculate the behavior of minerals and changes in aqueous chemistry based on chemical equilibrium conditions (Parkhurst and Appelo, 2013).

### 1.11.1 Geochemistry for Central Loving Project

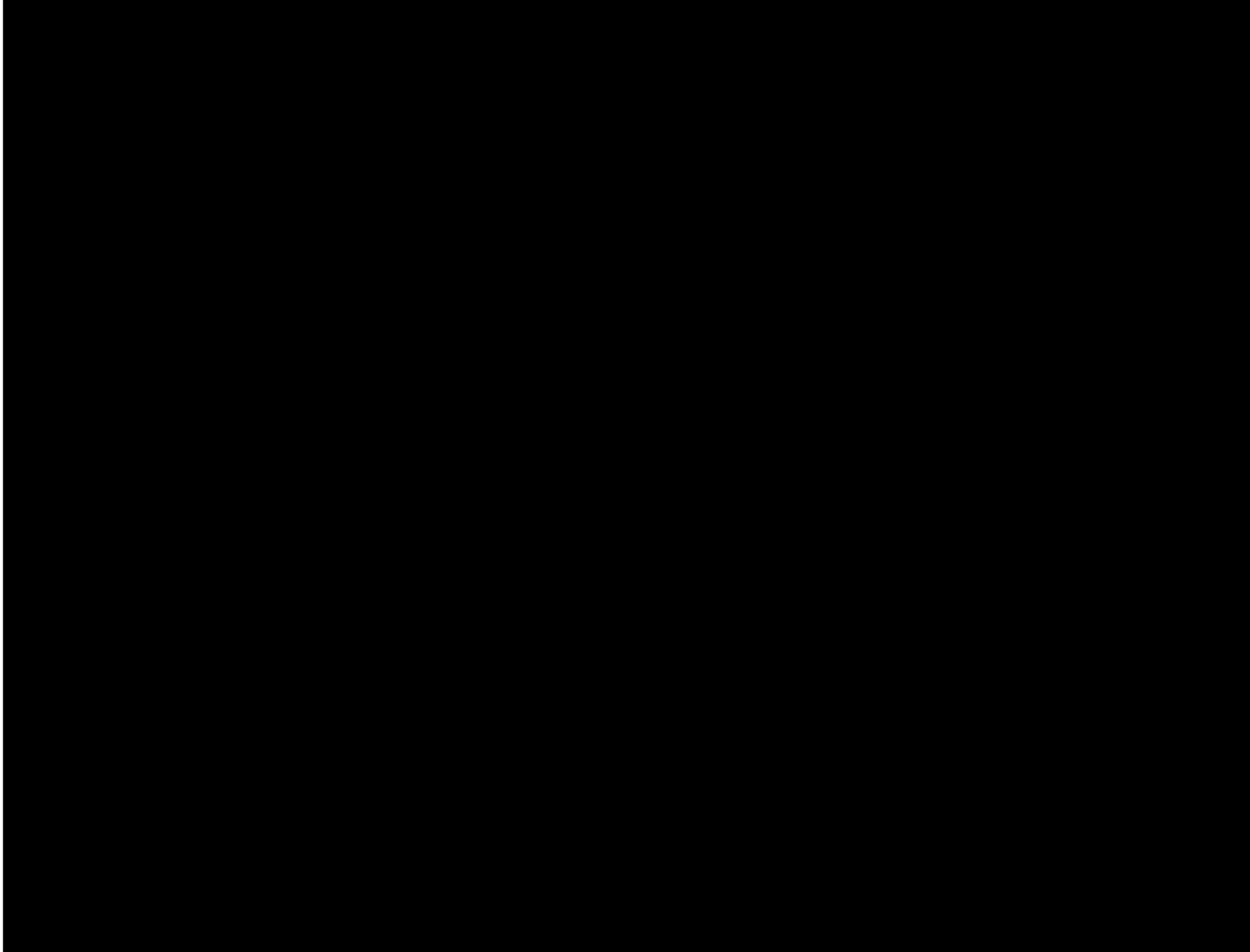
The Facility is located in the Delaware Basin that is part of the Permian Basin.

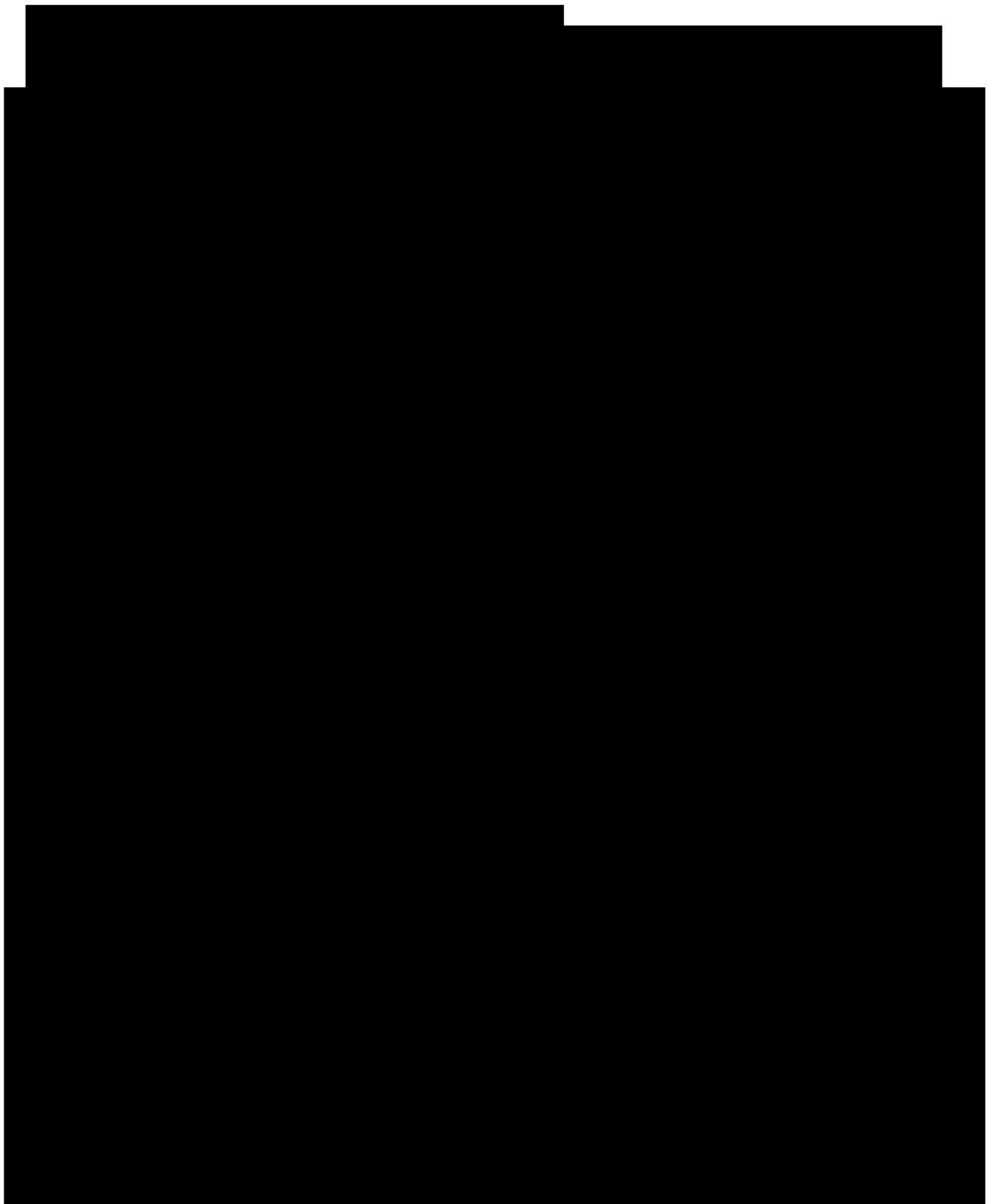


While rocks are buried in the Earth's crust, weathering and chemical reactions between the rocks and groundwater are termed diagenesis, which involves the dissolution of minerals into groundwater and precipitation of minerals from solution. Reactions are driven by fluid movement, temperature, and pressure changes due to burial depth and compaction. Over time, minerals and cements may dissolve and form new minerals. Important reactions that have occurred in the rocks of the Delaware Basin include the following:

- Precipitation and dissolution of cements and authigenic minerals, consisting of various minerals including quartz, clays, potassium feldspar (K-feldspar), plagioclase feldspar, and particularly calcite, and dolomite
- Dissolution of feldspars, quartz, and carbonates
- Formation of feldspar and quartz overgrowths
- Precipitation of illite, smectite and other clays

#### ***1.11.1.1 Brine Geochemistry***





**1.11.2.1 Geochemical Database**

For reactions involving water and minerals, the equilibrium relationship between products and reactant activities (concentrations) can be calculated using known values for parameters like Gibbs free energy found in thermodynamic databases (Parkhurst and Appelo, 2013). Thermodynamic values for these calculations are compiled in databases from several entities including the USGS and Lawrence Livermore National Laboratory (LLNL). A database developed at the Lawrence Livermore National Laboratory (LLNL.dat) was used for this evaluation. The LLNL.dat database includes a temperature range for the thermodynamic data provided from 0 to 300-degC. This database is appropriate for the groundwater concentrations, pressure, and temperature used in the modeled scenarios.

When modeling saline waters, the Pitzer database (Parkhurst and Appelo, 2013) is often used, but it has thermodynamic data for a limited number of minerals including calcite, dolomite, gypsum, and quartz. The Ellenburger and Devonian injection zones are predominantly composed of minerals that are not included in the Pitzer database; therefore, the LLNL.dat database was used because it also includes smectite, illite, and the minerals listed in Table 1-23.

**1.11.2.2 Saturation Indices**

Saturation indices (SIs) were calculated to represent whether a particular mineral (e.g., calcite) is in chemical equilibrium with the groundwater. (Hem, 1985) SI calculations (1-8) are used to predict if a mineral is likely to precipitate or dissolve in the groundwater and if these reactions changed the concentrations of dissolved elements.

Chemical equilibrium was assumed for the reactions in the model. Equilibrium modeling sets the saturation indices to a zero (0) value for a given mineral. Minerals used in the modeling scenarios were set to their relative abundances. The assumption of chemical equilibrium allows dissolution and precipitation reactions to be quantified in the model.

The formula for calculating SI is as follows:

$$SI = \frac{IAP}{K_{sp}}$$

where SI = saturation index

IAP = ion activity product

| K<sub>sp</sub> = solubility product

(1-8)

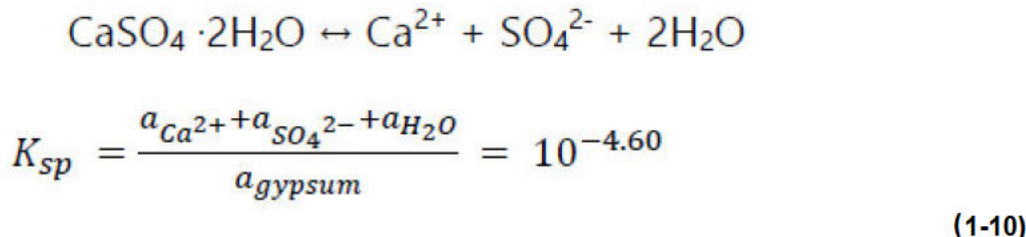
Using gypsum as an example (Hem, 1985), the ion activity product of gypsum (IAP<sub>gypsum</sub>) is the product of the activity (a, activity is approximately equal to concentration in dilute solutions) of calcium (Ca) and sulfate (SO<sub>4</sub>):

$$IAP = a_{Ca^{2+}} \times a_{SO_4^{2-}}$$

(1-9)

The solubility product,  $K_{sp}$ , is an indication of the relative solubility of a mineral in water. A value less than zero ( $<0$ ) indicates that the mineral will dissolve and contribute ions to solution and may result in a relatively high activity or concentration. A value greater than zero ( $>0$ ) indicates that the mineral has a low solubility, may precipitate from solution, and will not contribute many ions to the solution.

For the mineral gypsum, the  $K_{sp}$  based on the dissociation reaction of gypsum in water is:



Interpreting the results of the SI calculation is straightforward:

- Log SI  $> 0$  indicates that mineral is supersaturated in solution and may precipitate onto aquifer matrix.
- Log SI = 0 indicates that mineral is at chemical equilibrium with the water.
- Log SI  $< 0$  indicates that mineral is undersaturated in solution and may dissolve from aquifer matrix.

Due to potential systematic errors introduced during sampling and analysis, results within the range of  $\pm 0.5$  of zero are typically considered in or near chemical equilibrium.

### 1.11.3 Geochemical Model Pressure and Temperatures

To construct the equilibrium models in PHREEQC, site-specific data were used as input, including measured water chemistry, and calculated temperature and pressure.



### 1.11.4 Geochemical Modeling Results and Discussion

#### 1.11.4.1 Modeling Steps

Model results showing the changes in mineralogy designated as equilibrium phases in PHREEQC are presented for the modeled geologic units in Tables 1-25 and 1-26. Model results are presented in Table 1-27 for the water chemistry based on the equilibrium phases. The modeling steps were as follows:

- [REDACTED]
- [REDACTED]
- [REDACTED]
- [REDACTED]

#### **1.11.4.2 Equilibrium Modeling Results**

Model results showing the changes in mineralogy designated as equilibrium phases in PHREEQC are presented for the modeled geologic units in **Tables 1-25** and **1-26**. Model results are presented in **Table 1-27** for the water chemistry based on the equilibrium phases. Initial results are before injection begins and final results are at the end of injection with elevated pressures.

- [REDACTED]





## 1.12 Mineral Resources

11. **What is the primary purpose of the *Journal of Clinical Endocrinology and Metabolism*?**

—

10. **What is the primary purpose of the *Journal of Clinical Endocrinology and Metabolism*?**



## 1.13 Site Suitability [40 CFR 146.83]

[REDACTED]

[REDACTED]

[REDACTED]

### 1.13.1 Subsurface Distribution of Fractures – Implications for CO<sub>2</sub> plume migration

[REDACTED]

[REDACTED]

[REDACTED]

[REDACTED]

### 1.13.2 Injectability

[REDACTED]

[REDACTED]

[REDACTED]

### 1.13.3 Carbon Dioxide Containment



### 1.13.4 Secondary Confinement Zones



#### 1.13.5 Carbon Dioxide Interaction with Well Materials and Formation

[REDACTED]

[REDACTED]

#### 1.13.6 Total Storage Capacity

[REDACTED]

## 1.14 Well Index Tables

As noted in **Section 1.3** overview of the AoR, due to the difficulty of reading well names for the large amount of water wells, and oil and gas wells above the injection zone, these wells have been indexed into tables: **Table 1-29** and **1-30**. Each existing non-project well is denoted by its index number throughout permit **Section 1.3**.

### 1.14.1 Water Well Index Table

Index	Well Name	Latitude	Longitude	Depth (ft)
1	W1	35.88888888888889	-100.88888888888889	1000
2	W2	35.88888888888889	-100.88888888888889	1000
3	W3	35.88888888888889	-100.88888888888889	1000
4	W4	35.88888888888889	-100.88888888888889	1000
5	W5	35.88888888888889	-100.88888888888889	1000
6	W6	35.88888888888889	-100.88888888888889	1000
7	W7	35.88888888888889	-100.88888888888889	1000
8	W8	35.88888888888889	-100.88888888888889	1000
9	W9	35.88888888888889	-100.88888888888889	1000
10	W10	35.88888888888889	-100.88888888888889	1000
11	W11	35.88888888888889	-100.88888888888889	1000
12	W12	35.88888888888889	-100.88888888888889	1000
13	W13	35.88888888888889	-100.88888888888889	1000
14	W14	35.88888888888889	-100.88888888888889	1000
15	W15	35.88888888888889	-100.88888888888889	1000
16	W16	35.88888888888889	-100.88888888888889	1000
17	W17	35.88888888888889	-100.88888888888889	1000
18	W18	35.88888888888889	-100.88888888888889	1000
19	W19	35.88888888888889	-100.88888888888889	1000
20	W20	35.88888888888889	-100.88888888888889	1000
21	W21	35.88888888888889	-100.88888888888889	1000
22	W23	35.88888888888889	-100.88888888888889	1000
23	W24	35.88888888888889	-100.88888888888889	1000
24	W25	35.88888888888889	-100.88888888888889	1000
25	W26	35.88888888888889	-100.88888888888889	1000
26	W27	35.88888888888889	-100.88888888888889	1000
27	W28	35.88888888888889	-100.88888888888889	1000
28	W29	35.88888888888889	-100.88888888888889	1000
29	W30	35.88888888888889	-100.88888888888889	1000
30	W31	35.88888888888889	-100.88888888888889	1000
31	W32	35.88888888888889	-100.88888888888889	1000
32	W33	35.88888888888889	-100.88888888888889	1000
33	W34	35.88888888888889	-100.88888888888889	1000
34	W35	35.88888888888889	-100.88888888888889	1000
35	W36	35.88888888888889	-100.88888888888889	1000
36	W37	35.88888888888889	-100.88888888888889	1000
37	W38	35.88888888888889	-100.88888888888889	1000
38	W39	35.88888888888889	-100.88888888888889	1000
39	W40	35.88888888888889	-100.88888888888889	1000
40	W41	35.88888888888889	-100.88888888888889	1000
41	W42	35.88888888888889	-100.88888888888889	1000
42	W43	35.88888888888889	-100.88888888888889	1000
43	W44	35.88888888888889	-100.88888888888889	1000
44	W45	35.88888888888889	-100.88888888888889	1000
45	W46	35.88888888888889	-100.88888888888889	1000
46	W47	35.88888888888889	-100.88888888888889	1000
47	W48	35.88888888888889	-100.88888888888889	1000
48	W49	35.88888888888889	-100.88888888888889	1000
49	W50	35.88888888888889	-100.88888888888889	1000
50	W51	35.88888888888889	-100.88888888888889	1000
51	W52	35.88888888888889	-100.88888888888889	1000
52	W53	35.88888888888889	-100.88888888888889	1000
53	W54	35.88888888888889	-100.88888888888889	1000
54	W55	35.88888888888889	-100.88888888888889	1000
55	W56	35.88888888888889	-100.88888888888889	1000
56	W57	35.88888888888889	-100.88888888888889	1000
57	W58	35.88888888888889	-100.88888888888889	1000
58	W59	35.88888888888889	-100.88888888888889	1000
59	W60	35.88888888888889	-100.88888888888889	1000
60	W61	35.88888888888889	-100.88888888888889	1000
61	W62	35.88888888888889	-100.88888888888889	1000
62	W63	35.88888888888889	-100.88888888888889	1000
63	W64	35.88888888888889	-100.88888888888889	1000
64	W65	35.88888888888889	-100.88888888888889	1000
65	W66	35.88888888888889	-100.88888888888889	1000
66	W67	35.88888888888889	-100.88888888888889	1000
67	W68	35.88888888888889	-100.88888888888889	1000
68	W69	35.88888888888889	-100.88888888888889	1000
69	W70	35.88888888888889	-100.88888888888889	1000
70	W71	35.88888888888889	-100.88888888888889	1000
71	W72	35.88888888888889	-100.88888888888889	1000
72	W73	35.88888888888889	-100.88888888888889	1000
73	W74	35.88888888888889	-100.88888888888889	1000
74	W75	35.88888888888889	-100.88888888888889	1000
75	W76	35.88888888888889	-100.88888888888889	1000
76	W77	35.88888888888889	-100.88888888888889	1000
77	W78	35.88888888888889	-100.88888888888889	1000
78	W79	35.88888888888889	-100.88888888888889	1000
79	W80	35.88888888888889	-100.88888888888889	1000
80	W81	35.88888888888889	-100.88888888888889	1000
81	W82	35.88888888888889	-100.88888888888889	1000
82	W83	35.88888888888889	-100.88888888888889	1000
83	W84	35.88888888888889	-100.88888888888889	1000
84	W85	35.88888888888889	-100.88888888888889	1000
85	W86	35.88888888888889	-100.88888888888889	1000
86	W87	35.88888888888889	-100.88888888888889	1000
87	W88	35.88888888888889	-100.88888888888889	1000
88	W89	35.88888888888889	-100.88888888888889	1000
89	W90	35.88888888888889	-100.88888888888889	1000
90	W91	35.88888888888889	-100.88888888888889	1000
91	W92	35.88888888888889	-100.88888888888889	1000
92	W93	35.88888888888889	-100.88888888888889	1000
93	W94	35.88888888888889	-100.88888888888889	1000
94	W95	35.88888888888889	-100.88888888888889	1000
95	W96	35.88888888888889	-100.88888888888889	1000
96	W97	35.88888888888889	-100.88888888888889	1000
97	W98	35.88888888888889	-100.88888888888889	1000
98	W99	35.88888888888889	-100.88888888888889	1000
99	W100	35.88888888888889	-100.88888888888889	1000
100	W101	35.88888888888889	-100.88888888888889	1000
101	W102	35.88888888888889	-100.88888888888889	1000
102	W103	35.88888888888889	-100.88888888888889	1000
103	W104	35.88888888888889	-100.88888888888889	1000
104	W105	35.88888888888889	-100.88888888888889	1000
105	W106	35.88888888888889	-100.88888888888889	1000
106	W107	35.88888888888889	-100.88888888888889	1000
107	W108	35.88888888888889	-100.88888888888889	1000
108	W109	35.88888888888889	-100.88888888888889	1000
109	W110	35.88888888888889	-100.88888888888889	1000
110	W111	35.88888888888889	-100.88888888888889	1000
111	W112	35.88888888888889	-100.88888888888889	1000
112	W113	35.88888888888889	-100.88888888888889	1000
113	W114	35.88888888888889	-100.88888888888889	1000
114	W115	35.88888888888889	-100.88888888888889	1000
115	W116	35.88888888888889	-100.88888888888889	1000
116	W117	35.88888888888889	-100.88888888888889	1000
117	W118	35.88888888888889	-100.88888888888889	1000
118	W119	35.88888888888889	-100.88888888888889	1000
119	W120	35.88888888888889	-100.88888888888889	1000
120	W121	35.88888888888889	-100.88888888888889	1000
121	W122	35.88888888888889	-100.88888888888889	1000
122	W123	35.88888888888889	-100.88888888888889	1000
123	W124	35.88888888888889	-100.88888888888889	1000
124	W125	35.88888888888889	-100.88888888888889	1000
125	W126	35.88888888888889	-100.88888888888889	1000
126	W127	35.88888888888889	-100.88888888888889	1000
127	W128	35.88888888888889	-100.88888888888889	1000
128	W129	35.88888888888889	-100.88888888888889	1000
129	W130	35.88888888888889	-100.88888888888889	1000
130	W131	35.88888888888889	-100.88888888888889	1000
131	W132	35.88888888888889	-100.88888888888889	1000
132	W133	35.88888888888889	-100.88888888888889	1000
133	W134	35.88888888888889	-100.88888888888889	1000
134	W135	35.88888888888889	-100.88888888888889	1000
135	W136	35.88888888888889	-100.88888888888889	1000
136	W137	35.88888888888889	-100.88888888888889	1000
137	W138	35.88888888888889	-100.88888888888889	1000
138	W139	35.88888888888889	-100.88888888888889	1000
139	W140	35.88888888888889	-100.88888888888889	1000
140	W141	35.88888888888889	-100.88888888888889	1000
141	W142	35.88888888888889	-100.88888888888889	1000
142	W143	35.88888888888889	-100.88888888888889	1000
143	W144	35.88888888888889	-100.88888888888889	1000
144	W145	35.88888888888889	-100.88888888888889	1000
145	W146	35.88888888888889	-100.88888888888889	1000
146	W147	35.88888888888889	-100.88888888888889	1000
147	W148			

#### **1.14.2 Oil and Gas Well Index Table**













